UNIVERSITAT DE BARCELONA

Towards the validation of a druggable amyloid-beta oligomer as a target for Alzheimer´s disease

Cap a la validació d'un oligomer de beta-amiloide com a diana en la malaltia d'Alzheimer

Martí Ninot Pedrosa

Programa de doctorat de Química Orgànica

Towards the validation of a druggable amyloid-beta oligomer as a target for Alzheimer´s disease

Cap a la validació d'un oligomer de beta-amiloide com a diana en la malaltia d'Alzheimer

Martí Ninot Pedrosa

Tesi doctoral dirigida per:

Dra. Natàlia Carulla Casanovas

Institut de Recerca Biomèdica (IRB Barcelona)

Institut Européen de Chimie et Biologie (IECB)

UNIVERSITAT DE BARCELONA

Barcelona 2018

« Le vrai combat commence quand on doit combattre une part de soi-même. Jusque-là, c'est trop facile; mais on ne devient un homme que par de tels combats. Il faut toujours rencontrer le monde en soi-même, qu'on le veuille ou non. »

Ximénès – à l'Espoir (André Malraux)

Agraïments

“nanos gigantum humeris insidentes”

A vegades podem creure que estem on estem per les nostres qualitats, capacitats i intel·lecte. Però com deia Newton, si hi veiem lluny és perquè, tot i ser nans, estem sobre espatlles de gegants. De la mateixa manera que la meva feina no seria imaginable sense tota la gent citada en les referències, tampoc hagués sigut jo capaç de fer-la sense un munt de gent dels quals molts pocs apareixen en el dit apartat.

Primerament el principal d’aquests “gegants” és la Natàlia, per tantíssim. Perquè tots els que hem passat pel teu grup som conscients que hem sigut uns afortunats, pel teu esperit crític, pel teu rigor i fermesa, per la teva lluita incessant amb una energia i dedicació infinites per això que ens apassiona. Però sobretot, pel tracte humà, i per l’empatia que tens amb la gent amb qui treballes, en el meu cas, també per la paciència que has tingut. Ets un grandíssim exemple a seguir tant per els que hem tingut la sort de treballar al teu grup, com per les teves filles. Gràcies. Després, l’altre persona que ha estat un pilar aquests anys, òbviament, ha estat la Montserrat, també amb la paciència d’un sant. Treballar amb tu va ser genial, va ser tenir ganes d’anar al laboratori cada matí, va ser una complicitat molt especial i molts bons moments junts, poder compartir alegries i decepcions, i sobretot, va ser tenir una amiga d’un talent científic i humà excepcional. Gràcies.

També vull agrair a l’Ernest la seva didàctica, tant com a professor a la facultat com aquests anys en els seminaris de grup. Però a l’Ernest també li vull agrair la seva manera de ser, gràcies a la gent que escull i al seu tarannà senzill, ha aconseguit tenir el grup que té, on dóna gust treballar. No em podria oblidar de la gent que ha fet les coses senzilles, de la Eva, sempre disponible amb un somriure i gran eficiència i la Cristina Garcia amb qui hem compartit gran afició a la muntanya. També la Zuri! Tot i que vam coincidir pocs anys al lab, van ser prous! M’encanten els nostres vermuts i les nostres discussions!

I l’ambient al laboratori ha estat genial. Hi ha passat moltíssima gent, tots aquells que van marxar d’hora com els Bernats, el Benji, l’Abraham, el Miguel i la Rubi amb qui vaig

compartir poc temps però que sempre fa molta il·lusió tornar-los a veure. El Xavi Vila i les nostres aventures per Rio! I la Mendi! La meva companya perica per excel·lència. La Marta Mena i els seus invents per purificar des del sofà de casa. També gent com la Laura Nevola (i les seves recomanacions teatrals) i la Núria Bayó, sempre molt properes.

I com no, què haurien estat aquests anys sense l'Amyloid Team! Sense una gran Sílvia Turboprinyó! Gran companya i estricta jefa de l'Aurelio (hehe, com se't va trobar a faltar després pel lab!) quina pena que no ens apuntéssim a ballar swing! I grans moments que hem passat a Bordeaux o per les festes de Sants. I l'Aurelio amb els teus e-mails inigualables i les converses interessantíssimes ets una persona "digna de admirá", la Natàlia, la Montserrat i el Bernat, ja esmentats, ma anche Robi Mazzucata! Ti ricordi quando siamo andati alla festa di Okupi? E Anto, come dimenticare ogni mese che sei stato nel laboratorio, grazie per avermi insegnato un po d'Italiano, e per tuto! I ja més tard, va arribar l'Edu, company de llargues nits al laboratori però també hem passat bones nits de birres per Bordeaux, tornades amb bicicleta i has estat el meu professor particular de surf, merci nen! I finalment la Sonia, una altra de les que ha hagut de tenir més paciència amb mi. Ja mentre feies la tesi, em vas haver d'aguantar al costat tots els anys, i no contenta amb això, vas i entres a l'Amyloid Team, i com no, a Bordeaux t'ha tocat altre cop el torracollons del Martí al costat, et desitjo moltes dosis de paciència que encara et queden uns mesets més! Podria comentar nits de festa, visites a Centelles, cafès al vespre, bolera, sopars i moltes més coses, simplement moltes gràcies aquí estaré sempre.

Però no tot és Amyloid Team, què hauria sigut del lab del Giralt sense en Pep? Quin tio! Hem passat molt bons moments i hem pres bones cassalletes per allà baix (no coment), molts pokers, algunes curses i sempre tocant els picarols pel lab (però ja el dia que et vas endur una queixalada ja en vas aprendre! haha). I per suposat, res hauria sigut igual sense el company de batalles, Salvata! Amb tu ens hem apuntat a un bombardeig des del principi. Des del 1st PhD retreat com a organitzadors, el ja extint Beers for Science amb l'Àlbert i companyia que ens va donar molt bones tardes, amb el SciDF, les excursionetes amunt i avall i com no, les nostres curses d'orientació,... Tela! Gràcies per voler compartir tant amb mi, espero que això no canviï i seguim igual de liats a saco. També el Polanski, tot i que ara des de Yale, van ser molts anys d'hores intempestives al

lab, de tots els teus problemes amb en Pere, amb els dissolvents, dels riures que ens fèiem amb els de manteniment! “Has visto a Pol?” De molts cafès, algun poker? (i mira que és teu el joc),bones tardes berenant o calant foc a la barbacoa de la Sonia junt amb en Jesús! Vaya un altre! Haha Amb els seus problemes gatunos, perfumils,... Els seus donetes i mai cap mala paraula per ningú (Bueno, o en tot cas que tu te n’adonessis, perquè quins riures a l’esquiada amb la Cristina! xD). I tela amb la Fustera, tot i que no feia tant que havia arribat, no ens hem rigut ni res, de festa, amb lo tiquis-miquis que ets amb el menjar, amb la raquetada, les esquiades, i sobretot al laboratori, moles molt! I como no, la “leader”, qué haría este laboratorio sin ella! Macarena, eres una persona muy especial, con una gran empatía (a veces demasiado buena y todo), con una gracia innata que encajas con una sensatez que da gusto. ¡Ha sido una suerte conocerte y verte soñando como una niña super “groupie”! I Txell (sobretot que ningú pipetegi el TFA amb la boca!), Daniele y sus plantas arriba y abajo; Daniela speaking any number of languages; Monica, sempre ammirevolmente laboriosa; Toni y sus licores macedonios; also Mark, with your funny group meetings. I per suposat també l’Adam, crec que has aconseguit posar prou ordre en aquest laboratori i a més hem compartit la mitja de Granollers i molt bones tardes berenant al lab. També recordar la Júlia i els seus maldecaps amb l’FPLC (els buffers que es tornaven boles de nadal al posar-los a la nevera). La Cristina Díaz, tot i haver fet la carrera junts no ens havíem conegut abans, i amb el teu estil calmat ens hem anat coneixent. Ets molt treballadora i això segur que et portarà lluny. Es fa llarg però no em puc oblidar de les minions! L’Esther i la Ma, companyes de “uni”, i que després ha estat una grata sorpresa treballar amb vosaltres i compartir raquetades, tardes, sopars, etc. I darrerament també van arribar la Sílvia i la Maria i vàreu portar uns catalàs molt macos al laboratori a part de molt bon rotllo. E Federica e Fabio, è stato breve ma intenso, grazie anche a voi. Igual que contigu Daniel, un placer conocerte. Però a part del laboratori de’n Giralt, els de l’Albericio han estat com uns més del laboratori. Sobretot l’Helena, hem compartit caps de setmana, amics en comú, sortides, dinars, moltes pujades i baixades a la facultat per paperassa i sobretot, molts bons moments! Però també l’Iván, com hem rigut amb tu, sempre tenies un somriure per tothom i encomanaves bon rotllo, recordo molt la cursa d’orientació per Montjuic, haha vas morir molt! I com no, la Judith, déu ni do, quina paciència, haver-te hagut d’aguantar aquestes últimes setmanes al laboratori sempre queixant-te de tot,

ha estat molt dur... Quina dona! Haha Però si te'n vas a Canadà, se't trobarà a faltar! I finalment amb l'Alejandro, recordo molt el viatge a Boí xerrant tot el viatge, també hem compartit prou caps de setmana i birres, i que no pari! També tota la gent d'iProteos, Núria, Sandra, Pep,... que quasi heu estat uns més al laboratori.

Però a part de la gent del lab, vaig tenir la sort el meu primer any de doctorat, de conèixer i juntar-me amb un grup de gent genial d'altres labs de l'IRB. Què hauria sigut d'aquests anys sense valtros? Jordi gràcies pel finde a Boí, va ser brutal! Gemma, ex-veïna i gran amiga, saps que has estat important per a mi, merci. Laura i les nostres xerrades intenses i els bons riures. Jürguen, are you still alive after the week-end with paragliding and pica d'Estats? better Tagamanent, pica was crazy! And Craig, we also shared some nice hikes, ski trips, Passanant and so many others (like hair-length competition). I Ricardo y Adrián, ¡que risas en la excursión BTT por el río! L'Helena Roura i la seva finor, l'Àlbert que també hem passat molts bons moments i he pogut gaudir dels teus concerts. L'Anna, i els seus tallers de maquillatge i l'Ernest i les seves manies! També l'Adrià i tants altres que òbviament no els puc nomenar tots. Però sobretot amb tots vosaltres he passat grans caps de setmana i festes realment memorables. Sou genials! I com no, Serru i Ari, bones amigues ja a la uni i després encara hem compartit molts moments, molts ànims!

Però fora de la feina, he de donar mil gràcies als Bastoners del Casc Antic per aguantar-me tants anys! A tots els Castellers de la Sagrada Família i d'una manera molt especial, als cucs. Guapos, sabeu que sou molt necessaris per a mi!! Sara, Anneta, Pol, Amando, Coquito, Sareta, Lídia, Mayné, Maria, Aina, Bolinches, Noe, Roig. Sou un amor! I com no, Turi, Llena, Lali, què seria jo sense valtres? Encara que a vegades m'enfado, sou imprescindibles, gràcies per haver entrat i quedat tants anys a la meva vida. I Clarona, Toti, Adela, Adri, per seguir arreglant el món i trobar-nos molts més anys. Thal, per tants anys, per tot, merci. I Júlia, perquè d'una manera o altra, aquests 4 anys sempre hi has estat i jo no seria el mateix sense tu. Arnau i Lori, perquè per molts anys ens seguim reunint. Clàudia, després de tants anys i tot el viscut, merci per tot el que has volgut compartir amb mi, i per molts anys. Victor i Dani, per ser-hi sempre, moltíssimes gràcies. I gràcies també Èlia, pel suport i les lluites compartides.

Pour mes gents de Grenoble, merci énormément Diego, Kai, Hind, … je ne serais pas où je suis sans votre aide et votre amitié, j'espère vous revoir bientôt. Merci aussi à Juan, Anne, Yvain, Claudine, Adrien, Roman, Sarah, et tout l'équipe de métalloprotéines, je m'en souviens beaucoup de vous, car j'ai appris énormément dans votre laboratoire.

También tuve la suerte de estar en Bruselas, como no, Roberto, ¡tenemos que volver a salir por los bares! Joar, Francisco, gracias por los buenos momentos. Dank je wel ook aan Serge, for all the help in my stage and all the collaboration and meetings to finally make these Nanobodies possible. But of course, I'm super glad to have known, Ema, muito obrigado for all your help and everything you taught me, with your hard work you can get whatever you want. In general, thanks to all CMIM people! Moreover, during the stage I had the luck to meet Chrystel. No need to say too much, I wish we will be seeing each other for long time, when next trip? Dank je wel for everything.

Et cette dernière année j'ai eu la chance de déménager à Bordeaux. Merci Magalie pour être ma famille ici et ne pas t'embêter avec mes semaines de stress. Also, I would like to thank Chiara, Thomas, Alba, Britta, Caro, and all the people from IECB for their warm welcome for all the pub quizzes, and the breaks together. Et bien sûr, merci beaucoup à Antoine pour m'encadrer pour mon stage, et énormément aussi à Denis, pour prendre ton temps pour m'apprendre une partie de cette thèse c'est grâce à toi.

I Papa, Mama, sóc molt desagraït amb vosaltres i vaig sempre a la meva i a vegades no sé com encara m'aguanteu, gràcies per la vostra paciència, per fer-me com sóc, per haver-me ensenyat tant i donar-me tants valors. I Xels, ets un puto crack, t'envejo en moltes coses sé que arribaràs molt lluny, t'estimo! Iaia, esto también va por ti, por ser un ejemplo de persona moderna, de mujer fuerte igual que mi madre y de lucha constante, gracias. I a tots els tiets i cosins, també va per vosaltres, perquè m'alegra tenir aquesta família.

I a part de la família, si algú és directament responsable de tot això, és el sistema d'educació pública i específicament a l'escola Dolors Monserdà-Santapau, també l'Institut Frederic Mistral-Tècnic Eulàlia i la Universitat de Barcelona, tots ells per donar-me una educació envejable. I a tots els contribuents per pagar-me un sou, espero haver-lo merescut.

També, i en la redacció d'aquesta tesi m'ha afectat d'una manera molt especial, he de tenir un record per tots els ferits de l'1-O, especialment pel Roger, la Vicky i el Biel; també altre cop pels Castellers de la Sagrada família, que ens ha afectat tot plegat especialment. També vull demanar la llibertat tots els presos i exiliats polítics. Cal reivindicar més que mai els drets humans i la llibertat d'expressió, i cal esperar que canviïn aquests vents que, d'un temps ençà, tornen a apropar núvols foscos de temps passats.

Gràcies a tots vosaltres pel suport emocional imprescindible, per donar-me tota la força, tota la intel·ligència i tot l'entusiasme necessaris.

Cal intentar l'impossible per fer l'increïble

Contents

Agraïments I

Contents VII

Abbreviations XIII

Introduction 1

Dementia and Alzheimer's disease 3

Amyloid beta peptide 5

Aβ Oligomers 8

Beta-barrel Pore-Forming Oligomer (βPFO) 10

Ojectives 17

Chapter 1 : βPFO is stable in a native lipid environment 21

Context 23

Results 28

βPFO is not stable in DHPC-DMPC bicelles 28

DPC-DMPC can form bicelles 32

βPFO is inserted in DPC-DMPC bicelles 34

βPFO is stable and keeps its overall structural and functional properties in DPC-DMPC bicelles 35

βPFO can be directly formed and is stable in DPC-DMPC bicelles 38

Discussion 39

Materials & Methods 41

Reagents 41

Recombinant Expression of Aβ42 41

Purification of recombinant Aβ42 43
Preparation of monomeric Aβ42 from peptide synthesis 45
Quantification of Aβ42 peptide 45
Preparation of βPFO in micelles 45
Reconstitution of βPFO in DHPC-DMPC bicelles via proteoliposomes 46
Reconstitution of βPFO in DPC-DMPC bicelles in situ 47
Folding of βPFO in bicelles 47
SEC 48
NMR spectroscopy 48
CryoEM 49
Limited proteolysis 49
Electrical recordings with planar lipid bilayers 49

Chapter 2 : Generation of specific anti-βPFO Nanobodies 51

Context 53
Results 55
βPFO trapped into NAPol is a good antigen for *camelidae* immunization. 55
βPFO preserves its structure when immobilized in a solid support 57
Eleven Nanobodies were obtained after βPFO/NAPol immunization 60
The Nanobodies are specific for βPFO 62
Nanobodies interact with βPFO through different mechanisms 65
Nanobodies can block βPFO pores 67
Discussion 69
Materials & Methods 71
Reagents 71
βPFO trapping into NAPol 71

ELISA 71

Phage display panning and screening 73

Production of βPFO specific Nanobodies 75

Analysis of βPFO/Nanobody affinity by ELISA 77

Analysis of βPFO – Nb interaction by limited Proteolysis coupled to Western Blot 77

Analysis of βPFO – Nb interaction by electrical recordings with planar lipid bilayers 78

Appendix: Formation of amyloid oligomers in liposomes 79

Context 81

Results 83

HFIP is able to dissolve both Aβ42 and POPC 83

Liposomes containing Aβ42 are stable 85

Aβ affects every part of the POPC molecule 86

Discussion 89

Material & Methods 90

Reagents 90

Aβ42 proteoliposomes preparation 90

NMR spectroscopy 91

Conclusions 93

References 97

Abbreviations

AD	Alzheimer's disease
ADDLs	Aβ-derived diffusible ligands
AEBSF	4-(2-Aminoethyl)-benzenesulfonyl fluoride hydrochloride
AFM	Atomic force microscopy
AICD	APP Intracellular Domain
Apo E	Apolipoprotein E
ApoA-I	Apolipoprotein A-I
Apol	Amphipol
APP	Amyloid precursor protein
Asn or N	Asparagine
Aβ	Amyloid beta
βPFO	β-barrel pore forming oligomer
BB	Broad Band
BSA	Bovine serum albumine
C99	C-terminal fragment of 99 amino acids of APP
CCC	Chemically competent cell
CD	Circular dichroism
cDNA	complementary DNA
CDR	Complementary-determining region
C_H	Conserved domain of the heavy chain
CI	confidence interval
C_L	Conserved domain of the light chain
CMC	Critical micelle concentration
CryoEM	Cryo-Electron Microscopy
DB	Double band
DDM	Dodecylmaltoside
DHPC	1,2-dihexanoyl-sn-glycero-3-phosphocholine
DM	Decylmaltoside
DMPC	1,2-dimyristoyl-sn-glycero-phosphatidylcholine
DMSO	Dimethylsulfoxide
DNA	Desoxyribonucleic acid
DPC	dodecylphosphocholine
E. Coli	Escherichia coli
EC50	half maximal effective concentration
ECL	Enhanced chemiluminescence
EDTA	ethylenediamine-tetraacetic acid

ELISA	Enzyme-linked immunosorbent assay
EOAD	Early onset Alzheimer's disease
Fab	Antibody binding fragment
fAD	familial Alzheimer's disease
Fv	Variable domain of Fab
Gdn	Guanidinium
Gln or Q	Glutamine
HCAb	Heavy-chain Antibody
HFIP	1,1,1,3,3,3-hexafluoro-2-propanol
HMQC	Heteronuclear Multiple-Quantum Correlation
HPLC	High Performance Liquid Chromatography
HPLC-PDA	HPLC coupled to Photodiode Array Detector
HRP	Horseadish peroxidase
HSQC	Heteronuclear single quantum coherence spectroscopy
IECB	Institut Européen de Chimie et Biologie
IgG	Inmunoglobulin type G
IMAC	Immobilized-metal affinity chromatography
INEPT	Insensitive nuclei enhanced by polarization transfer
IPTG	Isopropyl β-D-1-thiogalactopyranoside
LB	Luria Bertani
LDAO	lauryldimethylamine-N-oxide
LOAD	Late onset Alzheimer's disease
LP	Limited proteolysis
LTP	long-term potentiation
MAS	Magic angle spinning
MS	Mass spectrometry
MSP	Membrane scaffold protein
NAPol	Non-ionic Apol
NFT	Neurofibrillary tangles
NHS	N-Hydroxysuccinimide
NMR	Nuclear magnetic resonance
OD	Optical density
OG	Octyl glucoside
OmpX	Outer membrane protein X

PC	Phosphocholine
PCR	Polymerase chain reaction
PE	Periplasmic extract
PEG	Polyethyleneglycol
PEN-2	Presenilin enhancer 2
PET	positron emission tomography
PF	Protofibrils
POPC	1-palmitoyl-2-oleoyl-sn-glycero-3-phosphocholine
PS1 or PSEN1	Presenilin-1
PS2 or PSEN2	Presenilin-2
RNA	Ribonucleic acid
sAPPα	secreted soluble APP α
sAPPβ	secreted soluble APP β
S_{CD}	Carbon-deuterium order parameter
scFv	Single-chain Fv
SDS	Sodium dodecyl sulfate
SDS-PAGE	SDS-Polyacrylamide gel electrophoresis
SEC	Size exclusion chromatography
ssNMR	solid-state NMR
TB	Triple band
TB	Terrific broth
TCEP	Tris(2-carboxyethyl) phosphine
TEA	Triethylamine
TEM	Transmission electron microscopy
TES	Tris, EDTA, Sucrose buffer
TFA	trifluoroacetic acid
THAM	Tris(hydroxymethil) acylamoidomethane
TRACT	1D [15N,1H]-TROSY for rotational correlation times
V_H	Variable domain of the light chain
V_HH	Variable domain of the heavy-chain antibody
V_L	Variable domain of the heavy chain
VUB	Vrije Universiteit Brussel
WB	Western Blot

Introduction

Dementia and Alzheimer's disease

Our memory, our language, our personality and most of the characteristics that define us as humans, progressively disappear when dementia appears. Dementia is defined as the loss of intellect and personality due to neuronal loss or damage. Alzheimer's disease (AD) is the most common type of dementia in humans, comprising 60-65% of all cases. As Robert Katzman defined it,[5]

"Alzheimer's disease is a democratic process. Physicians and psychologists, chess masters and physicists, mathematicians and musicians may become victims of this disorder"

AD affects people independently of social class, gender, profession or country of origin. Age is the main risk factor that predispose to develop AD. In its most common form, also called late onset AD (LOAD), the first symptoms appear around 65 years old and its prevalence doubles every 5 years. However, there are a 5% of cases where AD appears much earlier and in a very aggressive form, between 30-60 years old. This early onset AD (EOAD) is related to genetic mutations transmitted by Mendelian inheritance within the families. For this reason, EOAD is usually considered to be a familiar AD (fAD).[6]

The impact of AD in the world is dramatic both socially and economically. Last year, 47 million people were diagnosed with AD. The numbers are expected to increase as the length of life expectancy increases too. This, generates a huge and growing cost for both, public health systems (direct cost) and caregivers (social cost). Next year, global cost of the disease is expected to reach 1 trillion US$.[7] Moreover, inextricable to the economic cost there's the social impact in caregivers and families who see how patient's mind progressively disappears without any alternative. Even if many efforts have been done for a long time to find a cure for AD, only symptomatic treatments are available and the disease continues to progress without any cure up to now.

AD was first described in 1906 by Alois Alzheimer. He thought that the behavior of a demented 51-years-old patient was different from what he had seen until then. Thus, after 5 years of progressive dementia that prompted her death, he analyzed her brain *post-mortem*. Alzheimer found a dystrophic brain with vascular arteriosclerosis and neuronal death. Upon the use of chemical dyes, he found out the presence of "senile

plaques" in the extracellular space and the presence of "neurofibrillary tangles" (NFT) inside the neurons.[8-9] Later on, it was found that that NFT were formed by hyperphosphorilated versions of Tau protein,[10] a protein that stabilize microtubules giving shape and structure to the neurons and allowing the axonal transport. Moreover, plaques were found to be cumulations of amyloid fibrils, which later in 1984 were found to be formed by the consecutive arrangement of the amyloid beta peptide (Aβ).[11-12] From this point, two confronted hypotheses appeared. On one side, the discovery of other neurodegenerative disorders caused by tau malfunction without any other pathology so-called tauopathies, pointed to tau hyperphosphorylation as a possible responsible AD, within the "tau hypothesis".[13] On the other side, the discovery of other amyloidosis like the Creutzfeldt-Jakob disease pointed to Aβ as a possible prion protein responsible for AD, within the amyloid hypothesis. However, the genetic analysis of AD cases brought some light to this debate.

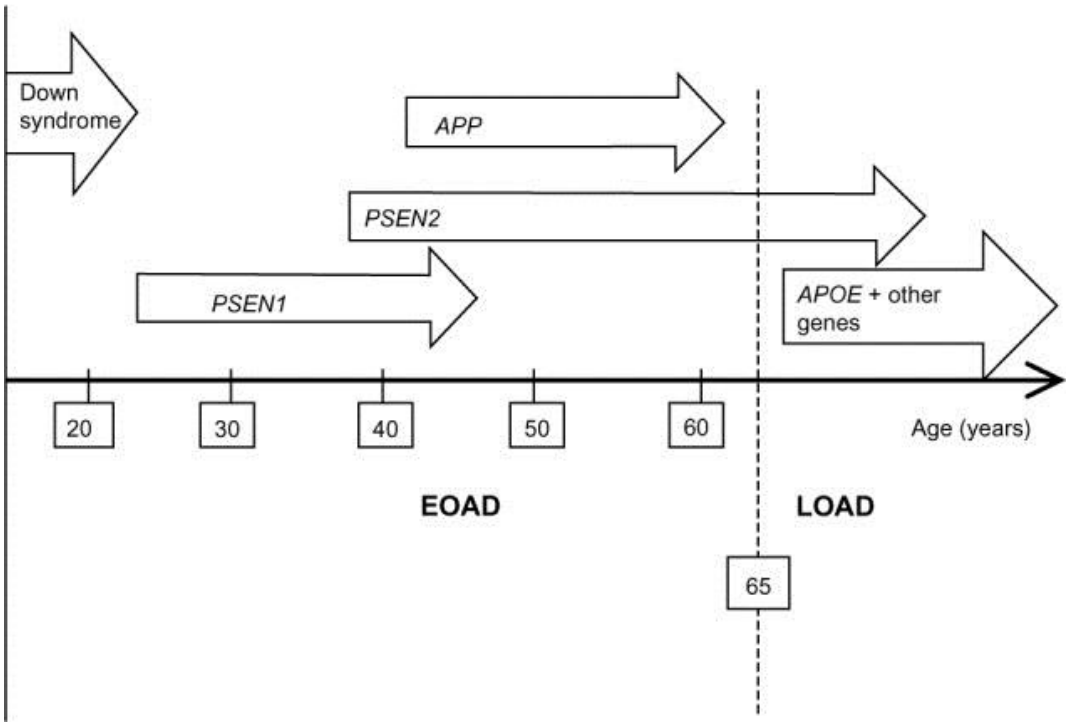

Figure 0-1: The range of ages of onset of AD, depending on the different involvement of genes. The onset can be dramatically early in Downs syndrome's patients, next for the people having certain mutations on the presenilin-1 (PSEN1) gene and then for the people having it for Presenilin-2 (PSEN2) and in the amyloid precursor protein (APP) respectively. The people carrying APOE risk factor genes, don't usually show EOAD. Reproduced with permission Bagyinszky *et al*.[2]

Genetic and populational analysis of LOAD cases pointed to Apolipoprotein E (Apo E) as the only gene established as an AD risk factor.[6,14] Apo E is one of the proteins responsible for Aβ clearance and have 3 different subtypes (ε2, ε3 and ε4). The ε2 having a protecting effect over AD, the ε3 being the most common in humans and the ε4 being a risk factor for AD. In fact, the individuals carrying of ε4/ε4 alleles have 10-fold more probabilities to develop dementia than the ε3/ε3 ones. However, the case of APOE only explains a 10% difference in the age of onset of dementia **[Figure 0-1]**.[15] The genetic analysis of EOAD cases showed a much more important relation between Aβ and AD. The genes found to be mutated in the people with fAD corresponded to the amyloid precursor protein (APP), the presenilin-1 (PS1), and the presenilin-2 (PS2). Notably, all these proteins are involved in the process of Aβ production.[2,6]

Apart from APOE and fAD mutations, there are other pieces of evidence that support the amyloid hypothesis. First, Down syndrome people develop the very early AD due to the trisomy of the 21st chromosome. This chromosome encodes for APP, the protein from which Aβ is obtained. Thus, implying three copies of the Aβ sequences inside the APP gene. Second, the toxic effect of Aβ soluble species to hippocampal and cortical neurons. And finally, the neuropathological and behavioral changes similar to AD that transgenic mice mutated with human APP show in a time dependent manner.[16] All these evidence make the amyloid hypothesis more robust. Even thought, the role of tau is indubitable. Indeed, a dual-cause neurotoxicity seems to be the main guideline nowadays,[17] in which tauopathy seems to be a consequence of amyloidosis, and thus, a so-called, “secondary tauopathy”.[18]

Amyloid beta peptide

APP is an integral transmembrane protein that upon digestion by different secretases, can generate the Aβ peptide. Several secretases are known to target APP. The cleavage produced by α-secretase followed by that of γ-secretase releases three parts: The innocuous p3 peptide without a clear biological role, the secreted soluble APP α (sAPPα) with a neuroprotective effect and the APP Intracellular Domain (AICD).[19] This cleavage pathway is called the non-amyloidogenic pathway since it does not lead to the production of Aβ **[Figure 0-2** left**]**. On the contrary, when APP is cleaved first by β-secretase followed by γ-secretase, three different parts are released. After the β-

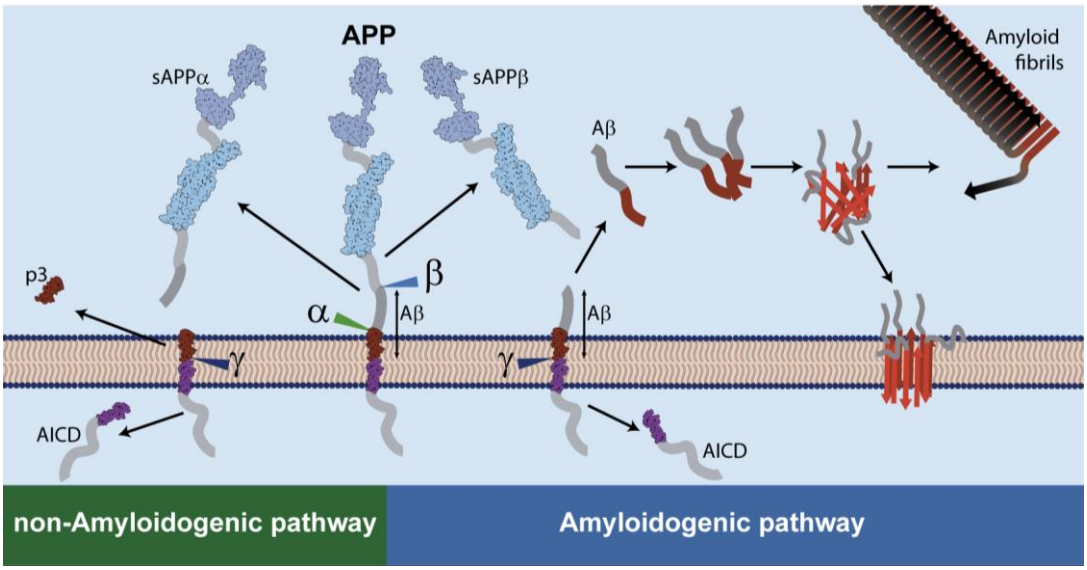

Figure 0-2: Scheme of APP proteolysis and Aβ aggregation. APP can be proteolyzed through the non-amyloidogenic pathway by the action of α-secretase and γ-secretase or through the amyloidogenic pathway by β-secretase and γ-secretase. After release from the membrane, Aβ starts to oligomerize through different oligomeric states until forming amyloid fibrils. Additionally, the low order oligomers have been proposed to interact with the membrane to form pores.

secretase cleavage, secreted soluble APP β (sAPPβ) without any neuroprotective effect, is released. The resulting C-terminal fragment of 99 amino acids (C99) is then cleft by γ-secretase to produce Aβ and AICD **[Figure 0-2** right**]**. γ-secretase is a multi-subunit protease complex made of four transmembrane proteins: PS1 or PS2, Presenilin enhancer 2 (PEN-2), nicastrin and APH-1. The catalytic center of the complex is found in the presenilins were, as previously commented, several mutations have been found to lead to fAD **[Figure 0-1]**.[19-22] γ-secretase cleavage is not specific, therefore, it sequentially cuts the C99 fragment by several points giving place to different Aβ variants. Generated Aβ variants range from 38 to 43 amino acids in length. Being Aβ40 and Aβ42 being the majoritarian ones.[23] While Aβ40 is the most abundantly produced (~90 %), Aβ42 (~10 %) is the most strongly linked to the etiology of the disease.[24] The two additional hydrophobic amino acids of Aβ42 compared to Aβ40, make it more prone to aggregate. This, makes it hard to handle, being called, even in the scientific literature, "the peptide from hell"[25]. Moreover, the genetic mutations on APP lead to an increase in Aβ production, Aβ aggregation propensity or an increase in the Aβ42/Aβ40 ratio. The latter effect is also found with the mutations of fAD present in PS1 and PS2.[6] This

genetic profile of the disease points to Aβ42, the most prone to aggregate, as the Aβ variant responsible of the neurotoxicity.

Indeed, it has been described that Aβ self-assembly is a must for the neurotoxicity to have place.[16] Aβ is present in the brains of healthy individuals, thus its mere presence does not cause neurotoxicity. However, in AD individuals, once the peptide is secreted and reaches a certain concentration, it starts to self-associate. Starting from dimers, different intermediate species commonly referred to as Aβ oligomers, are sequentially formed until forming fibrillization nucleus were amyloid fibrils, the main component of the neuritic plaques, start to build up.

If Aβ production and aggregation is the main player in AD, one way to validate the amyloid hypothesis would be to design drugs that would decrease Aβ production and inhibit Aβ aggregation. Unfortunately, most clinical trials focusing on either Aβ production or Aβ plaque clearance have failed, inducing some skepticism about the Amyloid hypothesis. However, there is not objective data actually opposing it.[26-27] On the contrary, the failings of solanezumab, a plaque clearer antibody, and verubecestat, a β-secretase inhibitor, may be explained if the harm of the disease is not proportional to the amount of Aβ. This opens different scenarios: First, that Aβ have to reach a threshold to start the neurotoxicity. Thus, if the lowering of Aβ is not going below this threshold, no significant improvement will be shown. Second, that Aβ triggers the disease process and once is triggered, Aβ clearance is worthless.[28-29] Third, that Aβ clearance process may not be cleaning the proper target. Until last year with aducanumab, an anti-Aβ antibody not targeting the monomer,[30] the clinical trials did not show a good target engagement. Not being able to prove a good target engagement hardens obtaining robust conclusions from the trials when they fail. The development and optimization of molecular positron emission tomography (PET) imaging made possible, in this last case, the visualization of plaque clearance. Fourth, patient selection could be a concern as the disease is thought to start a decade before the first symptoms appear. Indeed, it has been described nondemented cases having both Aβ plaques and NFT.[18,31] Therefore, some of the negative controls could already be developing AD. As previously stated, it is known that Aβ aggregation is needed to cause the neurotoxicity as Aβ monomers are a natural non-toxic product commonly present in healthy

individuals and even neurite-promoting.[32] But the amount of Aβ fibrils don't correlate with the degree of cognitive decline.[16,33-34] On the basis of this poor correlation, the amyloid hypothesis shifts to consider the main cause of neuron damage in AD soluble Aβ intermediate species. [16,35-42]

Aβ Oligomers

For a long time, Aβ senile plaques were the center in AD's research. However, for the past few years, most efforts have focused on the study and characterization of Aβ oligomers. Aβ oligomers are intermediate species formed in between the secreted monomer and the final fibrils. Since these intermediate species are heterogenous and transient, it has been hard to isolate, freeze the stage and characterize them.

Post-mortem Aβ oligomers from humans and transgenic mouse developing AD, have been extracted. In one case, Walsh *et al.* injected human AD-patient's soluble Aβ fraction into rats showing neurotoxicity by inhibiting long-term potentiation (LTP) from non-monomeric and non-fibrillar Aβ forms. [40] Also from human brain samples, Shankar *et al.* also administered human oligomers to rats and characterized a dimer as the smallest synaptotoxic specie.[43] Moreover, Lesné *et al.* characterized a 56 kDa oligomer from transgenic mouse developing AD which was found to be neurotoxic by inhibiting LTP when administered into rats.[44] However, a big concern exists regarding how the extraction method is affecting the original sample. Moreover, sample limitation is an issue when working with *in vivo* samples or *post-mortem* samples which limits as well the techniques that can be used to characterize them. For instance, it has been demonstrated that the use of sodium dodecyl sulfate (SDS) produces artifacts on oligomerization of Aβ42 peptides questioning the validity of the techniques such as SDS polyacrylamide gel electrophoresis (SDS-PAGE) to characterize Aβ oligomers.[45] For these reasons and with the advantage of cheap and relatively easy Aβ peptide synthesis, the importance of synthetic peptide increased and *in vitro* generated oligomers started to be developed.

First, protofibrils (PF), spherical and curvilinear soluble *in vitro* Aβ oligomers that appeared before fibril formation were described. They were formed by Aβ40, Aβ42 and E22Q (Dutch mutation) Aβ40 with curly fibril structures ranging from 6-10 nm in

diameter and up to 200 nm in length.[16,46] PF showed neurotoxicity when applied to neuronal cultures.[47] Afterwards, Aβ-derived diffusible ligands (ADDLs) were described as preparations of Aβ oligomers free of amyloid fibrils and with a similar structure to PF. ADDLs were prepared by incubating Aβ with clusterin and were found to be soluble, highly neurotoxic and spheres from 4 to 5 nm in diameter. But in contrast to PF, ADDLs could be formed by Aβ42 but not by Aβ40.[37] However, in both cases, due to their heterogeneity no structural characterization is available up to date. A less native oligomer preparation are the globulomers. Briefly, they were formed upon 1,1,1,3,3,3-hexafluoro-2-propanol (HFIP) resuspension followed by evaporation and dimethylsulfoxide (DMSO) resuspension with a final SDS-enriched phosphate-buffered saline (PBS) dilution. After incubation a 38-48 kDa globular oligomer was formed. Globulomers are shown to be formed in the presence of some fatty acids instead of SDS and they showed neurotoxicity by LTP inhibition. [48] The use of SDS was also employed to prepare a 150 kDa olifomer, from which a little structural information was obtained showing an antiparallel arrangement[35] which is a characteristic from the neurotoxic species.[49]

It has been described that neurons from AD brains present calcium dysregulation, oxidative stress synaptic loss and the formation of intracellular NFT. Calcium dysregulation, oxidative stress and formation of tau neurofibrillary tangles are processes occurring in the interior of the cells while Aβ is excreted and accumulated extracellularly. Consequently, it is very likely that neurotoxicity involves the cell membrane. Researchers pointed out different options: The Aβ peptide interacts with receptors from the membrane,[50] binds to the membrane nonspecifically disrupting it[41] or forms ionic pores that permeate the membrane.[51-53]

Some researchers already focused on membrane oligomers and studied the interaction of Aβ with liposomes. On one side, Kourie *et al.* and and Hirakura *et al.* showed the ability of Aβ to allow undefined conductance across lipid bilayer forming pores.[54-55] On another side, Lin *et al.* showed the formation of membrane oligomers reconstituting Aβ42 in lipid membranes. Using AFM, they showed a donut-like shape with an outer diameter from 8 to 12 nm. These oligomers also showed pore behavior across lipid

bilayers on electrical recordings.[53] However, further structure characterization was not obtained.

Beta-barrel Pore-Forming Oligomer (βPFO)

Following this research line, in the last years, Dr. Carulla's group has been studying the formation of Aβ oligomers using the same approaches as those used in the study of membrane proteins. In these studies, it is of paramount importance the use of a suitable biomimetic environment. The most commonly used, for their price and ease to manage are detergents[56-58]. Detergents, are amphiphilic molecules having a hydrophobic and a hydrophilic moiety. Their main characteristic is that when found in solution and the concentration is above its characteristic critical micelle concentration (CMC) they aggregate forming micelles. Micelles are spherical aggregates of 40-100 units of detergent molecules organized with the polar heads on the surface and the hydrophobic moiety remaining protected in the core of the micelle. Below its CMC, detergent molecules are either on the water surface/interface or in solution. Detergent micelles are a common system to solubilize membrane proteins. By forming a micelle around the hydrophobic belt of the membrane protein, they avoid protein aggregation by simulating the hydrophobic core of the membrane. Due to their small size compared to other biomimetic membrane environments, detergent micelles enable the use of solution nuclear magnetic resonance (NMR) allowing to obtain high-resolution structural and dynamical information of the protein under study. However, every detergent has different physicochemical and geometrical properties requiring an extensive screening to find those that match the geometry of the membrane protein and thus preserve its native structure and function. Moreover, not only the detergent type but the detergent concentration is important as the detergent-protein interaction may compete with

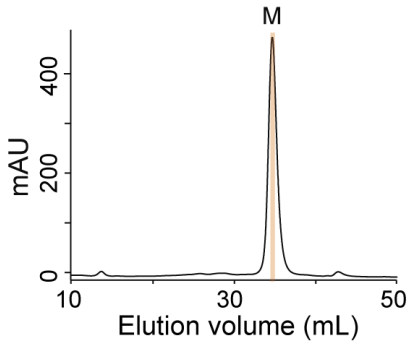

Figure 0-3: SEC characterization of monomeric Aβ40 sample prepared in SDS. The Aβ40 sample was analyzed immediately after being reconstituted in SDS micelles at an [Aβ]:[micelle] ratio of 1:4.7. In SEC tandem Superdex 200 Increase-Superdex 200 HR10/300 columns were used at 4°C, which showed that monomeric Aβ40 eluted at 34.7 mL.

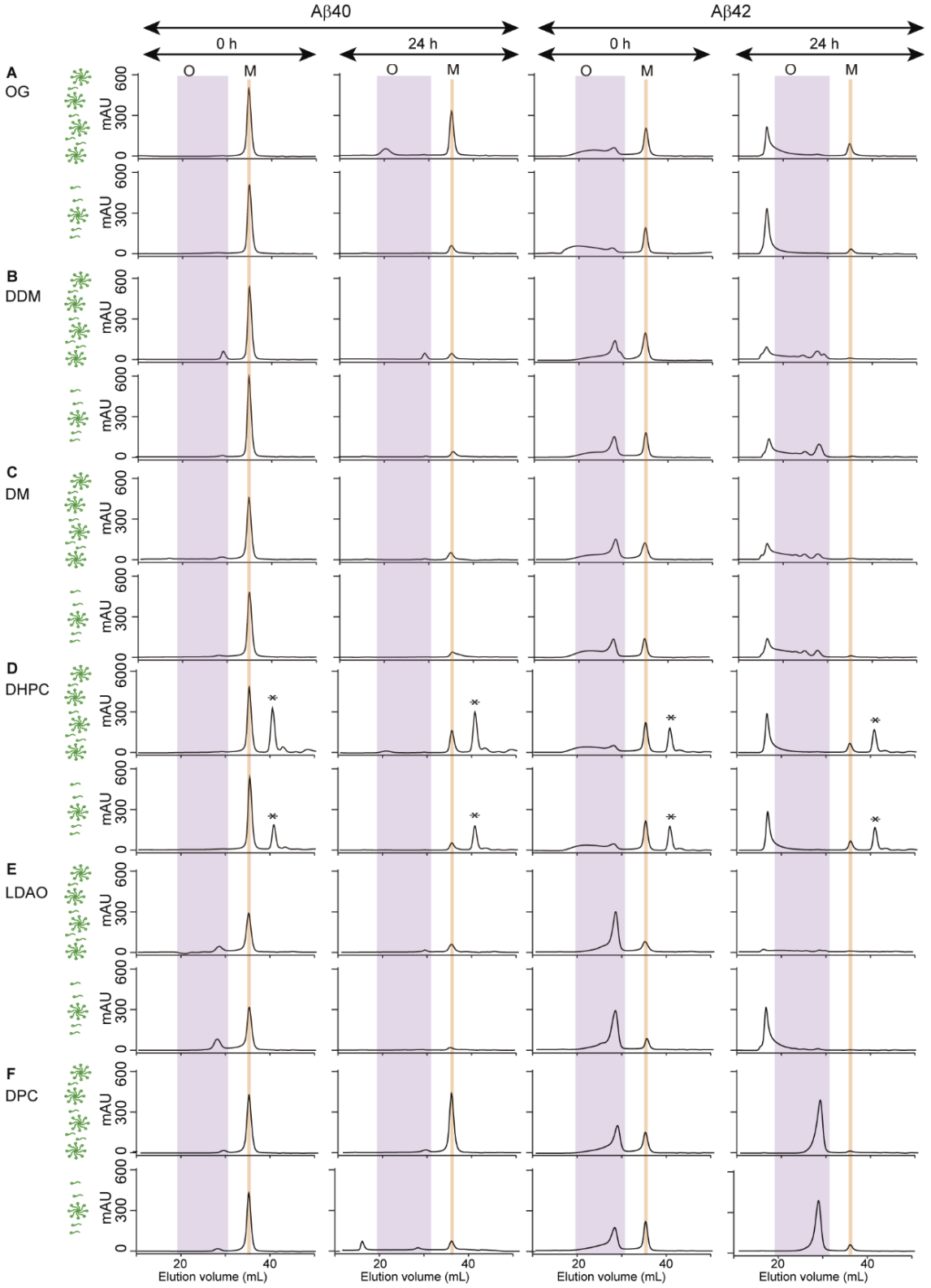

Figure 0-4: SEC characterization of Aβ40 and Aβ42 samples reconstituted under high and low micelle conditions using different detergents. Schematics of four micelles and one micelle, shown in green, represent high ([Aβ]:[M] 1:4.7) and low ([Aβ]:[M] 1:0.5) micelle conditions, respectively. Samples were analyzed at an Aβ concentration of 150 µM immediately after being reconstituted in micelles (t = 0 h) and after 24 h incubation at 37°C. SEC chromatograms of Aβ samples reconstituted in (A) OG, (B) DDM, (C) DM, (D) DHPC (the asterisk corresponds to DHPC micelles), (E) LDAO and (G) DPC. Chromatograms

were monitored at 220 nm. The orange line and purple band correspond, respectively, to the elution volume of our monomeric Aβ40 control and to the range of Aβ oligomers detected under the distinct detergent micelle conditions tested throughout this work.

the specific protein-protein interactions that we can expect in the case of an oligomer.[59] Therefore, several types of detergent micelles at different micelle concentrations were extensively screened by Serra-Batiste *et al.* using size exclusion chromatography (SEC).[60] The aim was to find a condition that matched the properties of Aβ oligomers described in liposomes with pore activity.[53] As a control for these studies, SDS-Aβ40 was used as monomer control to know the monomer retention time **[Figure 0-3]**.[58] Next, Six different detergents were screened to assess oligomer formation. These include: octyl glucoside (OG), dodecylmaltoside (DDM), decylmaltoside (DM), 1,2-dihexanoyl-sn-glycero-3-phosphocholine (DHPC), lauryldimethylamine-N-oxide (LDAO), and dodecylphosphocholine (DPC); at two different [Aβ]/[micelle]molar ratios: 1:4.7 referred to as high micelle condition and 1:0.5 as low micelle conditions; working with both Aβ40 and Aβ42; and analyzed at time 0 h and 24 h at 37°C **[Figure 0-4]**.

Different oligomerization behavior was found among the different detergents with many significant differences between Aβ40 and Aβ42. Aβ42, despite having only two extra amino acids, had much less monomeric propensity and more oligomeric propensity, while Aβ40 was mostly found as a monomer before incubation or disappeared after incubation forming, most likely, high molecular weight aggregates, as amyloid fibrils, that were lost upon sample filtration **[Figure 0-4]**.

The only conditions that kept Aβ42 stable after 24h incubation were the DPC-incubated samples at both micelle conditions. The chromatograms showed mainly a major symmetric peak eluting earlier than the monomer, thus, indicating the formation of a homogeneous population of Aβ42 oligomers in terms of size. When comparing with Aβ40 under the same conditions after 24h, it stayed either as a monomer, in high micelle conditions, or aggregated forming fibrils, at low micelle conditions. The formation of fibrils could be seen by transmission electron microscopy (TEM) **[Figure 0-5]**. This differential effect might be related to the differential relevance of Aβ40 and Aβ42 in the

disease. After these results, the conditions of Aβ42 at low micelle conditions of DPC micelles after 24h incubation at 37°C were choosen for next studies.

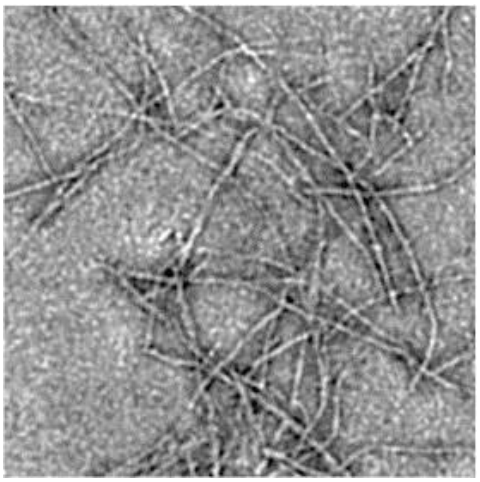

Figure 0-5: Transmission Electron Microscopy (TEM) image of Aβ40 fibrils. Aβ40 was incubated for 24h incubation at 37°C in 1:0.5 Aβ:micelle ratio.

The micelle Aβ42 oligomeric preparation at low micelle conditions was further studied by electrical recordings with planar lipid bilayers to establish its pore-forming ability as described for Aβ in the literature.[51-52,54-55,58] First, Aβ40 in low micelle conditions and also detergent micelles were analyzed as controls without giving any change in conductivity (data not shown). The addition of monomeric Aβ42 induced fast, transient, and heterogeneous ionic current **[Figure 0-6** E**]**. This "spiky" behavior was previously reported for Aβ and attributed to the formation of a highly heterogeneous population of Aβ pores.

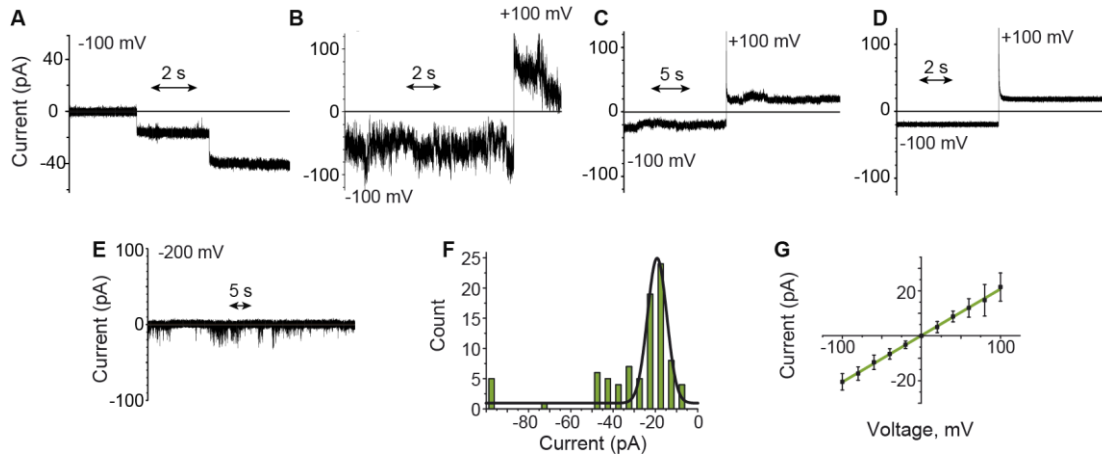

Figure 0-6: Electric recordings on planar lipid bilayers. Aβ42 oligomers incorporate into lipid bilayers as well-defined pores. (A) Multiple pore insertions. Typical current traces for (B) type 1, (C) type 2, (D) and type 3 pores of oligomeric DPC/Aβ42. (E) Typical current fluctuations induced by Aβ42 monomers. Electrical recordings were carried out on diphytanoyl-sn-glycero-3-phosphocholine planar lipid bilayers at the indicated applied potentials. (F) Histogram and (G) voltage versus current curve for type 2 and type 3 pores.

Regarding the sample under study, after 5-15 min of sample addition, step-wise changes in bilayer conductance were observed **[Figure 0-6** A**]**, behavior typical of the incorporation of individual proteins that form nanopores in membrane bilayers. These pores could be classified in three different types. Type 1, observed in about 17% of the experiments, was characterized by fast and noisy transitions with undefined open pore conductance values **[Figure 0-6** B**]**. Type 2, observed in about 48% of the experiments, showed a reasonably well-defined open pore conductance **[Figure 0-6** C**]**. Finally, type 3, which was observed in 35% of the experiments, indicated the presence of a well-defined open pore with no current fluctuations **[Figure 0-6** D**]**. Type 2 and type 3 conductance showed an average open pore current of -19.2 ± 3.5 pA at -100 mV **[Figure 0-6** F**]**. Type 2 and 3 pore conductance were consistent with a cylinder with a diameter of about 0.7 nm.

After the assessment of the pore-forming activity, this preparation was studied at a structural level. In a first step, the structural characterization was done using three probes. The mobile methyl from the methionine 35 selectively labelled with ^{13}C ($^{13}CH_3(Met_{35})$-Aβ42) and the $^{15}NH_2$ from the side chains of asparagines and glutamines from U-[^{15}N]-Aβ42 and U-[^{2}H,^{15}N]-Aβ42 **[Figure 0-7** A**]**. For all of them, there was twice as peaks as probes. There were two peaks for the only methionine **[Figure 0-7** B**]** having a different chemical shift than monomeric Aβ42, and 4 doublets of peaks for the two residues, an asparagine and a glutamine **[Figure 0-7** C**]**, the double of expected peaks. This indicated that the Aβ molecules incorporated in the oligomer had two different environments. Further characterization of the oligomer was done by circular dichroism (CD), which showed that it adopted a β-sheet secondary structure **[Figure 0-7** D**]**. This type of secondary structure was further assessed with the fingerprint region of ^{1}H-^{15}N TROSY spectrum of the U-[^{2}H,^{15}N]-Aβ42 oligomer sample **[Figure 0-7** F**]**. A set of peaks were found in the downfield-shifted region and another set in the random coil region. This pattern is characteristic of a protein assembly dominated by β-sheet secondary structure with flexible regions and loops **[Figure 0-7** F**]**. These results pointed out to a β-barrel structure as is the only β-sheet secondary structure found in membrane proteins and compatible with the pore activity in lipid bilayers. This result was further assessed also by hydrogen deuterium exchange (data not shown) and limited proteolysis

experiment **[Figure 0-7** E**]** showing the same pattern of a protected β-sheet structure and an unprotected flexible part. To find additional evidence for a β-barrel arrangement, we analyzed Aβ42 oligomers by SDS-PAGE. The Aβ42 oligomer migrated as a folded protein in SDS-PAGE when the sample was not boiled whereas it appeared as a monomer when the sample was boiled **[Figure 0-7** E**]**. This behavior is also characteristic

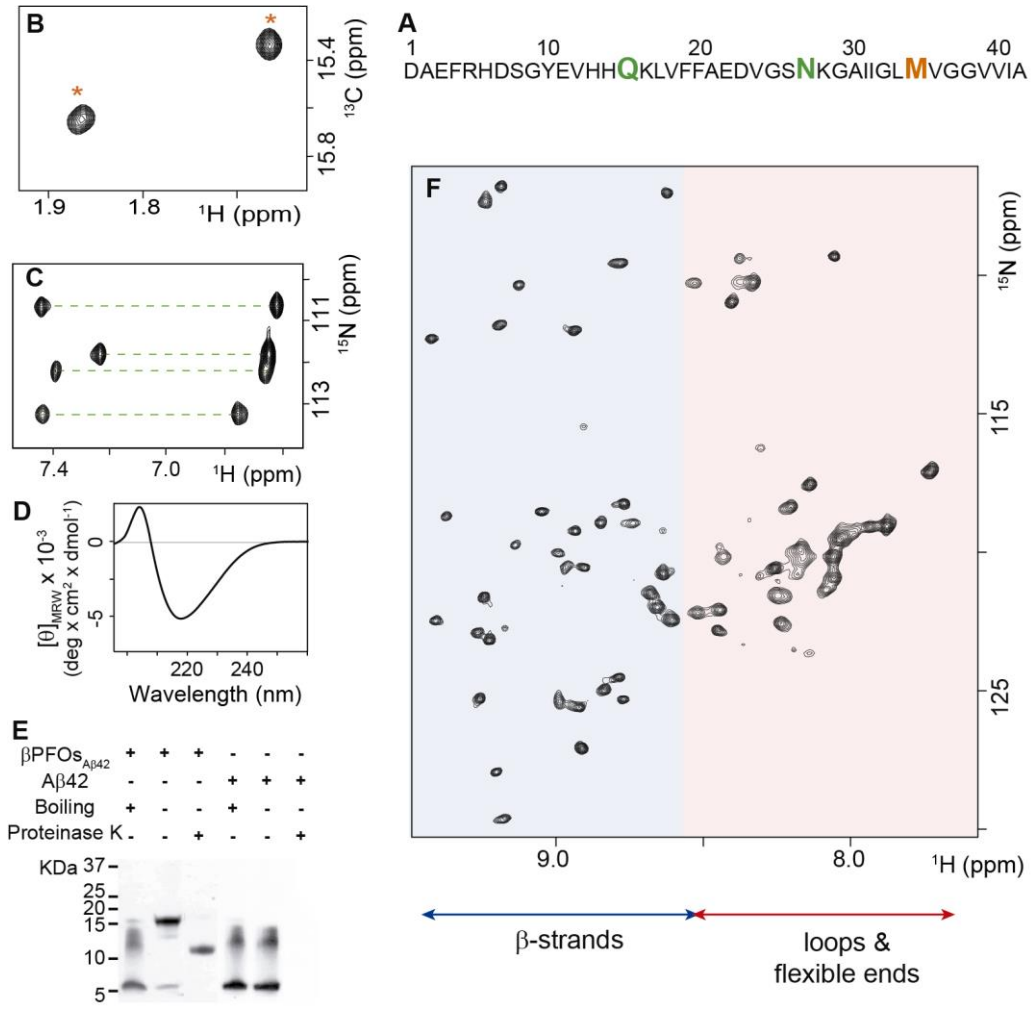

Figure 0-7: Characterization of the Aβ42 oligomer. (A) Aβ42 sequence highlighting probes Gln 15, Asn 27, and Met 35. (B) ^{1}H-^{13}C HMQC NMR spectrum of ^{13}C(Met$_{35}$)-Aβ42 oligomer. (C) Region of ^{1}H-^{15}N HSQC NMR spectra characteristic of the side chain amides of Gln and Asn residues. (D) Far-UV CD characterization of the Aβ42 oligomer. (E) SDS-PAGE analysis of monomeric Aβ42 and the Aβ42 oligomer (βPFO$_{Aβ42}$) samples with and without boiling them and before and after incubation with proteinase K. (F) ^{1}H-^{15}N TROSY-HSQC NMR spectrum of [^{2}H,^{15}N]-Aβ42 oligomer. The peaks clustered in the random coil region (region shown in red) would be attributable to the loops and flexible ends, while the downfield-shifted resonances would correspond to the β-strands of the β-barrel (region shown in blue).

from β-barrel structures[61-62]. Because of all these properties, the oligomer was called **β-barrel Pore Forming Oligomer** (**βPFO**).

βPFO is a good candidate to explain how Aβ contributes to the disease. It can explain how soluble oligomers interact with the lipid membrane and allow calcium entrance in the cell. However, from this work we only knew that βPFO forms in detergent micelles so its relevance in AD was unknown. Even if detergent micelles have been extensively used to study membrane proteins for decades, there are many concerns of whether this system mimics real lipid bilayers well enough.

Throughout this doctoral thesis, we aimed to establish the relevance of βPFO in AD. To this end, we first studied whether βPFO formed in vitro in the presence of more relevant biomimetic membrane environment comprising native lipids. Second, we generated βPFO-conformational specific antibodies to use them in AD human brain tissue samples, AD mouse models or neuronal cell cultures to establish βPFO's relevance in AD.

Ojectives

This thesis had two main objectives:

1. **The study of the β-barrel pore-forming amyloid-β oligomer (βPFO) in a biomimetic membrane environment comprising lipids.**

To accomplish this objective, the following specific goals were proposed:

- Characterize a new type of bicelles composed of DPC and DMPC at low concentrations.
- Establish a protocol for βPFO reconstitution into DPC-DMPC bicelles
- Determine the stability and structure integrity of βPFO reconstituted in DPC-DMPC bicelles

2. **The generation and characterization of conformational specific Nanobodies against βPFO to validate βPFO's relevance in Alzheimer's Disease.**

To accomplish this objective, the following specific goals were proposed:

- Prepare βPFO as a suitable antigen for alpaca immunization
- Select conformational specific Nanobodies against βPFO structure
- Characterize the βPFO-Nanobody interaction

Chapter 1 :
βPFO is stable in a native lipid environment

Context

Around 30% of the genes in humans, E. coli and S. cerevisiae are predicted to code for membrane proteins.[63] In their native state, membrane proteins, are found either totally surrounded or partially embedded within lipid bilayers. They have regions mostly comprising hydrophobic amino acids, which form a hydrophobic surface to which lipids interact through van der Waals interactions. Detergent micelles reach to solubilize membrane proteins upon imitating the hydrophobic core of lipids.[64-65] Even if for many years detergent micelles have been a straightforward way to study membrane proteins, they poorly imitate the native lipid environment in which the membrane proteins are found.[66] Some concerns appears on whether the structure, dynamics and function of membrane proteins are preserved when reconstituted under detergent micelles. For this reason, several biomimetic membrane environment systems have been developed. These include amphipols (APol), liposomes, nanodiscs and bicelles **[Figure 1-1** A, B, C **and** D, **respectively]**.

Amphipols are amphipathic polymers "that can keep membrane proteins water soluble in detergent-free solutions as small individual entities by adsorbing onto their transmembrane surface"[59] **[Figure 1-1** A**]**. They are chemically synthetized upon polymerization of different hydrophilic and hydrophobic moieties conferring them an amphiphilic character, ideal for membrane protein solubilization. After the first publication, more than 20 years ago, validating the A8-35 APol as a good biomimetic membrane environment able to solubilize functional membrane proteins[67] several other APol have been developed. APol are highly soluble in water and they form well defined aggregates hiding the hydrophobic chains as happens with detergent micelles. These APol, once in a detergent solution, they disassemble thanks to the detergent and stick to the hydrophobic core of the membrane proteins. Upon detergent depletion, Apols stay bound to the membrane protein in an irreversible way.

Liposomes, are lipid bilayers closed in the form of spheres **[Figure 1-1** B**]**, where membrane proteins can be integrated. When the target protein is integrated in the bilayer, they are called proteoliposomes. They represent a very good approach to mimic the native environment of membrane proteins, but they also present some problems. First, proteoliposomes, are not soluble and they precipitate upon centrifugation what

make them difficult to separate from protein aggregates. Second, they are not homogeneous in size and therefore not suitable for SEC. Finally, their big size makes them anisotropic and therefore not suitable for solution NMR spectroscopy.

The discovery of the lipid transporter Apoliprotein A-I (ApoA-I),[68] after some improvements, gave place to the use of engineered ApoA-I as membrane scaffold proteins (MSP). MSP adopts a circular shape and upon dimerizing, can enclose a piece of lipid bilayer inside. This strategy gives rise to nanometric lipid bilayers, that are referred to as nanodiscs **[Figure 1-1** C**]** Upon inserting the membrane protein in

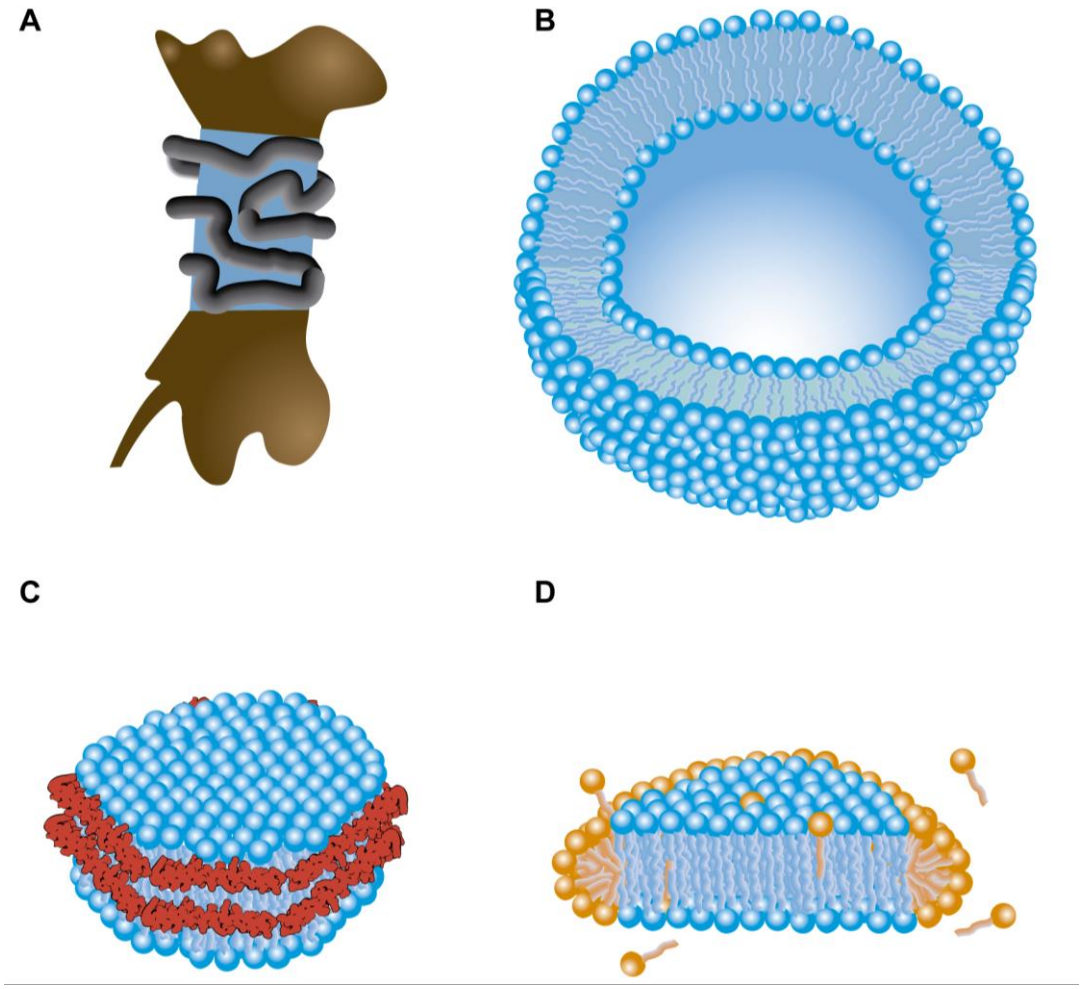

Figure 1-1: Scheme of different biomimetic membrane environment systems. (A) Membrane protein with its (brown) hydrophilic part and (blue) hydrophobic part solubilized by (dark lines) an amphipol. (B) Section of a liposome. (C) Nanodisc with the (blue) lipid bilayer enclosed into the (red) MSP. (D) Bicelle formed by lipids (blue) and detergent (gold).

nanodiscs, the limitations concerning the use of proteoliposomes are overcome keeping the membrane protein in direct contact with natural lipids.[69] However, in order to reconstitute a membrane protein into Nanodiscs, it is first necessary to have the target membrane protein reconstituted in lipid bilayers.

Last but not least, bicelles, are disc-shaped mixtures of lipids and detergents. They are formed by a discoidal lipid bilayer enclosed by a belt of detergent protecting the rims of the bilayer and thus avoiding the hydrophobic tails of the lipids to be water-exposed **[Figure 1-1** D**]**. Depending on their size, bicelles, are used in NMR either as small fast-tumbling isotropic bicelles in solution NMR, or as big slow-tumbling anisotropic bicelles aligned to the magnetic field in solid-state NMR[70]. Membrane proteins can be inserted in the lipid bilayer of the bicelle in order to study them in a lipid environment. Even if some characteristics of the cell membrane as lateral pressure are not kept, the lipid-protein interactions, not found with detergent micelles or amphipols, are.

All those lipid systems can be prepared using either natural lipids extracted from native membranes or with pure synthetic lipids. The use of natural lipid extracts allows us to work with a more native representation of the lipid mixture. However, the exact lipid composition of native bilayer is usually unknown. Consequently, the use of homogeneous synthetic lipids, although less representative compared to the natural lipid mixture in native lipid membranes, it allows us to have a more defined system, which also simplifies its characterization.

From all these biomimetic membrane environments containing lipids, several considerations are relevant to the system under study. Liposomes are not amenable to several techniques such as solution NMR and sample manipulation is more difficult. Nanodiscs require, first to have the protein reconstituted in liposomes. In contrast, bicelles may be prepared starting from the membrane protein reconstituted in detergent micelles.

Bicelles are mainly defined by the type of detergent and lipid used and the ratio between them. The changes in lipid/detergent molar ration or “q” **[Equations** 1**]** regulate the size of the disc. In addition, the magnetic behavior of the bicelles also changes in relation to disc size. The large bicelles, having a q>2.3 and total lipid and detergent concentrations

between 3-60 % w/v, get aligned when placed into a magnetic field with its normal perpendicular to it. This allows to align soluble or membrane proteins in relation to the magnetic field, and therefore, to turn an isotropic system into an anisotropic one. On the contrary, at low q values, most usually in between 0.25 - 0.5, the bicelles formed are isotropic and can tumble in the presence of magnetic fields. [71]

When preparing bicelles, it is very important to take into account that not all detergent molecules in the sample are part of the bicelles' structure. Some of the detergent molecules are soluble monomers in fast exchange with the bicelle bound ones. These monomeric detergent molecules are approximately at the CMC. As these soluble detergent molecules, are not part of the bicelles, the size of the bicelle at the same "q" can change as a function of the bicelle concentration, as a higher or lower percentage of the total detergent will be in the soluble part. The contribution of the soluble detergent, can be negligible when working at high bicelle concentrations. But when working at low bicelle concentrations, the contribution of the soluble detergent increases and it is useful to work with the effective concentration of detergent present in the bicelles ([detergent] – CMC). And using this value get the effective ratio "q_{eff}" **[Equations** 1-2**]**. Since CMC changes with the buffer pH, the ionic strength of the solution and the temperature, working at detergent concentrations near the CMC can be an issue.

Equations 1-2: (1) Molar lipid-detergent ratio and (2) effective molar lipid-detergent ratio.

$$(\mathbf{1}) \quad q = \frac{[lipid]}{[detergent]}$$

$$(\mathbf{2}) \quad q_{eff} = \frac{[lipid]}{[detergent] - CMC} = \frac{[lipid]}{[detergent_{in\ micelles}]}$$

To reconstitute a detergent-solubilized membrane protein into a bicelle there are several strategies. Throughout this work we talk about three of them **[Figure 1-2]**. The **first** strategy is the complete reconstitution **via proteoliposomes**.[72] Starting from a membrane protein reconstituted in a detergent-micelle system different from the target detergent used to form the bicelles. Upon adding the lipids to the sample, doing heat-cold cycles, mixed detergent-lipid micelles are formed. Then detergent is removed to

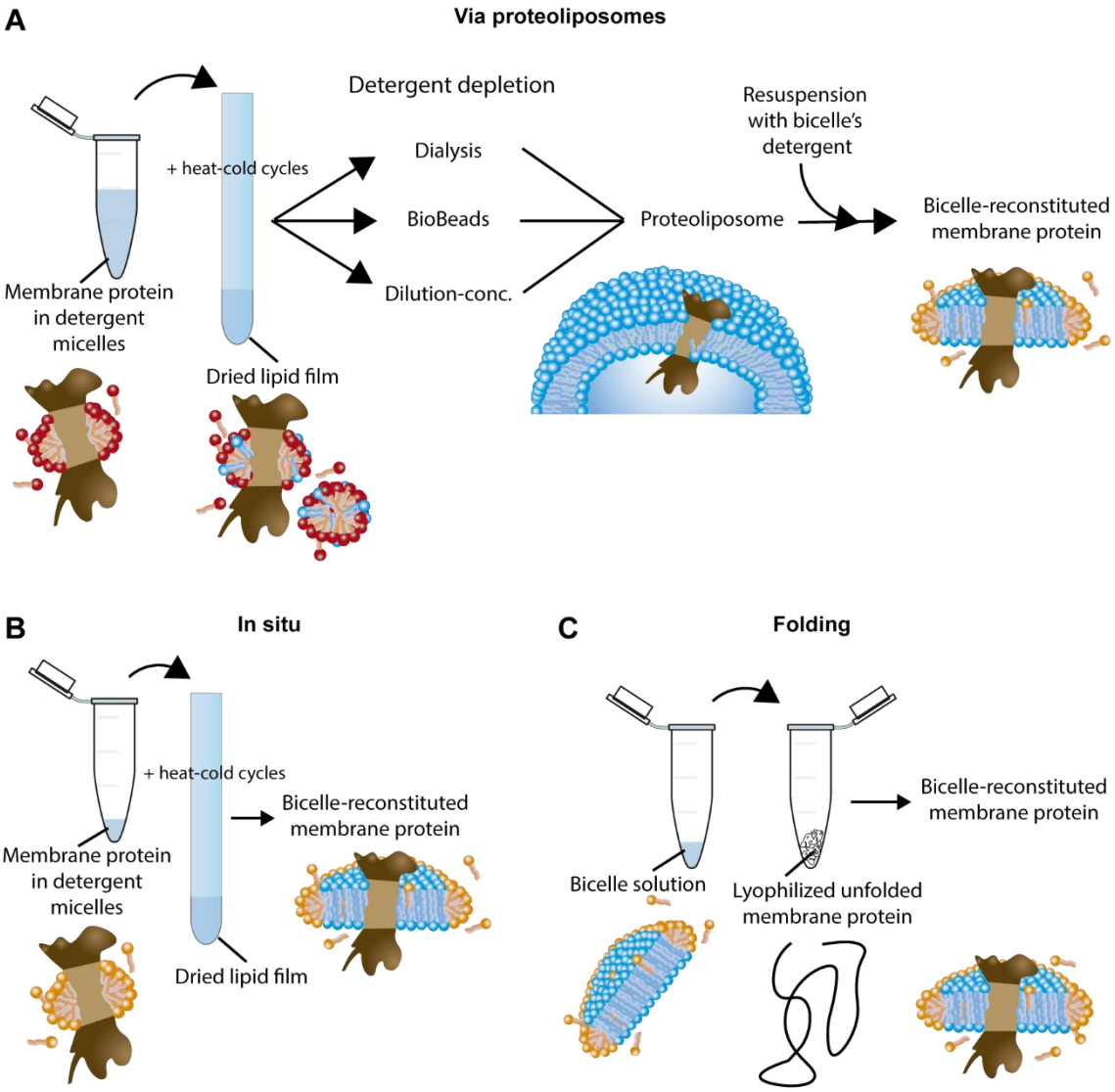

Figure 1-2: Three different strategies followed. (A) Via Proteoliposomes strategy were the lipid is added to the membrane protein making mixed micelles, then the detergent is depleted and the lipids form liposomes with the protein embedded. Bicelles are formed upon dissolving the liposomes with the selected detergent. (B) Directly mix the membrane protein reconstituted in micelles, with the lipids and form the bicelles with heat-cold cycles. (C) Unfolded, lyophilized protein is folded directly into pre-formed bicelles.

form proteoliposomes. Next, proteoliposomes are dissolved with the detergent buffer desired for the bicelles at the right concentration to finally have the target detergent-lipid mixture at the target concentration. The **second** strategy is the ***in situ*** bicelle formation. It consists in having the membrane protein already reconstituted in the detergent micelles used to produce the bicelles. Upon adding the lipids to it and doing some heat-cold cycles, insoluble lipids get solubilized and inserted in the detergent-protein system forming bicelles. The **third** strategy is directly **folding** the protein into

Lipid (PC)	CMC (mM)
5:0	90
6:0	15
7:0	1.4
8:0	0.27
9:0	$2.9 \cdot 10^{-2}$
10:0	$5.0 \cdot 10^{-3}$
12:0	$9.0 \cdot 10^{-5}$
14:0	$6.0 \cdot 10^{-6}$
16:0	$4.6 \cdot 10^{-7}$

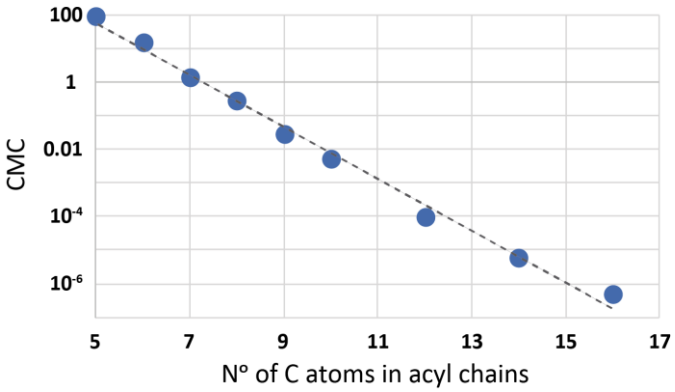

Figure 1-3: CMC change with acyl chain length. In the left, a table with the critical micellar concentration of different saturated phosphatidylcholines taken from Avanti Polar Lipids webpage. In the right the semi-log plot of these CMC values plotted compared to the acyl chain length.

pre-formed bicelles, either upon protein expression with cell-free systems or upon folding denatured proteins.

DHPC together with the long-chain lipid 1,2-dimyristoyl-sn-glycero-phosphatidylcholine (DMPC) can form one of the most used bicelle systems in the literature, the DHPC-DMPC bicelles.[70,73-83] DHPC is a short chain phosphatidylcholine lipid. Short-chain lipids (as well as lysophospholipids) are considered detergents, as they can form micelles and are partly soluble. This is because lipid monomeric solubility, or CMC, decreases exponentially with the elongation of acyl chains **[Figure 1-3]**. In the case of DHPC, the CMC is ~15 mM in pure water. For clarity, in this work, DHPC is treated as a detergent.

In this chapter we study the reconstitution of βPFO in DHPC-DMPC bicelles. Next, we establish a new bicelle system, DPC-DMPC at low concentration, not defined up to date. Finally, we reconstituted βPFO in this new bicelle system to assess its stability in a native lipid environment.

Results

βPFO is not stable in DHPC-DMPC bicelles

To determine whether the oligomer is inserted in bicelles, we used Aβ42 peptide with a carbon-13 label incorporated into the methyl group of the methionine side chain ($^{13}CH_3$(Met$_{35}$)-Aβ42). This labelling simplifies the spectra and allows us to easily

distinguish the type of assembly adopted by Aβ42 in the conditions under study (i.e. random coil monomers, oligomers, higher aggregates not visible by solution NMR, etc.).

In order to insert βPFO in a bicellar system, we chose the common DHPC-DMPC mixture. We studied βPFO reconstitution in this system. The first option was to reconstitute βPFO pre-formed in DPC micelles, into DHPC-DMPC bicelles with the first strategy, **via proteoliposomes**[72]. The detergent depletion step of this strategy was too harsh for our system. When depletion was done with BioBeads, a commercial detergent absorbent, after centrifugation of the detergent-depleted sample, a gel appeared instead of the expected lipid pellet. Upon resuspending the precipitate with DHPC, no signal was found by solution NMR (data not shown). So, this gel was most probably formed by Aβ42 fibrils. When the detergent depletion was done by dilution-concentration cycles or by dialysis,

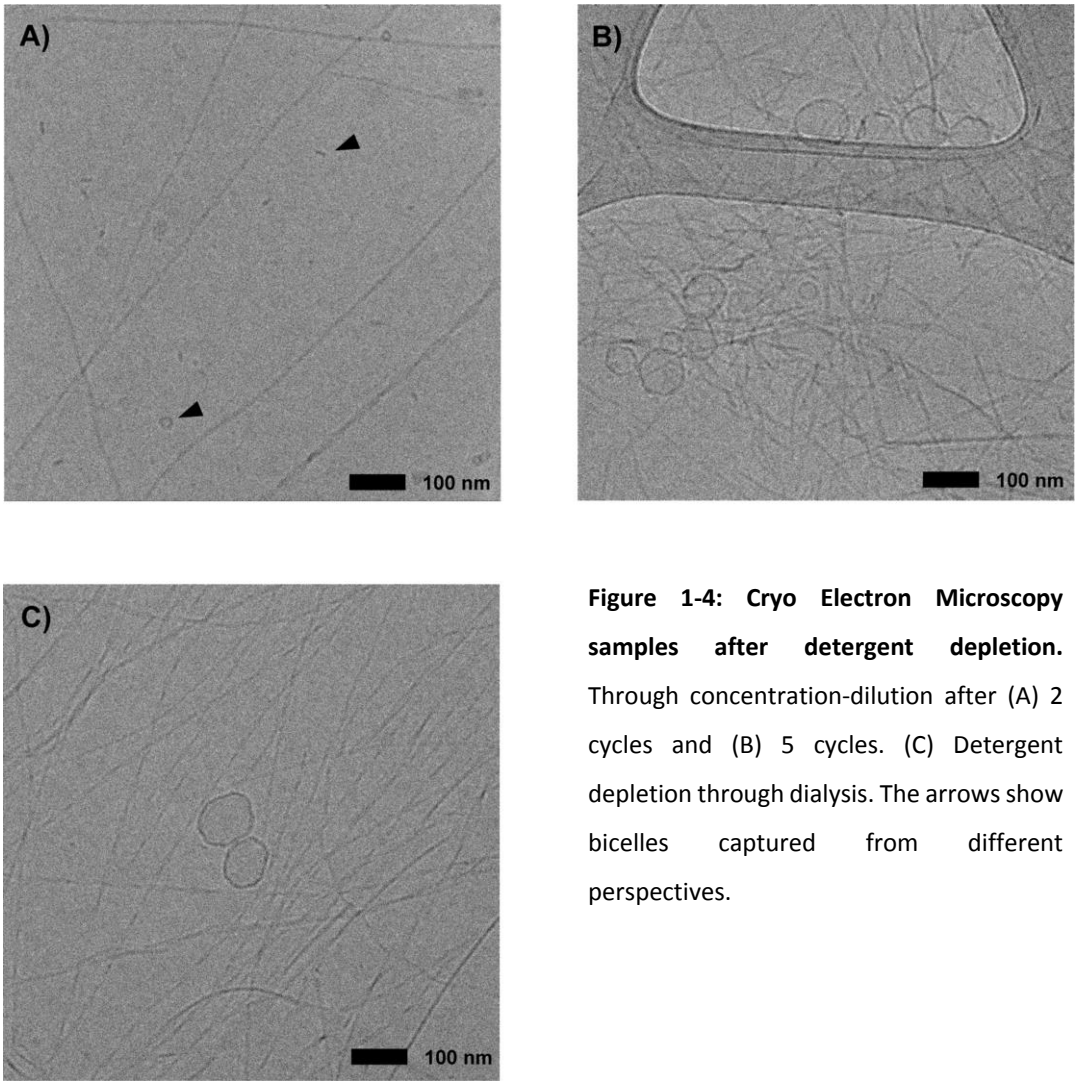

Figure 1-4: Cryo Electron Microscopy samples after detergent depletion. Through concentration-dilution after (A) 2 cycles and (B) 5 cycles. (C) Detergent depletion through dialysis. The arrows show bicelles captured from different perspectives.

also amyloid fibrils were formed in large amounts as seen by Cryo-Electron Microscopy (CryoEM) **[Figure 1-4** B **and** C **respectively]**.

Then we continued with the reconstitution using the second strategy of ***in situ*** bicelle formation. For this, we studied whether Aβ42 was able to fold and form βPFO using DHPC micelles. We incubated $^{13}CH_3(Met_{35})$-Aβ42 peptide in the presence of DHPC at 37 ºC inside the magnet to analyze the formation of βPFO as a function of time. At time 0 h, a low intensity peak characteristic from the monomer (at 14.43 ppm in the ^{13}C axis) appeared together with a wide and very low intensity signal in the oligomer region (between 14.8 and 15.0 ppm in the ^{13}C axis) **[Figure 1-5** A**]**. However, the putative signals assigned to an oligomer progressively disappeared with the time **[Figure 1-5** B**]**. These results indicate that something too large to be detected by solution NMR was formed. These results matched SEC results designed to assess βPFO formation in DHPC where we could detect the formation of larger aggregates appearing at the void volume after 24h incubation **[Figure 1-5** E**]**.

Next, we studied whether Aβ42 was able to fold into pre-formed DHPC-DMPC bicelles within the **folding** strategy. Even if the folding in DHPC did not lead to the formation of βPFO, we studied if the presence of the native lipid DMPC might confer a supplementary folding ability. We firstly made DHPC-DMPC bicelles by directly mixing DMPC and DHPC dissolved in chloroform and drying them together. Bicelles were prepared at a q = 0.33. The ratio was determined upon integration of the methyl peaks of both, DHPC and DMPC. Using this strategy, the heat-cold cycles used in the lipid insertion of the via liposomes strategy is not required as the lipid and the detergent are already well-mixed with the co-solubilization. We added 2% w/v of bicelles to lyophilized $^{13}CH_3(Met_{35})$-Aβ42. Folding on bicelles was monitored at 37 ºC in the magnet analyzing ^{1}H-^{13}C HMQC spectra as a function of time. Again, a low intensity peak corresponding to monomer was detected as well as a low intensity wide peak in the zone of the oligomer. Both disappeared as a function of time **[Figure 1-5** C-D**]**. This result shows that even with the presence of DMPC that might have stabilized the oligomer, DHPC causes Aβ42 to rapidly aggregate. Consequently, DHPC was discarded as detergent to make bicelles for βPFO reconstitution.

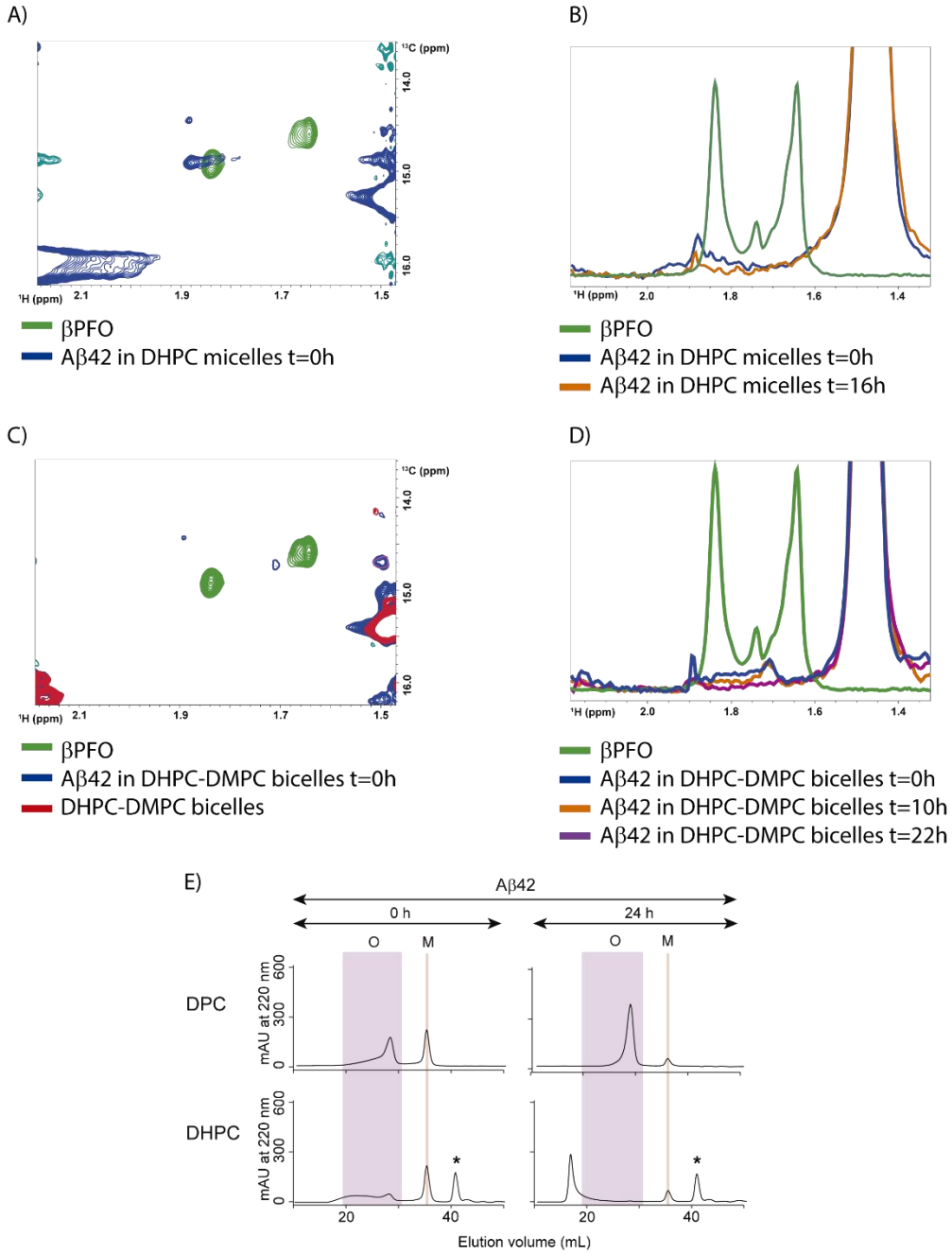

Figure 1-5: Aβ42 oligomer formation in DHPC micelles and DHPC-DMPC bicelles monitored by NMR and SEC. (A blue) 2D ^{1}H-^{13}C HMQC spectra of Aβ42 resuspended with DHPC micelles at time 0 h. (B blue) Projection of ^{1}H-^{13}C HMQC spectra of Aβ42 resuspended with DHPC micelles at time 0h and (B orange) t=16 h. (C blue) 2D ^{1}H-^{13}C HMQC spectra of Aβ42 with DHPC-DMPC bicelles at time 0 h and (C red) of bicelles without peptide. (D blue) Projection of ^{1}H-^{13}C HMQC spectra of Aβ42 with DHPC-DMPC bicelles at time 0 h, (D orange) t=10 h and (D purple) t=22 h. (A and C green) The typical 2D ^{1}H-^{13}C HMQC signal or (B and D green) projection of $^{13}CH_3(Met_{35})$-βPFO represented to show the region where oligomer is expected to appear. SEC of (E top) Aβ42 incubated at 37 °C in DPC or (E bottom) DHPC at (E left) t=0 h and (E right) at t=24h. Chromatogram was recorded at 220 nm. (E orange line) The monomer retention time was found out upon analyzing SDS incubated Aβ40. The (E purple area) oligomer region was set between the void volume peak and the (E orange line) monomer peak. The * peak appeared also when analyzing DHPC solution without protein may correspond to DHPC micelle elution because of ester bond absorbance.

DPC-DMPC can form bicelles

As just shown, detergent depletion step from the first strategy, via proteoliposomes, promoted protein aggregation. For this reason, we studied whether the **in situ** bicelle formation with βPFO in micelles and the Aβ42 **folding** in bicelles was produced when using its own DPC together with DMPC. However, the DPC-DMPC bicelle system had only previously been established to prepare large anisotropic bicelles for solid-state NMR[84] or isotropic bicelles at high concentrations.[80]

As DPC-DMPC bicelles at low concentrations were not previously characterized, we studied whether this mixture produced isotropic bicelles or not. The main technique used to characterize DHPC-DMPC bicelles was ^{31}P NMR analysis. As both, DHPC and

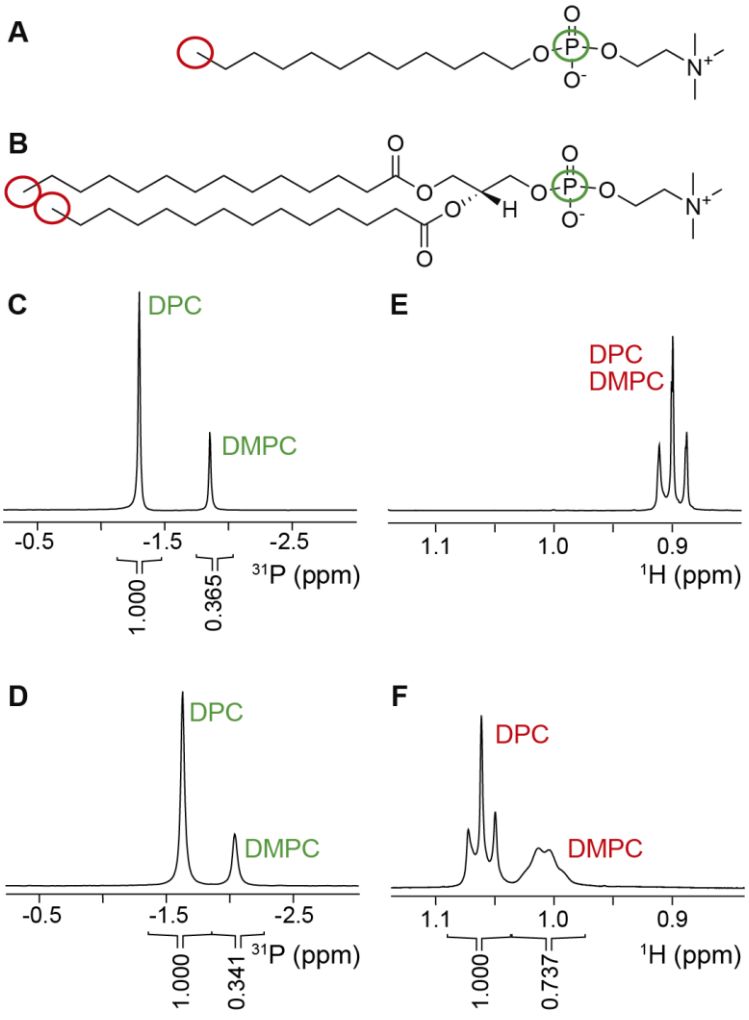

Figure 1-6: DPC-DMPC bicelle formation monitored by NMR. Structures of (A) DPC and (B) DMPC molecules with the (red circle) ω-methyl and the (green circle) phosphorous labelled. ^{31}P spectra of the bicelle system in (C) d_4-methanol and (D)D_2O. ^{1}H spectra of the bicelle system in (E) d_4-methanol and (F) D_2O.

DMPC, have an identical polar head they have an indistinguishable ^{31}P chemical shift when solubilized with organic solvents. However, when forming bicelles, peaks split showing the two different environments, the one in the bilayer and the one in the rim.[73] However, phosphorous resonances of DPC and DMPC have different connectivity with the alkyl chains **[Figure 1-6** A-B**]** and consequently have a different magnetic environment already when dissolved in methanol **[Figure 1-6** C**]**. This difference would difficult interpretation of ^{31}P changes in chemical shifts associated to bicelle formation **[Figure 1-6** D**]**. Instead, ^{1}H signals from ω-methyl distinct between DHPC and DMPC, are indistinguishable between DPC and DMPC when solubilized in methanol **[Figure 1-6** E**]**. In agreement with the fact that both, detergent and lipid, experience different magnetic environments in bicelles, by showing that these indistinguishable peaks become distinguishable in a DPC-DMPC bicelle's sample **[Figure 1-6** F**]**, we assessed that in these conditions DPC-DMPC bicelles were formed.

As βPFO needs a defined [micelle]:[Aβ42] ratio, working with high bicelle concentration would imply a big amount of Aβ42. But the lower the bicelle concentration is, the lower is the part of the detergent forming bicelles and the harder is to control the real q_{eff}. To know at which bicelle concentration could we work, we analyzed DPC-DMPC bicelles at different concentrations by ^{31}P NMR **[Figure 1-7** A**]**. The analysis of the chemical shift of the DPC shows a shift with the bicelle concentration. As soluble DPC and bicelle-bound

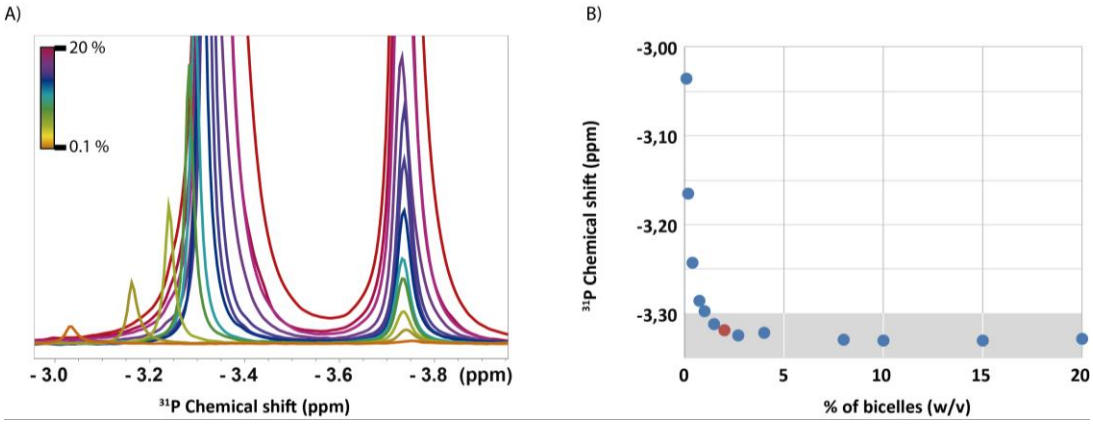

Figure 1-7: Bicelles at different concentrations. (A) Overlaid NMR spectra from different bicelle concentrations, each one indicated by a different color. DPC peak from -3.1 to -3.4 ppm and DMPC peak at 3.74 ppm. (B) Plot of the changes in DPC chemical shift as a function of the bicelle percentage. Grey area limits the chosen threshold, red dot is the 2 % w/v.

DPC are in fast exchange, the chemical shift of DPC is the average of both populations. We selected 1 % w/v of DPC-DMPC bicelles as a safe threshold to work as long as DPC chemical shift is not far from its chemical shift at high bicelle concentrations. At lower concentrations, q_{eff} could be unpredictable **[Figure 1-7** B**]**. Therefore, as the concentration of detergent micelles regulates the concentration of peptide required to form βPFO, we chose 2 % w/v of bicelles as a good bicelle concentration to have the peptide concentrated enough for NMR studies (> 1 mM). We therefore, assessed the formation of bicelles at 2 % w/v and at q = 0.33.

βPFO is inserted in DPC-DMPC bicelles

To assess that βPFO was inserted into the DPC-DMPC bicelles, we focused on the different size that micelles and bicelles have. Bicelles are quite larger than micelles as they have both, the protein and the micelle (as a rim), but also the discoidal bilayer. So, a way to assess the insertion of βPFO into bicelles is to analyze the hydrodynamic radius of both proteins. In this sense, we studied the effective rotational correlation time (τ_c) of both, βPFO in micelles and βPFO in bicelles, through 1D [^{15}N,^{1}H]-TROSY for rotational correlation times (TRACT) experiments. By only using the signals from the structured amides, the rotational correlation time of folded proteins correlates with the hydrodynamic radius increasing as a function of size. Usually, it also correlates to a good approximation with the molecular weight[85].

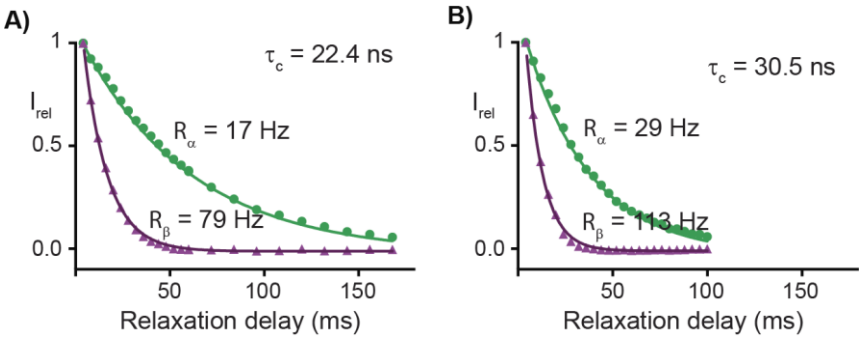

Figure 1-8: Curves resulting from TRACT experiment of βPFO. Decay curve of the two ^{15}N spins from 1D [^{15}N,^{1}H]-TRACT experiments. The two systems are represented, in (A) DPC micelles and in (B) DPC-DMPC bicelles. The (green) upper and (purple) lower curves correspond to the slowly relaxing α-spin state of ^{15}N and the more rapidly relaxing β-spin state, respectively. Exponential fits (solid lines) yielded relaxation rates of α- and β-spin states (R_α and R_β) used for τ_c estimation. Experiments were recorded at 37 °C.

After the analysis of the data, a τ_c value is obtained for each sample **[Figure 1-8]**. We got a significantly longer τ_c for the bicelles rather than for the micelles meaning that the system containing these signals was bigger. Thus, it confirmed the insertion of βPFO into DPC-DMPC bicelles.

βPFO is stable and keeps its overall structural and functional properties in DPC-DMPC bicelles

To determine whether βPFO reconstituted in bicelles kept their overall structure, we proceeded to analyze the samples using a range of structural strategies previously used to characterize βPFO in micelles. We showed that βPFO in bicelles had the same pattern of resistance to proteolysis than βPFO in micelles by using limited proteolysis and analyzing the samples by SDS-PAGE. In the same way than βPFO in micelles, after limited proteolysis by proteinase K, βPFO in bicelles was not completely proteolyzed but its overall size was partially diminished **[Figure 1-9** A**]**. Next, we used the three NMR probes that we also used in βPFO characterization in micelle. The ^{13}C-labelled methyl of methionine 35 (M) and the $^{15}NH_2$ side-chain of glutamine 15 (Q) and asparagine 27 (N) [**Figure 1-9** D**].** We compared the ^{1}H-^{13}C HMQC of $^{13}CH_3$(Met$_{35}$)-βPFO in bicelles and in micelles **[Figure 1-9** B**]**, what showed a slight shift in both proton and carbon axis and a

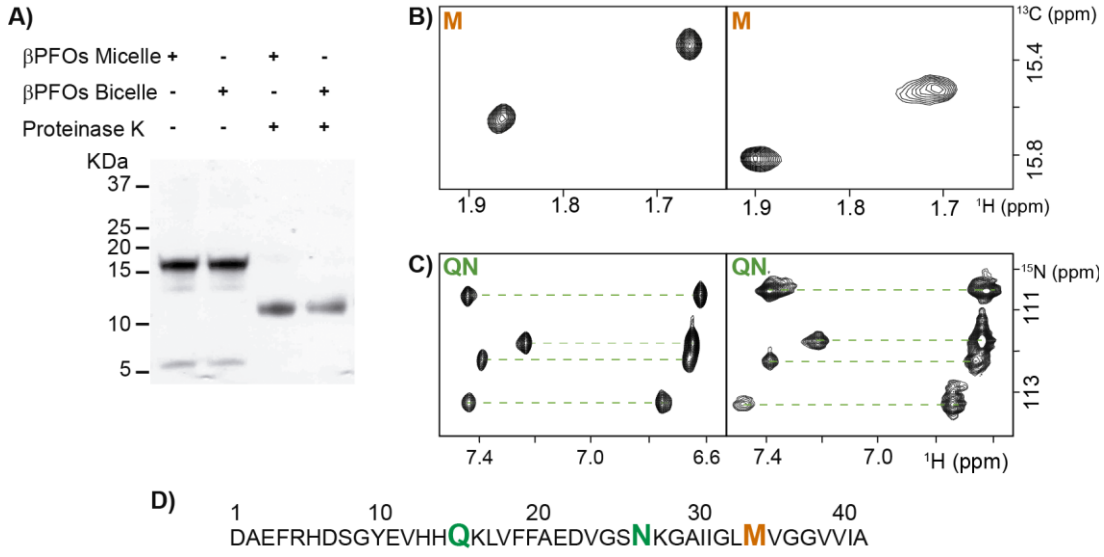

Figure 1-9: βPFO properties change between micelle and bicelle samples. (A) Limited proteolysis of βPFO in micelles and in bicelles analyzed by SDS-PAGE. (B) 2D ^{1}H-^{13}C HMQC spectra of ^{13}C(Met$_{35}$)-βPFO (left) in micelles and (right) in bicelles. (C) Window of the side chain region (Q and N) of 2D ^{1}H-^{15}N HSQC spectra of [^{15}N]-βPFO (left) in micelles and (right) in bicelles. (D) Aβ42 amino acid sequence with the three probes colored.

peak widening in the βPFO in bicelle's sample. The latter effect was consistent with the longer relaxation time of the βPFO in bicelle. Alternatively, asparagines and glutamines were detected through ^{1}H-^{15}N HSQC. They did not show any differences in chemical shifts in the micelle sample compared to the bicelle one. As expected, asparagines and glutamines also showed peak widening in the bicelle sample **[Figure 1-9** C**]**. All of them showed two different environments, a feature characteristic of βPFO. ^{1}H-^{13}C HMQC was also used to monitor βPFO stability as a function of time in bicelles. The $^{13}CH_3(Met_{35})$-βPFO in bicelles was completely stable for 3 days at 37 °C. It did only lose 30 % and 50 % of its signal after 12 days and 3 weeks at 37 °C respectively (stability evaluation on peak height).

In addition, to provide additional evidences on βPFO structure in bicelles, ^{1}H-^{15}N HSQC of U-[^{15}N,^{13}C,^{2}H]-βPFO was analyzed. Amide backbones did not show significant changes in chemical shifts. The number of peaks and their positions were approximately the same as those found in the micelle sample, but with much wider signals **[Figure 1-10** A-B**]**. By comparing, we can observe that data quality is reduced when βPFO is in bicelles

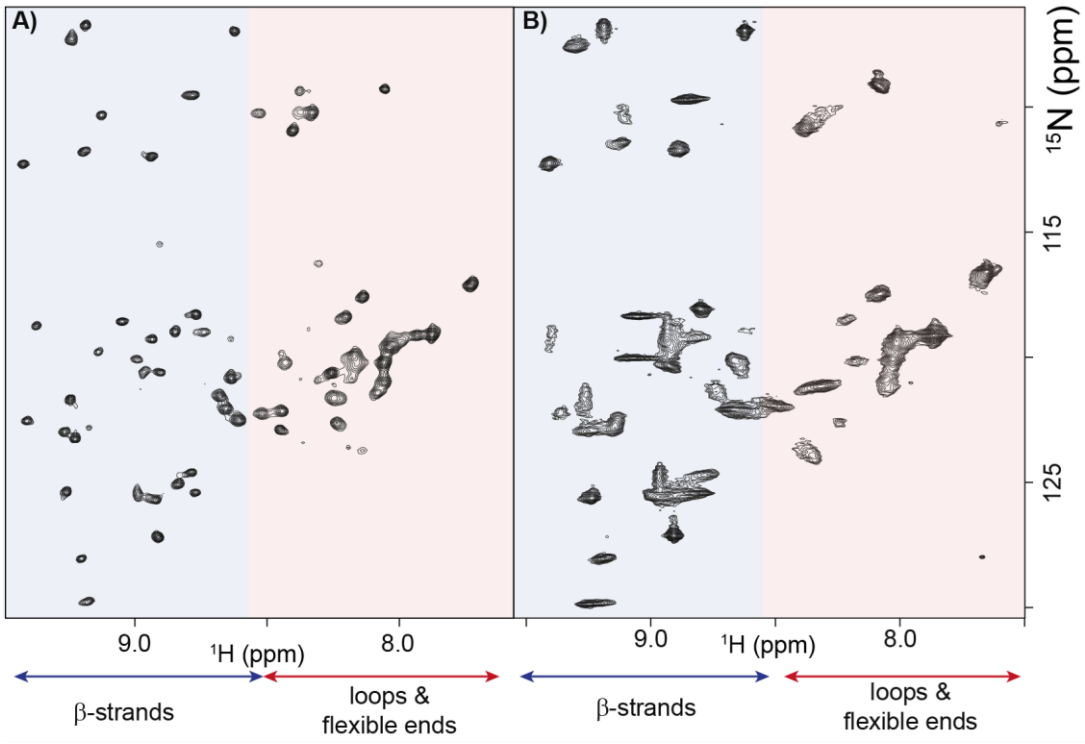

Figure 1-10: Amide region of 2D ^{1}H-^{15}N HSQC spectra of U-[^{15}N,^{2}H] βPFO (A) in micelles and (B) in bicelles. 2D spectra is divided in two parts, (blue) the β-strand region and (red) the flexible regions.

but also that we can affirm that βPFO structure is mainly preserved when inserted in DPC-DMPC bicelles and thus that βPFO is stable in native lipid environments.

To verify whether the pore function was also kept when βPFO was inserted in bicelles, we analyzed the bicelle sample using electrical recording in Planar Lipid Bilayers in collaboration with Mariam Bayoumi and Dr. Giovanni Maglia from the University of Gröningen. βPFO reconstituted in DPC-DMPC bicelles incorporated into diphytanoyl-sn-glycero-3-phosphocholine planar lipid bilayers in the same manner that βPFO in micelles. βPFO in bicelles also formed three different types of pores as βPFO in micelles and approximately in the same proportions. Type 1 had fast and noisy transitions with undefined open pore conductance values **[Figure 1-11** A**]**. Type 2 had a quite well-defined conductance but still noisy **[Figure 1-11** A**]**. Type 3 had a well-defined open-pore conductance with no fluctuation **[Figure 1-11** A**]**. The pores of type 2 and 3 formed by βPFO in bicelles showed a slightly higher average conductance than the ones in micelles **[Figure 1-11** B**]**.

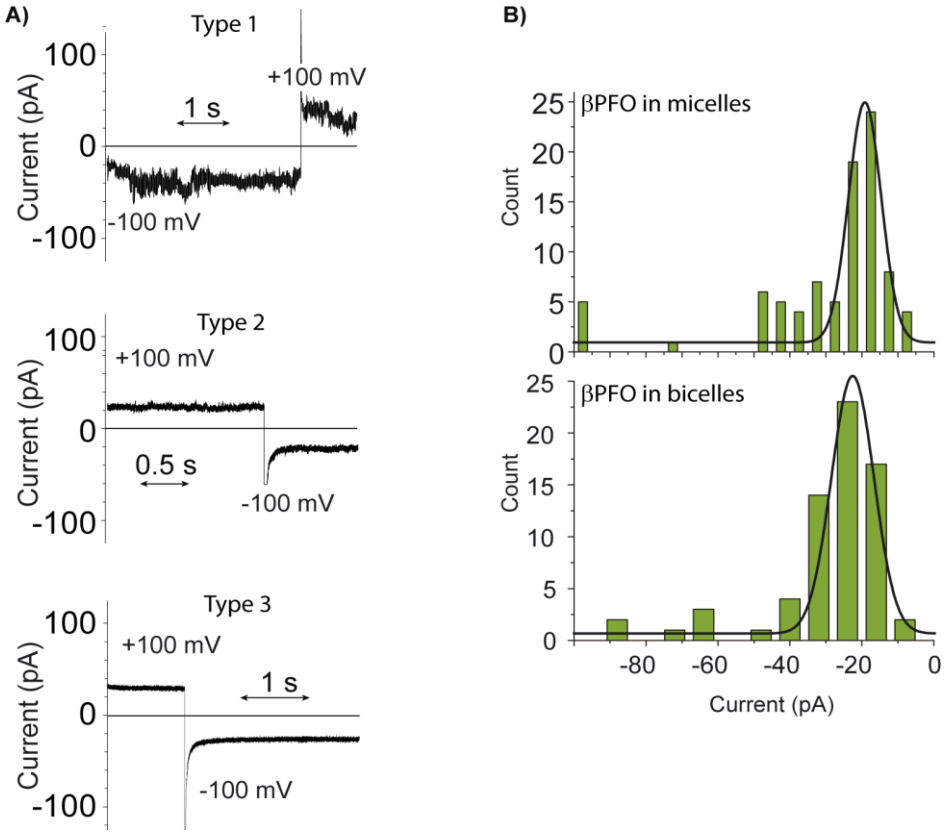

Figure 1-11: Electrical recordings of βPFO in bicelles and Aβ42 folding in bicelles. (A) Three types of pores found when analyzing the βPFO in DPC-DMPC bicelles in electrical recordings on planar lipid bilayers. (B) Comparison between the conductivities shown by βPFO in micelles and βPFO in bicelles.

We have demonstrated that βPFO was reconstituted in DPC-DMPC bicelles and that it conserved βPFO's overall structure and all the properties found in βPFO in micelles.

βPFO can be directly formed and is stable in DPC-DMPC bicelles

Finally, the third strategy of protein insertion into bicelles through **folding** was also used. Bicelles were produced at 2 % w/v. After the heat-cold cycles, we used the pre-formed bicelles to resuspend the $^{13}CH_3$(Met$_{35}$)-Aβ42 peptide and we incubated the sample at 37 °C in the magnet. The sample was analyzed along the time by ^{1}H-^{13}C HMQC for a week. One of the peaks corresponding to one of the environments was already formed in the first experiment. The other peak appeared progressively. After 1.5 days peaks arrived to its maximum but the mid-peaks continued to disappear progressively until the last analysis **[Figure 1-12]**.

We, therefore, showed that Aβ42 can be directly folded into DPC-DMPC bicelles giving the same ^{1}H-^{13}C HMQC signal than for reconstitution of βPFO in bicelles. The environment around 1.9 ppm was immediately formed while the one at 2.05 ppm was

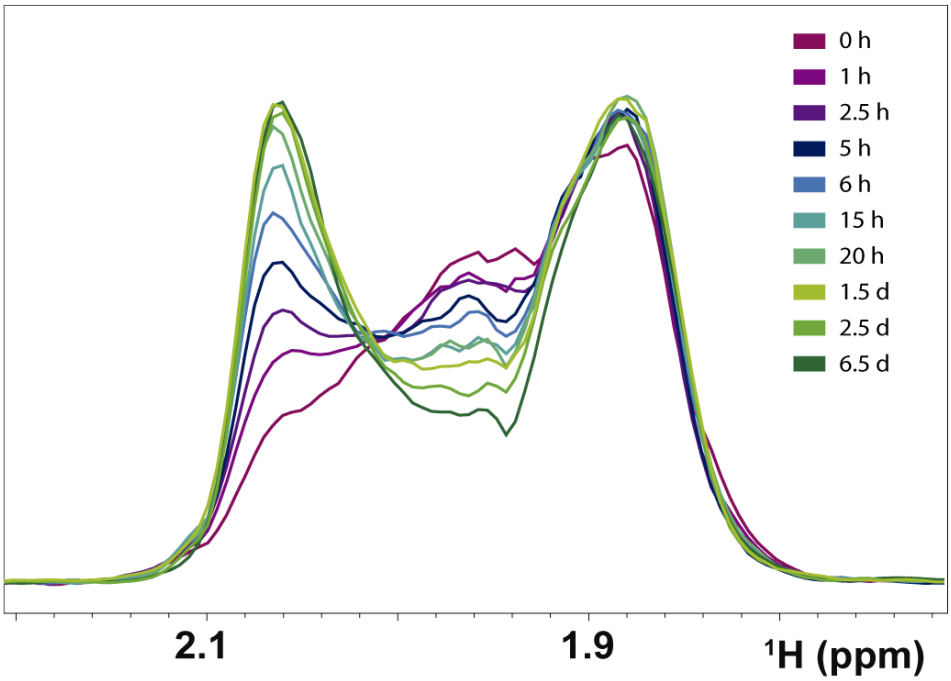

Figure 1-12: Folding of Aβ42 on DPC-DMPC bicelles. Overlay of projections of 2D ^{1}H-^{13}C HMQC of the folding of Aβ42 in DPC-DMPC bicelles along the time incubated and analyzed at 37°C.

formed after incubation. The two environments characteristics of βPFO were completely formed after 1.5 days at 37°C and its intensity was unchanged after almost 6.5 days. So, we demonstrated that DPC-DMPC bicelles is an excellent system for βPFO.

Discussion

In this chapter we showed that βPFO can be inserted, formed and is stable in a lipid environment.

We first showed that the common DHPC-DMPC bicelle system was not compatible with βPFO formation as DHPC promoted Aβ42 aggregation. Other researchers, studied the effect of DHPC on Aβ40 aggregation obtaining conflicting results. Either Aβ40 fibrillization was inhibited by DHPC[86] or it was promoted.[87] Here, we showed that DHPC made Aβ42 to aggregate in large aggregates not detectable by solution NMR. In view of the results, we developed a new isotropic bicelle system based on DPC-DMPC at low concentrations. Other authors showed the bicelle formation at high concentrations[80] and at an anisotropic q.[84] However, no one used them at the same conditions we required, to our knowledge, before our description of these DPC-DMPC bicelles[60]. Recently another paper appeared using isotropic DPC-DMPC bicelles for membrane protein study.[88] Next, we demonstrated that βPFO were inserted in the bicelle by TRACT experiments. The overall correlation time (τ_c) of βPFO at 37 °C was 22.4 ns in micelles and 30.5 ns in bicelles. These values are consistent with previously reported τ_c for the Outer membrane protein X (OmpX), an 18-kDa β-barrel protein reconstituted in DHPC micelles (τ_c = 21–24 ns measured at 30 °C)[85] and DHPC-DMPC bicelles (τ_c = 35 ns measured with q = 0.5, at 30 °C)[73] and are in complete agreement with the fact that bicelles are larger than micelles. Moreover, we established this βPFO preparation in bicelles was stable for several days at 37 °C.

We also proved that the structure of βPFO in bicelles was preserved with the three side-chains probes: methionine, glutamine and asparagine. Using these probes, we could see the two environments characteristics from βPFO. Furthermore, βPFO in bicelles, had the same degree of protection to proteolysis than βPFO in micelles. Finally, to stablish structure similarity, we showed by ^{1}H-^{15}N HSQC that the footprint of βPFO in micelles

and in bicelles is similar with few shifts and that peaks were wider in the case of bicelles as biomimetic environment, what is consistent with its bigger size.

Finally, we showed that βPFO in bicelle had the same functional pore activity than βPFO in micelle by planar lipid bilayer electrical recording. Having optimized the DPC-DMPC bicelle system we also showed that Aβ42 was able to fold in the form of βPFO directly on the bicelles and that was stable for several days at 37 ºC.

For long time the research in Aβ oligomers focused in soluble oligomers. However, membrane implication in the disease pushed researchers towards the membrane-bound oligomers. Lal and coworkers showed that Aβ42 could be reconstituted into lipid bilayers and that was able to form pores.[53] Disregarding the controversy of the use of chloroform to solubilize Aβ42, which apparently is not able to solubilize Aβ42[89], they obtained a signal in electrical recordings in planar lipid bilayers that they adjudge to Aβ42 pores. Also, they showed good AFM images consistent with pore formation. Alternatively, using Aβ40 Korshavn and coworkers showed that upon zwitterionic liposome binding, Aβ40 took a defined α-helical structure. They proposed this structure as a first intermediate of the interaction of Aβ40 with lipids leading to the antiparallel ionic pore oligomer.[90] Alternatively, also with Aβ40, Bhowmik and coworkers developed the SERS system in which they studied Aβ40 attached to lipid coated nanoparticles.[91] With this study using Aβ40 they found that Aβ was forming a β-strand, turn, β-strand with an antiparallel arrangement characteristic from the toxic oligomers allowing a “porin” like β-barrel structure.[49]

In conclusion, this work is a step forward in the discovery of the neurotoxic form of Aβ in neurons. Up to now, βPFO was characterized in detergent micelles, which is not an environment that can be found in brain. Now we have successfully shown that βPFO can form and insert in DPC-DMPC bicelles, demonstrating that βPFO can be formed and is stable into a lipid environment, and thus reinforcing it as a potential new target for AD.

Materials & Methods

Reagents

Lipids and detergents were purchased from Avanti Polar Lipids or Affymetrix-Anatrace. Deuterated reagents were purchased from Cambridge Isotope Laboratories except deuterated dimyristoyl-sn-glycero-3-phosphocholine (d_{54}-DMPC) that was purchased from Cortecnet and deuterium oxide (D_2O) that was purchased from Euriso-top. All other reagents were supplied by Sigma-Aldrich unless otherwise stated.

Recombinant Expression of Aβ42

For both, ^{15}N-Aβ42 and [^{2}H,^{15}N]-Aβ42, the recombinant expression was done as published[92] using auto-induction and M9 minimal media respectively.

Stock solutions. For the U-[^{15}N] Aβ42, the 20x ^{15}N-NPS and 50x 5052 solutions were prepared as previously described[93]. Briefly, the 20x ^{15}N-NPS solution contained 142 g Na_2HPO_4, 136 g KH_2PO_4, 50 g $^{15}NH_4Cl$ and 14.2 g Na_2SO_4 per L and the 50x 5052 solution contained 250 g glycerol, 25 g D-glucose and 100 g α-lactose per L. The 500x trace metal solution was also prepared based on previous descriptions with small adjustments[94]. Briefly, 1 L of 500x trace metal solution contained 8 mL 5 M HCl, 5 g $FeCl_2{\cdot}4H_2O$, 184 mg $CaCl_2{\cdot}2H_2O$, 64 mg H_3BO_3, 18 mg $CoCl_2{\cdot}6H_2O$, 4 mg $CuCl_2{\cdot}2H_2O$, 340 mg $ZnCl_2$, 605 mg $Na_2MoO_4{\cdot}2H_2O$, and 40 mg $MnCl_2{\cdot}4H_2O$. These three solutions were heat-sterilized and stored at room temperature until use. The 100x vitamin solution was prepared by dissolving 50 mg thiamine hydrochloride, 10 mg D-biotin, 10 mg choline chloride, 10 mg folic acid, 10 mg niacin, 10 mg pantothenic acid, 10 mg pyridoxal, and 1 mg riboflavin in 100 mL MilliQ water. This solution was sterilized using a 0.2 µm filter, wrapped in aluminum foil, and stored at -20°C until use.

For the U-[^{2}H,^{15}N] Aβ42 various stock solutions were required: the 30x salt solution was prepared as a 50-mL aliquot of D_2O containing 10.2 g anhydrous Na_2HPO_4, 4.5 g anhydrous KH_2PO_4, 0.75 g NaCl and 0.37 g $MgSO_4$; the 100x vitamin solution and the 500x trace metal solution were prepared as detailed above using D_2O instead of H_2O.

Media solutions. For the production of U-[^{15}N] Aβ42, ^{15}N-labeled P-5052 medium for auto-induction was prepared from 2 mL of 1 M $MgSO_4$ solution, 50 mL of the 20x ^{15}N-

NPS, 20 mL of the 50x 5052, 2 mL of the 500x trace metal solution and 916 mL heat-sterilized MilliQ water. The resulting medium was heat-sterilized and subsequently 10 mL of the previously filtered 100x vitamin solution was added to it.

For the U-[^{2}H,^{15}N] Aβ42, M9 minimal media was prepared from 33.3 mL of the 30x salt solution, 10 mL of the 100x vitamin solution, 1 g NH_4Cl, and 4 g D-glucose and brought to 1 L with 50% H_2O/50% D_2O or 100% D_2O for the pre-cultures. For the final culture, 1 g $^{15}NH_4Cl$ and 2 g D-glucose were added in 100% D_2O. The resulting solutions were sterilized by filtering them through a 0.2-µm filter. Afterwards, 2 mL of heat-sterilized 500x trace metal solution were freeze-dried, resuspended in D_2O and finally added to each of them.

Protein expression. Rosetta (DE3) pLysS *E. coli* cells (Novagen) were transformed with the expression vector and grown overnight at 37°C on Luria Bertani (LB)-agar plates containing 1% glucose. All cell cultures were also supplemented with 35 µg/mL chloramphenicol and 50 µg/mL kanamycin.

For U-[^{15}N] Aβ42, single colonies were picked and grown overnight in 2 x 12.5 mL LB, 1% glucose. The pre-cultures were centrifuged at 3,000 *g* for 10 min at 25°C. Each pellet was transferred to 0.5 L ^{15}N-labeled P-5052 auto-inducing media with the appropriate antibiotics using a 3-L Erlenmeyer flask. The resulting cultures were grown for 6 h at 37°C and 180 rpm. The temperature was then lowered to 25°C, and the culture was incubated 22 h more at 180 rpm. The cells were then harvested by centrifugation at 9,000 *g* for 15 min at 4°C and then frozen at -80°C.

For U-[^{2}H,^{15}N] Aβ42 expression, single colonies were picked and grown overnight in 4 x 3 mL LB, 1% glucose. The LB pre-cultures were centrifuged at 3,000 *g* for 10 min at 25°C. The pellets were then transferred to 120 mL M9 medium, containing 50% H_2O/50 % D_2O and the corresponding antibiotics. The 50% D_2O pre-culture was grown for 7 h at 37°C and centrifuged at 2,000 *g* for 20 min. The pellet was re-suspended and inoculated in 240 mL M9 medium in 100% D_2O. The 100% D_2O pre-culture was grown overnight. The next morning, the pre-culture was centrifuged at 2,000 *g* for 20 min, and the pellet was re-suspended and inoculated in 1 L M9 100% D_2O medium, containing 1 g/L $^{15}NH_4Cl$ and 2 g/L D-glucose. The culture was grown at 37°C and 180 rpm and induced at OD_{600} ~0.8

by the addition of IPTG to a final concentration of 0.5 mM. After further growth for 3 h, the cells were harvested by centrifugation at 9,000 *g* for 15 min at 4°C and then frozen at -80°C.

Purification of recombinant Aβ42

Cell lysis. The cell pellet was resuspended in 6 mL buffer A (300 mM NaCl, 50 mM sodium phosphate, 20 mM imidazole, 1% Tween-20 and 1 mM tris(2-carboxyethyl)phosphine (TCEP) pH 8.0), supplemented with half a pill of ethylenediaminetetraacetic acid (EDTA)-free Complete protease inhibitor (Roche) and 1 mg DNAse (Roche) per g of cells, supplemented with 1 EDTA-free Complete protease inhibitor pill (Roche) and 1 spatula of DNAse (Roche) per 50 mL of buffer. The resuspended cells were lysed using a cell disruptor (Constant Systems Ltd. U.K.) operating at 20,000 psi. The cell extract was then centrifuged at 30,000 *g* for 30 min at 4ºC, the supernatant filtered using a 0.45 µm and subsequently purified by IMAC.

IMAC. The supernatant was loaded at 1 mL/min onto a HisTrap HP 5-mL Ni column (GE Healthcare), which was previously equilibrated with 5 column volumes of buffer A. After the loading step, the resin was washed with buffer B (300 mM NaCl, 50 mM sodium phosphate, 40 mM imidazole, 0.05% Tween-20 and 1 mM TCEP pH 8.0) for 10-15 column volumes, until UV absorbance was stable. An amount of fusion protein without the Aβ42 sequence was also produced. It was independently eluted at 2-5 mL/min using the following 3-step elution method: (a) a 15 mL linear gradient from 0 to 15% of buffer C (300 mM NaCl, 50 mM sodium phosphate, 500 mM imidazole, 0.05% Tween-20 and 1 mM TCEP pH 8.0), followed by (b) a 20 mL isocratic step at 15% buffer C and (c) a second isocratic step at 100% buffer C until UV absorbance was stable **[Figure 1-13]**.

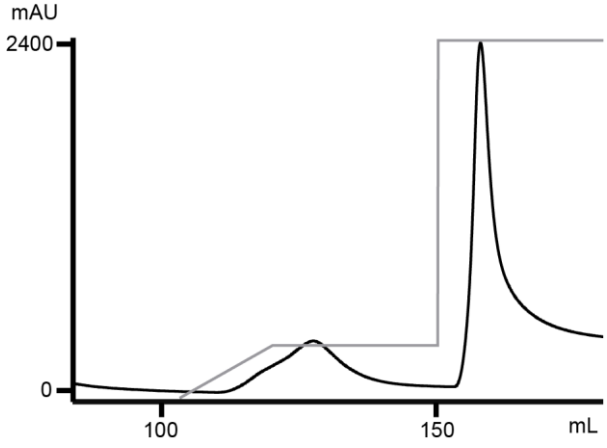

Figure 1-13: Typical chromatogram from IMAC purification of recombinant Aβ42. In grey the 3-stepped gradient of buffer B. In black the absorbance at 280nm. At around 125 mL appears the SUMO peak separately from the SUMO-Aβ42.

Fusion protein removal. IMAC fractions were analyzed by sodium dodecyl sulfate polyacrylamide gel electrophoresis (SDS-PAGE), and those containing the fusion protein were pooled in batches of 10 mL. Subsequently, buffer was exchanged using a HiPrep 26/10 desalting column (GE Healthcare) equilibrated with 50 mM ammonium carbonate and 1 mM TCEP. Afterwards, the concentration and purity of protein was determined by nanodrop and RP-HPLC, respectively. Afterwards, to cleave Aβ42 from the SUMO fusion tag, samples were incubated overnight at 4 °C with SUMO protease[95] in a 1:50 protease:protein ratio. The concentration of Aβ42 peptide after the cleavage was determined by RP-HPLC analysis.

SEC Purification. Subsequently, aliquots containing 3.75 mg Aβ42 were prepared and freeze-dried. Each of these aliquots was solubilized with 6.8 M guanidinium thiocyanate (GdnSCN) to 2.5 mg Aβ42/mL and sonicated for 5 min in an ice bath. Afterwards, the sample was further diluted with MilliQ water to 1.5 mg Aβ42/mL and 4 M GdnSCN, and centrifuged at 10,000 g for 6 min at 4 °C. Finally, 2.5 mL of the 1.5 mg Aβ42/mL was injected into a HiLoad Superdex 30 prep grade column (GE Healthcare), previously equilibrated with 50 mM ammonium carbonate, and eluted at 4°C at a flow rate of 1 mL/min. The peaks corresponding to SUMO and monomeric Aβ42 were collected separately and their purity and concentration were determined by RP-HPLC. Both pools were freeze-dried, and the Aβ42 pool was subjected to the same GdnSCN solubilization

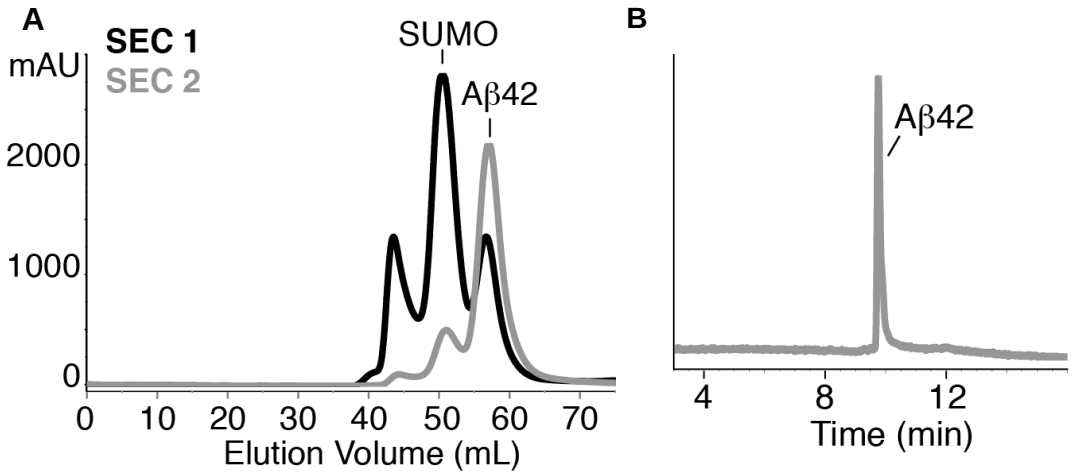

Figure 1-14: Typical SEC purification of recombinant Aβ42. (A) The typical (black) first and (grey) second SEC chromatograms were the first peak is formed by high molecular weight aggregates, the second peak is formed by SUMO and the third peak is formed by Aβ42. (B) The HPLC chromatogram of the purified Aβ42.

protocol and SEC fractionation, as described. Pure Aβ42 was obtained after the two SEC steps **[Figure 1-14]**. It was then aliquoted in the desired amounts, freeze-dried, and kept at -20ºC until use.

Preparation of monomeric Aβ42 from peptide synthesis

Aβ42, and $^{13}CH_3$(Met$_{35}$)-Aβ42 were synthesized and purified by Dr. James I. Elliott (New Haven, CT, USA). Pure ^{15}N-Aβ42 and [^{2}H,^{15}N]-Aβ42 were obtained by recombinant expression and purification as just described. Independently of the labels of the Aβ peptide under study, monomeric Aβ42 was obtained using SEC. Aβ42 peptide was dissolved in 6.8 M Gdn·SCN (Life Technologies) at 8.5 mg/mL, sonicated for 5 min, and diluted to 5 mg/mL of peptide and 4 M Gdn·SCN with H_2O. It was then centrifuged at 10,000 g for 6 min at 4 °C and passed through a 0.45-µm Millex filter (Millipore). The resulting Aβ42 solution was injected into either a HiLoad Superdex 75 prep grade column (GE Healthcare) or a HiLoad Superdex 30 prep grade column (GE Healthcare). The columns were equilibrated with 50 mM ammonium carbonate and eluted at 4°C at a flow rate of 1 mL/min. The peak attributed to monomeric Aβ42 was collected and its peptide concentration was determined by High Performance Liquid Chromatography coupled to Photodiode Array Detector (HPLC-PDA). Aliquots with the desired amount of peptide were prepared, freeze-dried, and kept at -20 °C until use for reconstitution into detergent micelles.

Quantification of Aβ42 peptide

The concentration of monomeric Aβ42 was determined by HPLC-PDA (Waters Alliance 2695 equipped with 2998 photodiode array detector). HPLC-PDA analysis was done using a Symmetry 300 C4 column (4.6 × 150 mm, 5 µm, 300 Å; Waters) at a flow rate of 1 ml/min and a linear gradient from 0 to 60 % B in 15 min (A = 0.045 % trifluoroacetic acid (TFA) in water, and B = 0.036 % TFA in acetonitrile) at 60 °C. A calibration curve was generated based on Aβ42 solutions that had previously been quantified by amino acid analysis.

Preparation of βPFO in micelles

DPC micelles. Freeze-dried monomeric Aβ42 peptide was dissolved in 50 mM ammonium carbonate at a concentration of 15 mM and immediately diluted to 150 µM

with 10 mM Tris·HCl pH 9.0 containing the appropriate concentration of DPC to reach 1:0.5 [Aβ]:[micelle]. The [micelle] is the difference between the detergent concentration ([D]) and its CMC divided by its aggregation number (i.e. ([D]-CMC)/aggregation number). At an [Aβ] of 150 µM, the concentration of DPC required to achieve [Aβ]/[MDPC] ratios of 1:0.5 (low micelle conditions) was 5.5 mM DPC. The CMC of DPC was taken to be 1.5 mM[56] [96] and the DPC aggregation number 54[96].

DHPC micelles. βPFO in DHPC micelles was prepared in the same way as described for DPC micelles but, with different detergent concentration. For the SEC **[Figure 1-5** E**]**, the ratio [Aβ]:[micelle] was 1:0.5 and thus, DHPC concentration was 17 mM. For the bicelle-formation samples **[Figure 1-5** A-B**]** the concentration of DHPC was 25 mM.

Reconstitution of βPFO in DHPC-DMPC bicelles via proteoliposomes

A βPFO sample in micelles was produced at high concentration (1.7 mM Aβ42, 47.4 mM DPC 10 mM Tris pH 9) and incubated for 24h at 37°C. In two different glass tubes, 5.11 mg of DHPC in chloroform and 2.65 mg of DMPC in chloroform were dried under N_2 flow while rolling the tube to make a lipid film around the glass walls. A low N_2 flow was let overnight to eliminate chloroform traces. On the same glass tube, 250 µL were used to resuspend the DMPC. Three heat-cold cycles were performed (4°C - 40°C). Samples were diluted 6.5-fold for the detergent depletion step that was carried out through three different techniques.

Bio Beads. To 500 µL of the diluted samples, 125 mg of Bio Beads (BioRad) were added and sample was incubated in a roller for 1h. Then Bio Beads were changed for new ones and sample was incubated overnight. Then Bio Beads were changed again for new ones and sample cas incubated 1h.

Figure 1-15: Sketch of the cut Eppendorf and the dialysis foil. The sample was added in the cap and then the circle was closed on the cap trapping the dialysis foil in the middle.

Dyalisis. The reservoir of a 5 mL Eppendorf LoBind is cut just leaving the cap and the circle to close it

[Figure 1-15]. Then, 500 µL of the diluted sample are inserted in a 5 ml Eppendorf cap and pre-hydrated "Biotech RC Dialysis" membrane (Spectra/Por SpectrumLabs) is trapped between the cap and the circle that encloses the system. With this system, sample was dialyzed against 3 x 1 L of 10 mM Tris Buffer pH 9.

Concentration-dilution. 500 µL of sample were concentrated using Vivaspin 500 of 3 kDa MWCO and then diluted with 10 mM Tris buffer pH 9. Five concentration-dilution cycles were performed and presence of DPC was checked by ^{31}P NMR. Proteoliposomes were monitored with CryoEM.

Reconstitution of βPFO in DPC-DMPC bicelles in situ

First, $^{13}CH_3$(Met$_{35}$)-βPFO was produced in micelles upon resuspending $^{13}CH_3$(Met$_{35}$)-Aβ42 with 47.4 mM d_{38}-DPC, 9 mM d_{11}-Tris, 1 mM Tris, 100 % D_2O pH* 8.6 at 1.7 mM peptide concentration. Sample was incubated in a shigemi tube for 24h at 37 ºC. DMPC dissolved in chloroform was dried under nitrogen flow in a glass tube upon rolling it. Slight nitrogen flow was let pas overnight to avoid chloroform traces. Next, the βPFO sample was used to resuspend the lipid film formed in the glass tube vortexing. Heat-cold cycles were performed putting the sample at 40 ºC for 5 min, on ice for 5 min, then vortexed and centrifugated. If pellet appeared the process was repeated after vortexing. Usually three to five cycles were enough.

The U-[^{15}N,^{2}H]-βPFO was produced by resuspending U-[^{15}N,^{2}H]-Aβ42 with 34.8 mM d_{38}-DPC, 9 mM d_{11}-Tris, 1 mM Tris, 10 % D_2O, pH 9.0. Sample was directly incubated in the magnet to detect βPFO formation. In the form of powder, d_{54}-DMPC was added to the sample. Heat- cold cycles were performed as previously described.

Folding of βPFO in bicelles

Bicelles were formed by directly mixing the detergent with the lipid in chloroform in at q = 0.33 drying them together as previously explained. In the case of DHPC-DMPC bicelles, samples were produced at 150 µM $^{13}CH_3$(Met$_{35}$)-Aβ42, 2% bicelles and 10 mM Tris buffer pH 7.4. In the case of DPC-DMPC bicelles, samples were produced at 1.23 mM $^{13}CH_3$(Met$_{35}$)-Aβ42, 2% bicelles and 10 mM Tris buffer pH 9. Heat-cold cycles were not required.

SEC

A control sample corresponding to monomeric Aβ was prepared by dissolving freeze-dried Aβ40 (Aβ40 was prepared in the same way as described for Aβ42) in 50 mM ammonium carbonate at a concentration of 15 mM and immediately diluting it to 150 µM with 10 mM Tris·HCl pH 7.4 containing 46.4 mM SDS ([Aβ]/[micelle] ratio of 1:4.7). These conditions are reported in the literature to lead to a monomeric Aβ solution adopting an α-helix.[58] Also samples of Aβ42 reconstituted into DPC and DHPC micelles at ratio 1:0.5 [Aβ]:[micelle] were prepared as described previously. Samples of 100 µL were loaded onto tandem Superdex 200 Increase-Superdex 200 HR 10/300 columns (GE Healthcare). The columns were equilibrated with 0.36 mM DDM, 10 mM Tris·HCl, and 100 mM NaCl at pH 7.4. SEC was carried out at 4°C at a flow rate of 0.5 ml/min, and monitored at 220 and 280 nm. Samples were first passed through 0.45-µm filters (Millipore) to remove any insoluble aggregates. Control monomeric Aβ40 sample was analyzed immediately after being prepared. Aβ40 and Aβ42 samples reconstituted into detergent micelles were analyzed before and after incubation at 37°C for 24 h.

NMR spectroscopy

HMQC. ^{1}H-^{13}C HMQC spectra were recorded for $^{13}CH_3$(Met$_{35}$)-βPFO prepared in d_{38}-DPC micelles (1.2 mM Aβ42 concentration) and for $^{13}CH_3$(Met$_{35}$)-βPFO reconstituted in d_{38}-DPC-d_{54}-DMPC bicelles (1.2 mM Aβ42 concentration) in 100% D_2O, 9 mM d_{12}-Tris·DCl, 1 mM Tris·DCl at pH* 8.6. Unless otherwise stated, the spectral window used to acquire these spectra was 5 ppm (^{1}H dimension) and 9 ppm (^{13}C dimension).

HSQC. ^{1}H-^{15}N HSQC and ^{1}H-^{15}N TROSY-HSQC spectra were recorded, using pulse sequences in which evolution of water magnetization is carefully controlled so the intensity of the amide protons is affected only by their intrinsic relaxation times and not by the slowly relaxing water protons, for ^{2}H,^{15}N βPFO prepared in d_{38}-DPC micelles (1.2 mM Aβ42 concentration) and for ^{2}H,^{15}N βPFO reconstituted in d_{38}-DPC-d_{54}-DMPC bicelles (1.2 mM Aβ42 concentration) in 90% H_2O/10% D_2O, 9 mM d_{12}-Tris·DCl, 1 mM Tris·DCl at pH 9.0. These samples were also used to determine the rotational correlation time of βPFO in micelles and bicelles using the 1D [^{15}N, ^{1}H]-TRACT pulse scheme[85]. All measurements were carried out at 37 °C on a Bruker 600 MHz or a 800 MHz

spectrometer equipped with a cryogenic probe head. All data were processed and analyzed using TopSpin software from Bruker.

1D spectra. ^{31}P and ^{1}H spectra were recorded for a 2 % DPC-DMPC bicelle sample (11.5 mM and 34.8 mM, DMPC and DPC, respectively) in 100% D_2O 9 mM d_{12}-Tris·DCl, 1 mM Tris·DCl at pH* 8.6 and for a DPC-DMPC mixture prepared at the same concentration and dissolved in methanol-d4. Also 20% DPC-DMPC bicelles at q = 0.33 together with their subsequent dilutions were analyzed by ^{31}P spectra. The spectral window used to acquire ^{31}P and ^{1}H spectra were 159.53 and 9 ppm, respectively. A trimethyl phosphine/acetoned6 (TMP) inset in D2O was used as external reference for ^{31}P experiments. All measurements were carried out at 37°C on a Bruker 600 MHz. All data were processed and analyzed using TopSpin software from Bruker.

CryoEM

CryoEM grids were prepared by Electron Microscopy facility staff with two different conditions, CDD Acquire and vitrobot. The best images were obtained using the vitrobot condition. Samples were read on a Tecnai F20 (FEI Company) with *field emission gun* of 200 kV.

Limited proteolysis

Proteinase K from tritirachium album was added to βPFO prepared in DPC micelles at pH 9.0 (1.2 mM Aβ42 concentration), and to βPFO reconstituted in DPC-DMPC bicelles (1.2 mM Aβ42 concentration) at a protease:Aβ42 molar ratio of 1:20 (proteinase K). After incubating the samples for 45 min at 37 °C, the protease was inhibited by adding the serine protease inhibitor 4-(2-Aminoethyl)benzenesulfonyl fluoride hydrochloride (AEBSF). They were then diluted to 30 µM Aβ42 concentration with 10 mM Tris·HCl and 1.5 mM DPC at pH 9.0 and analyzed by SDS-PAGE without boiling.

Electrical recordings with planar lipid bilayers

Electrical recordings with planar lipid bilayers were performed in the university of Leuven by our collaborators as previously described.[60] Ionic currents were measured from planar bilayers formed from diphytanoyl-snglycero-3-phosphocholine in 10 mM Tris·HCl and 150 mM NaCl at pH 7.5 and 23 °C applying a 2 kHz low-pass Bassel filter with a 10 kHz sampling rate. Potentials were applied, and the current was recorded using

Ag/AgCl electrodes connected to a patchclamp amplifier (Axopatch 200B, Axon Instruments). Current recordings were analyzed using the Clampfit 10 software package (Molecular devices). Open-pore currents were measured by a Gaussian fit to all point histogram. The center of the peak corresponds to the open-pore conductance and the width at half height to the error. Each electrophysiology chamber contained 500 µL 10 mM Tris·HCl and 150 mM NaCl at pH 7.5. Two samples were analyzed, βPFO (150 µM Aβ42 concentration) that was diluted from 1:250 to 1:100 in the chamber; N>40 and βPFO reconstituted in DPC-DMPC bicelles (1.2 mM Aβ42 concentration) that was diluted 1:500 in the chamber; N>20. For βPFO in micelles, type 1, 2 and 3 were observed in 17%, 48% and 35% of the experiments (N=105). For βPFO reconstituted in DPC-DMPC bicelles, Type 1, 2, and 3 were observed in about 17.5%, 44.4%, and 38.1% of the experiments (N=74). Type 2 and type 3 conductance showed an average open pore current of –27.5 ± 1.7 pA at -100 mV **[Figure 1-11]**. Controls were carried out to establish that the concentration of the detergent micelles presents in the samples did not affect the stability of the bilayer.

Chapter 2 :
Generation of specific anti-βPFO Nanobodies

Context

βPFO is a membrane associated Aβ42 oligomer that our group found out that was able to form pores in lipid membranes[60]. This *in vitro* generated Aβ42 oligomer could then be responsible for calcium dysregulation in neurons[38,97-98] and thus be the paramount Aβ specie responsible for AD neurotoxicity. However, we need a specific antibody or probe that allow us to establish that βPFO is formed *in vivo*. This probe needs to be conformational-specific against βPFO to distinguish it from the different Aβ42 forms present in the brain such as monomers, fibrils, soluble oligomers and other membrane oligomers.

Antibodies are proteins produced by the B cells of the immune system and are developed to bind specifically certain antigens. This binding specificity makes antibodies good probes. However, antibodies are very big (~150 kDa), difficult and expensive to produce. Alternative systems using antibody fragments have been proposed and used, like antibody binding fragment (Fab), variable domains of Fab (Fv) and single chain Fv (scFv). However, these fragments have less affinity compared to the entire antibodies. Moreover, antibodies in general recognize a specific sequence of amino acids, what makes them not good to distinguish between different forms of the same protein.[99]

In 1993, it was discovered that all the *camelidae* family comprising camels, dromedaries, lamas, alpacas, etc. had a different class of antibodies apart from conventional antibodies.[100] It was found that these new antibodies lacked the light chain. This new type of antibodies devoid of light chain were called Heavy Chain Antibodies (HCAb) **[Figure 2-1** middle**]** and were not found in the rest of mammal families. In conventional antibodies, the paratope recognizing the antigen is formed by both variable domains from the heavy chain and from the light chain (V_H and V_L respectively) **[Figure 2-1** left**]**. On the contrary, the paratope in HCAb is only found in the variable domain of the heavy chain of the HCAb (V_HH). As V_HH domain has no contacts with other domains of the antibody, it is formed by single sequence and has complete antigen-recognition capacity, it can be easily produced separately from the rest of the HCAb. This domain, when it is produced alone is referred to as Nanobody **[Figure 2-1** right**]**.[99] Nanobodies have many properties that make them very interesting compared to conventional antibodies. Nanobodies are easily generated and produced, they usually have a good

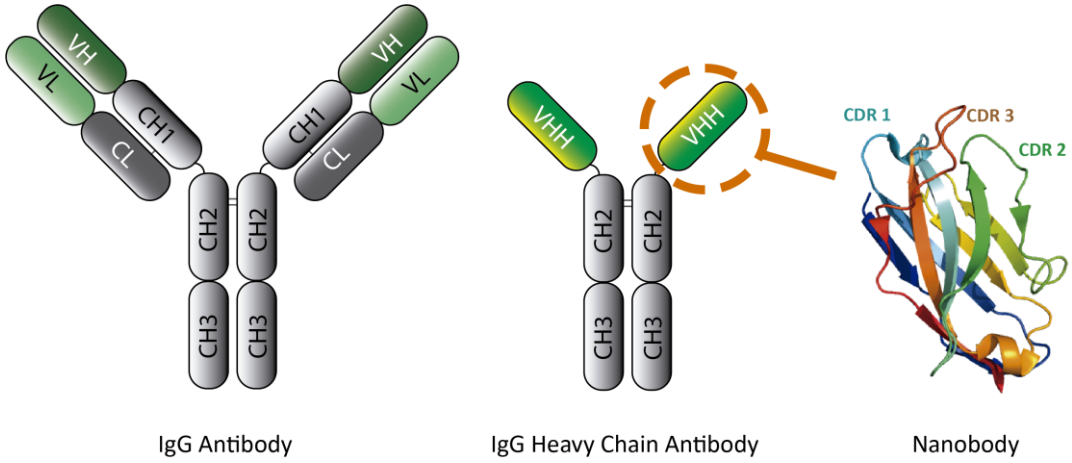

Figure 2-1: Schematic representation of the conventional IgG Antibody, the Camelian IgG Heavy Chain Antibody (HCAb) and a Nanobody. (left) Conventional IgG antibodies are formed by two heavy chains, linked to each other through two or more disulfide bridges, and two light chains each linked through a disulfide bound to a heavy chain. The heavy chain is formed by three conserved domains (C_H1, C_H2 and C_H3) and the variable domain (V_H), the antigen recognition domain. The light chain is formed by a conserved domain (C_L) and a variable domain (V_L), also recognizing the antigen. (middle) HCAb only have two heavy chains linked to each other through two or more disulfide bonds. The heavy chain is formed by only two conserved domains (C_H2 and C_H3) and a variable domain (V_HH). (right) The V_HH domain is stable and functional by its own, therefore, when produced alone it is called Nanobody. Here 2X10 Nanobody against Gesolin is shown as an example.[4]

antigen affinity, they are soluble because of the lack of contacts with other domains, they are very stable to both denaturizing conditions and proteases, and they are non-immunogenic. All these properties open the door to their therapeutic use in humans.

Regarding their structural properties, Nanobodies are formed by two faced β-sheets usually bound by a cysteine bridge, thus, they are very small in size (~15 KDa). The sequence of the β-strands is conserved for each specie while the sequence of three of the loops is completely variable for every Nanobody. This is due to the fact that these variable loops are the responsible for antigen binding, therefore, they are referred to as complementary-determining region (CDR).[101] In the case of conventional antibodies, there are 3 CDR in the V_L domain and 3 CDR more in the V_H domain **[Figure 2-1** left**]**. On the contrary, V_HH only have 3 CDR for antigen binding. However, the third one, CDR3, tends to be much longer than in V_H. Also, it tends to adopt a defined structure upon binding, producing a gain in enthalpy that compensate the lack of CDRs from the V_L. Moreover, the longer CDR3 tends to recognize cavities and active sites from enzymes.

The latter makes Nanobodies better at binding conformational epitopes than conventional antibodies. We envisioned that the ability of Nanobodies to recognize cavities could be very appropriate for selectively targeting of βPFO.

In this work we have generated 11 different Nanobodies specific against βPFO structure. Specificity was assessed against βPFO, Aβ42 monomers and Aβ42 fibrils. The βPFO-Nanobody interaction was characterized by limited proteolysis (LP) and planar lipid bilayer electric recordings. Through these techniques we demonstrated the βPFO-Nanobody interaction at the molecular level and that the Nanobodies interact with βPFO through different mechanisms. These results open the door to the use of these Nanobodies to validate βPFO relevance in AD.

Results

βPFO trapped into NAPol is a good antigen for *camelidae* immunization.

To generate specific Nanobodies against βPFO, we first used βPFO stabilized in DPC micelles as antigen. We then immunized a llama with the βPFO/DPC complex. However, this immunization did not produce any Nanobody hit. We attributed this lack of hits to micelle dispersion upon dilution below the CMC of DPC when injecting the βPFO/DPC complex in the llama tissue. Dispersion of the micelle into detergent monomers would leave the hydrophobic core of the oligomer unprotected, causing βPFO disruption and/or subsequent aggregation.

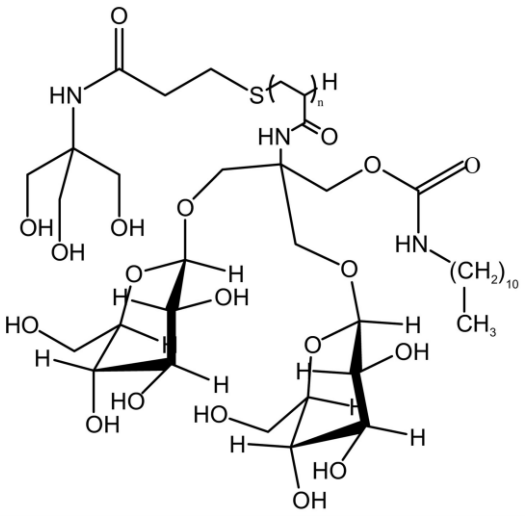

Figure 2-2: Chemical structure of NAPol. Aliphatic chains surround the hydrophobic residues while glucose solubilizes the complex. Reproduced with permission from Watkinson *et al.* [3]

As explained in the introduction, Amphipols (APol) are a biomimetic membrane environment that allow membrane protein solubilization. Nevertheless, in contrast to detergents, once APol are bound to the membrane protein, they can stand dilution as APol do not solubilize as monomers in absence of competing detergent and so the membrane protein/APol interaction is irreversible in this case.[59,67,102] In our laboratory we have been working with different APols. Dr. Serra-Batiste in our research group demonstrated that βPFO could be reconstituted into non-ionic Amphipols (NAPols), a type of Apols decorated with two glucoses and a C11 hydrophobic chain per monomeric unit **[Figure 2-2]**.[103-104][105] Indeed, after detergent depletion, βPFO trapped in NAPol maintained its structure as assessed through the following experiments. First, the βPFO/DPC complex migrated at the same position as βPFO/NAPol when both samples were analyzed by non-boiled SDS-PAGE. Moreover, both samples had the same behavior upon proteolysis **[Figure 2-3** A**]**. Second, by using $^{13}C(Met_{35})$-Aβ42 to form βPFO, and analyzing βPFO/DPC and βPFO/NAPol through a ^{1}H-^{13}C HMQC experiment, we detected the same two peaks with the same chemical shifts characteristics of βPFO **[Figure 2-3** B**]**. These peaks were broader in the case of the βPFO/NAPol than in the case of the

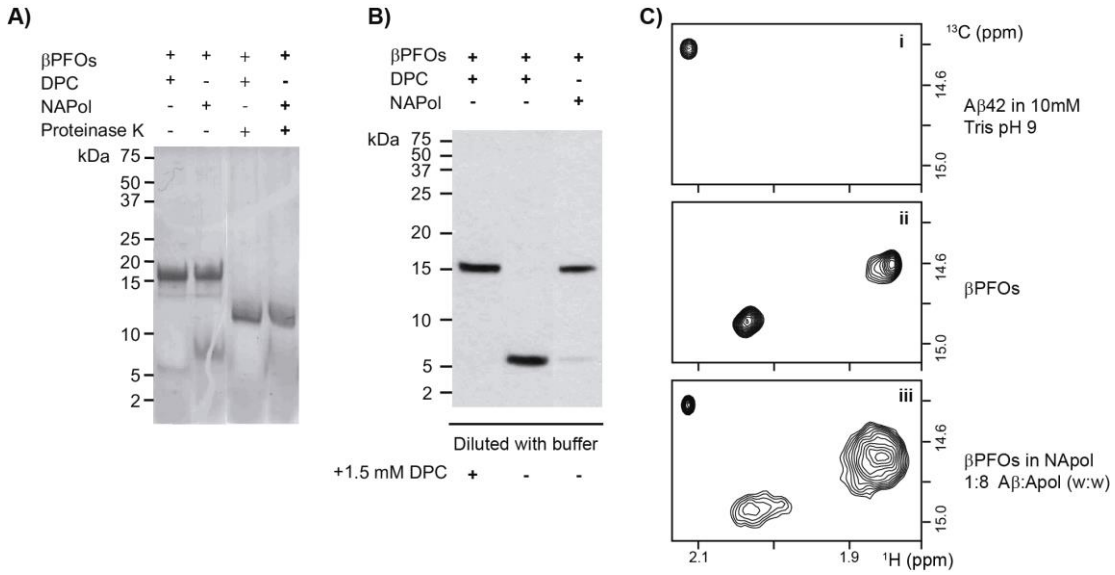

Figure 2-3: βPFO/NAPol complex characterization. (A) SDS-PAGE analysis of βPFO/DPC and βPFO/NAPol complex before and after proteolysis by proteinase K by SDS-PAGE without boiling the sample. (B) Western Blot (WB) analysis of βPFO/DPC or βPFO/NAPol diluted with 10 mM Tris pH 9 buffer with or without 1.5 mM DPC. (C) ^{1}H-^{13}C HMQC spectra of (top) monomeric $^{13}C(Met_{35})$-Aβ42 in Tris pH 9, (middle) $^{13}C(Met_{35})$-βPFO/DPC and (bottom) $^{13}C(Met_{35})$-βPFO trapped in NAPol.

βPFO/DPC. This can be explained not only because NAPol were non-deuterated, but also because Membrane Protein/APol complexes are described to comprise a thicker belt than membrane proteins/detergent micelle complexes, which makes NMR signals relax faster compromising their detection. ^{1}H-^{13}C HMQC also showed the appearance of a peak corresponding to random coil monomer after βPFO trapping into NAPol also visible in the Western Blot **[Figure 2-3** C **and** B **respectively]**.

Finally, Dr. Serra-Batiste also demonstrated that βPFO/NAPol was stable upon dilution. One of the problems of working with detergent micelles is that they have a CMC below which detergent is soluble and does not form micelles that can protect the hydrophobic region of the membrane protein. Because of that, when diluting the βPFO/DPC complex with Tris buffer, βPFO is no longer migrating in the non-boiled SDS-PAGE as an oligomer but as a monomer **[Figure 2-3** C**]**. However, if it is diluted with 1.5 mM DPC Tris buffer (being 1.5 mM the CMC of DPC), the oligomer is maintained **[Figure 2-3** C**]**. APol bind to the hydrophobic surface of membrane proteins in an irreversible manner in the absence of a competing detergent. Dr. Serra-Batiste showed that when working with βPFO/NAPol, the complex was stable even after dilution with Tris Buffer **[Figure 2-3** C**]**. All together, these experiments show that βPFO structure is preserved when trapped in NAPol including after high dilution conditions. Because of these properties, we considered βPFO/NAPol a good antigen for immunization. We, therefore, immunized the alpaca, called Paco, with the βPFO/NAPol complex.

βPFO preserves its structure when immobilized in a solid support

In order to obtain specific Nanobodies against βPFO, we required to immobilize βPFO in a solid support for phage display, screening, ELISA, etc. Several options were available. First, the use of biotinylated APols and streptavidin coated plates. However, biotinylated APols had been reported to give some false positives when used in phage display as a result of non-specific interactions (Manuela Zoonens, personal communication). Second, the preparation of biotinylated βPFO and the use of streptavidin coated plates. Third, the direct absorption of βPFO on polystyrene surface.

We started by optimizing the chemical biotinylation of βPFO. βPFO was formed under buffer conditions free of amines, (phosphate buffer was used instead of Tris), was left to react with N-Hydroxysuccinimide (NHS) functionalized with biotin and was finally purified by SEC. Next, we determined that βPFO structure was maintained after biotinylation by measuring a ^{1}H-^{13}C HMQC NMR spectrum of $^{13}C(Met_{35})$-βPFO. We detected peaks at similar chemical shifts than non-biotinylated βPFO indicating that the oligomer structure was maintained (data not shown). Moreover, we assessed the Aβ42 biotinylation ratio by Mass Spectrometry (MS) **[Figure 2-4]**. We found approximately a 25% of Aβ42 was biotinylated considering the same ionizability for βPFO than biotinylated βPFO.

In a parallel manner, Dr. Vazquez de la Torre in our group, developed an ELISA assay in which βPFO was directly absorbed on ELISA plates. The method was based on the use of 1.5 mM DPC, the CMC of DPC, in all the buffers. By doing so, we prevented dispersion of the micelles stabilizing the oligomer. By using this method, the oligomer was detected in a dose-dependent manner, using primary antibodies targeting the exposed flexible loops of βPFO such as 6E10 (3-8) and 4G8 (17-24). Whereas βPFO was not detected using antibodies targeting the hydrophobic core of the oligomer, protected by the micelle, such as MM26 (35-42) [**Figure 2-5** A**]**. This pattern of antibody detection was consistent

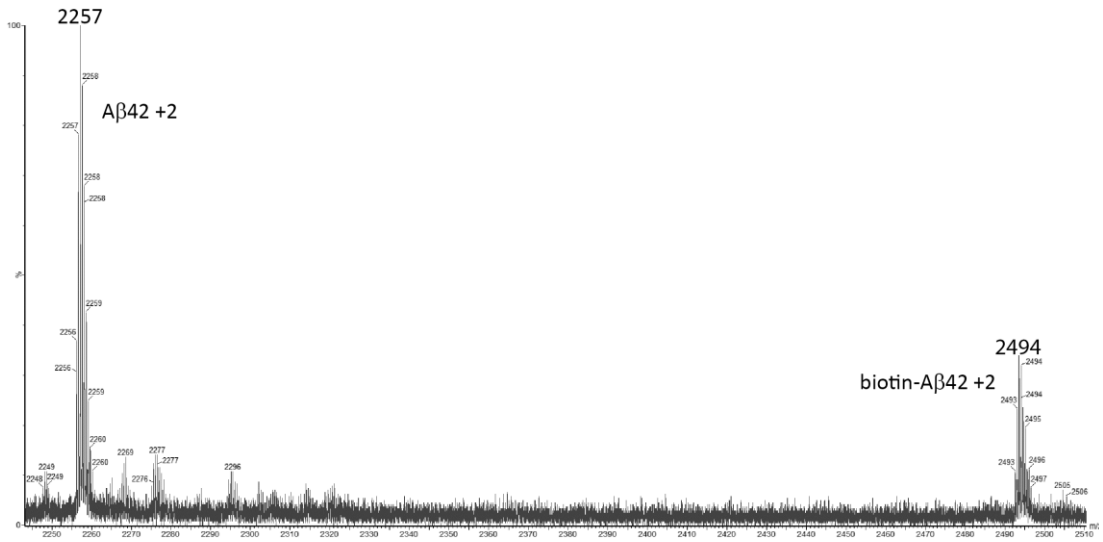

Figure 2-4: MS spectrum of biotinylated βPFO. Detection of non-biotinylated monomer with charge +2 at 2257 m/z and biotinylated monomer with a charge +2 at 2494 m/z. The area of the biotinylated peak corresponds to the 25% of the area of both peaks.

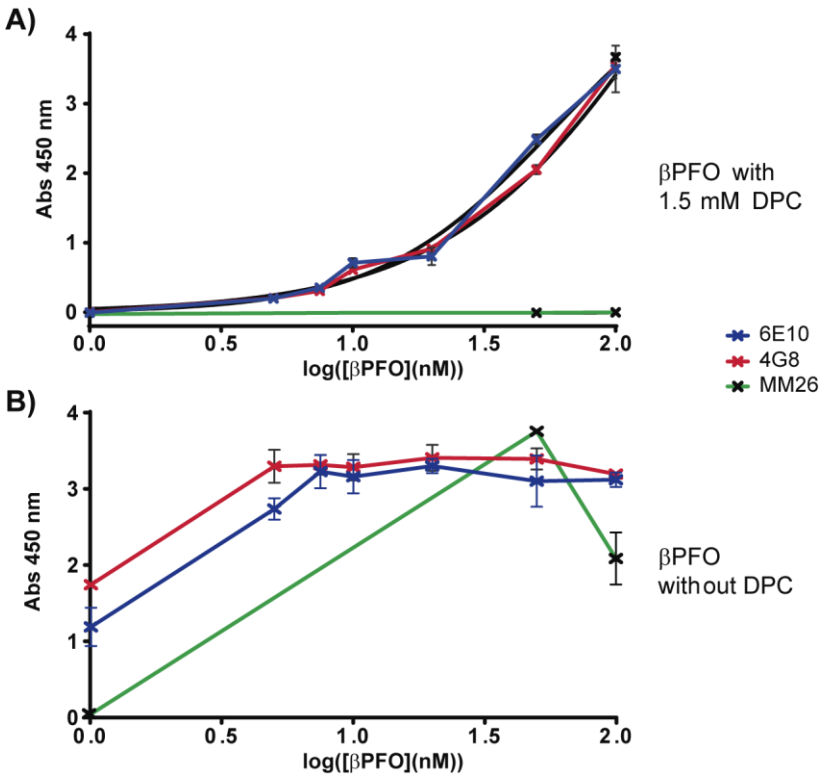

Figure 2-5: βPFO coating in ELISA plates. ELISA of βPFO immobilized at different concentrations detected by 6E10 (3-8), 4G8 (17-24) and MM26 (35-42). The same experiment was performed using (A) 1.5 mM DPC in all the buffers or (B) without DPC in all the buffers.

with structural data on βPFO obtained by other members of the group (data not published) and indicated that the oligomer was well folded when absorbed in the polystyrene surface.

On the contrary, when 1.5 mM DPC was not used in all the buffers, signal was detected for all the primary antibodies used including those targeting protected regions of βPFO such as MM26 **[Figure 2-5** B**]**. This result indicated that, when no DPC was present in the buffers, all regions of Aβ were exposed thus indicating that the structure of βPFO was no longer kept.

Since the direct absorption method using 1.5 mM DPC in all the buffers allowed maintaining the structure of the oligomer, we used it in all steps of Nb generation and selection that required βPFO immobilization in the solid support. Compared to βPFO biotinylation, this approach was more effective both in terms of βPFO manipulation and time.

Eleven Nanobodies were obtained after βPFO/NAPol immunization

Library generation

Nanobodies were generated in collaboration with Prof. Serge Muyldermans' group from the Vrije Universiteit Brussel (VUB). They performed immunization and generated the Nanobody plasmid library according to published protocols.[106] Briefly, the βPFO/NAPol complex was injected subcutaneously to the alpaca called "Paco" together with other antigens and "GERBU LQ" as immunostimulating adjuvant. Vaccination was carried out once a week. After 6 vaccinations, 100 mL of blood were extracted from the animal. The ribonucleic acid (RNA) of the B cells obtained from the blood was extracted and cloned to obtain complementary deoxyribonucleic acid (cDNA). The cDNAs corresponding to Nanobody sequences were amplified, and with the use of restriction enzymes they were inserted into pMECS vectors generating a plasmid library. The latter was transformed into bacteria to generate a bacterial library. From the bacterial library, upon phage attack, a phage display library was generated.

Panning and Screening

I carried out a research stage in Prof. Serge Muyldermans Laboratory at VUB with the invaluable help of Ema Romão, in order to obtain the anti-βPFO Nanobody positive hits from the phage display library. We started by the phage display library performing panning, which consisted on successive rounds of phage display involving three steps. First, phages from the phage library were incubated with the antigen pre-coated on a solid support. Second, non-bound phages were washed. Third, the bound phages were eluted under high pH conditions. After the elution, the pH was rapidly equilibrated to

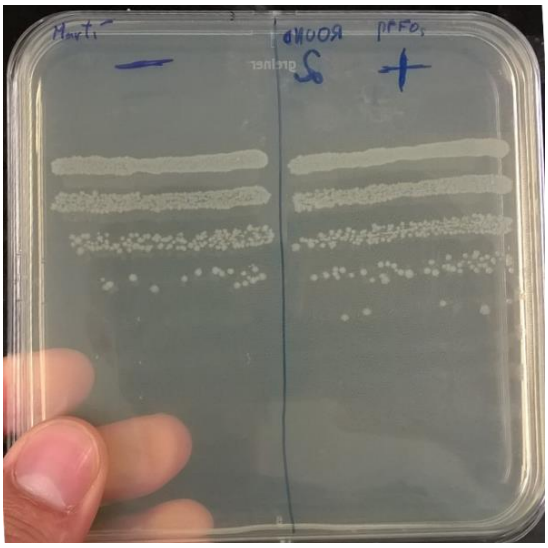

Figure 2-6: Analysis of enrichment in second panning round. Upon 10-fold dilution, the bacterial amount is analyzed. We can see one order of magnitude more concentration for the selected sample.

avoid protein hydrolysis. Afterwards, the obtained phages were used to infect bacteria. The new bacterial library enriched in specific binders was grown again. From this final bacterial library, a second round of panning was started again. Panning was repeated for 4 rounds changing the blocking agent every time (skim milk, BSA and casein). Only in the second round we found a significant enrichment in the antigen-recognizing phages compared to non-specific phages **[Figure 2-6]**. Despite the not-so-good results from panning, we moved on.

After the panning, we selected 95 discrete colonies and carried out a first screening using crude Nanobodies obtained from the Periplasmic Extract (PE). In this first screening, βPFO was coated in a 96-well ELISA plate. Afterwards, the plate was blocked with BSA and subsequently crude Nanobodies were added. After washing unbound Nanobodies, those that remained attached were detected by an antiHisTag antibody. The signal was compared with a control where no antigen was coated in the plate. The ratio of signal between the antigen-coated and the non-coated well provided qualitative information about the degree of binding and specificity of the Nanobody under study to the antigen. We performed screening under two different conditions. The first one was done at physiological pH 7.4, and gave 19 positive clones. Moreover, as our oligomer is more stable at pH 9.0 we wanted to find out also Nanobodies that were stable at this pH. For this reason, a second screening was carried out at pH 9.0 and 5 additional positive hits were found.

We started to analyze the clones obtained at pH 7.4. As 19 was a high enough number of colonies, we carried out a second screening to assess their relevance. To this end, WK6 cells were transformed with the plasmids. WK6 cells is the cell line in which Nanobodies are usually expressed. By ELISA, we compared the Nanobody affinity for βPFO, monomeric Aβ42 and non-coated wells (blank). Every clone was analyzed by triplicate. Most of them showed a higher signal for the βPFO than for the blank. And all of them showed a higher ratio of signal for βPFO/Blank than for monomeric Aβ42/Blank. In between all the colonies, 15 that showed more than 2-fold signal increase between βPFO and blank, were selected. The other 4 clones were discarded. Simultaneously, the 19 clones had been PCR amplified and their size was checked by agarose gel electrophoresis. Clone n°10 already discarded due to lack of specificity, was the only one

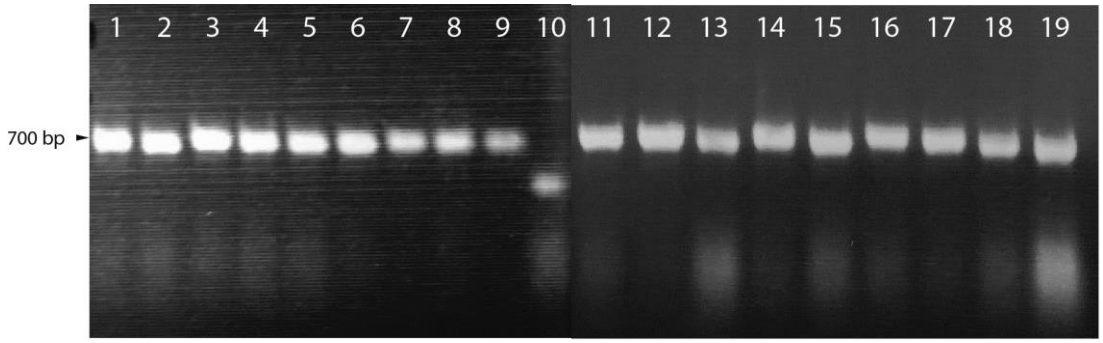

Figure 2-7: Agarose gel analysis of the Nanobody DNA fragments found at pH 7.4

not having the proper size (~700 bp) **[Figure 2-7].** The five clones from pH 9.0 were directly amplified and sequenced without carrying out a second screening.

Next, we sequenced the plasmids and eliminated duplicate sequences. This afforded 9 Nanobodies for the screening carried out at pH 7.4, and 4 Nanobodies for the one carried out at pH 9. Notably, one of the Nanobodies was found whether the screening was carried out at pH 7.4 or at pH 9. Thus, in a first moment, we generated 12 different Nanobodies that targeted βPFO. Nanobodies were named according to their complementarity-determining regions (CDRs). Indeed, they have 3 CDRs (CDR1, CDR2, and CDR3). CDR3 is the main responsible for antigen binding while the CDR1 and CDR2 just have an influence on the overall Nanobody affinity.[99] Nanobodies having different CDR3 were named with a different number in an consecutive manner (i.e. Nb (1.), Nb(2.), Nb (3.), etc.). Then, Nanobodies having the same CDR3 but different CDR1 were differentiated with a second number (i.e. Nb (1.1.) and Nb (1.2.)). Finally, Nanobodies having also the same CDR1 were differentiated with a third number (i.e. Nb (1.1.1.) and Nb (1.1.)). After numbering all the Nanobodies, we discarded Nb (8.) as sequencing was of poor quality and none of the well sequenced amino acids differed from the sequence of Nb (1.1.). In summary, we finally generated 11 different Nanobodies. From them, Nb (1.1.), Nb (1.2.), Nb (2.), Nb (3.), Nb (4.), Nb (5.), Nb (6.) and Nb (7.) were found when screening was carried out at pH 7.4, while Nb (1.1.1.), Nb (7.) again, Nb (9.) and Nb (10.) were obtained when screening was carried out at pH 9.0.

The Nanobodies are specific for βPFO

For the Nanobodies to be a good probe and thus be useful to validate βPFO in relevant AD models, it's critical that they selectively target βPFO versus other Aβ species present

in the brains such as Aβ42 monomers or Aβ42 fibrils. For this reason, we set to determine the specificity and the affinity of the obtained Nanobodies against the three above mentioned Aβ42 forms using ELISA. In these experiments, we compared our Nanobodies with "Nb_3", obtained previously by our collaborators against Aβ40 peptide.[107] We renamed this Nanobody from "Nb_3" to "Nb (0.)" for clarity purposes. Firstly, we coated either βPFO, Aβ42 monomers or Aβ42 fibrils on the surface of the well using coating buffer. Secondly, we blocked the wells with BSA. Then, we incubated the wells with decreasing concentrations of Nanobodies. Finally, we detected the bound Nanobodies with a primary antiHis-Tag antibody that recognized the His_6 tag of the

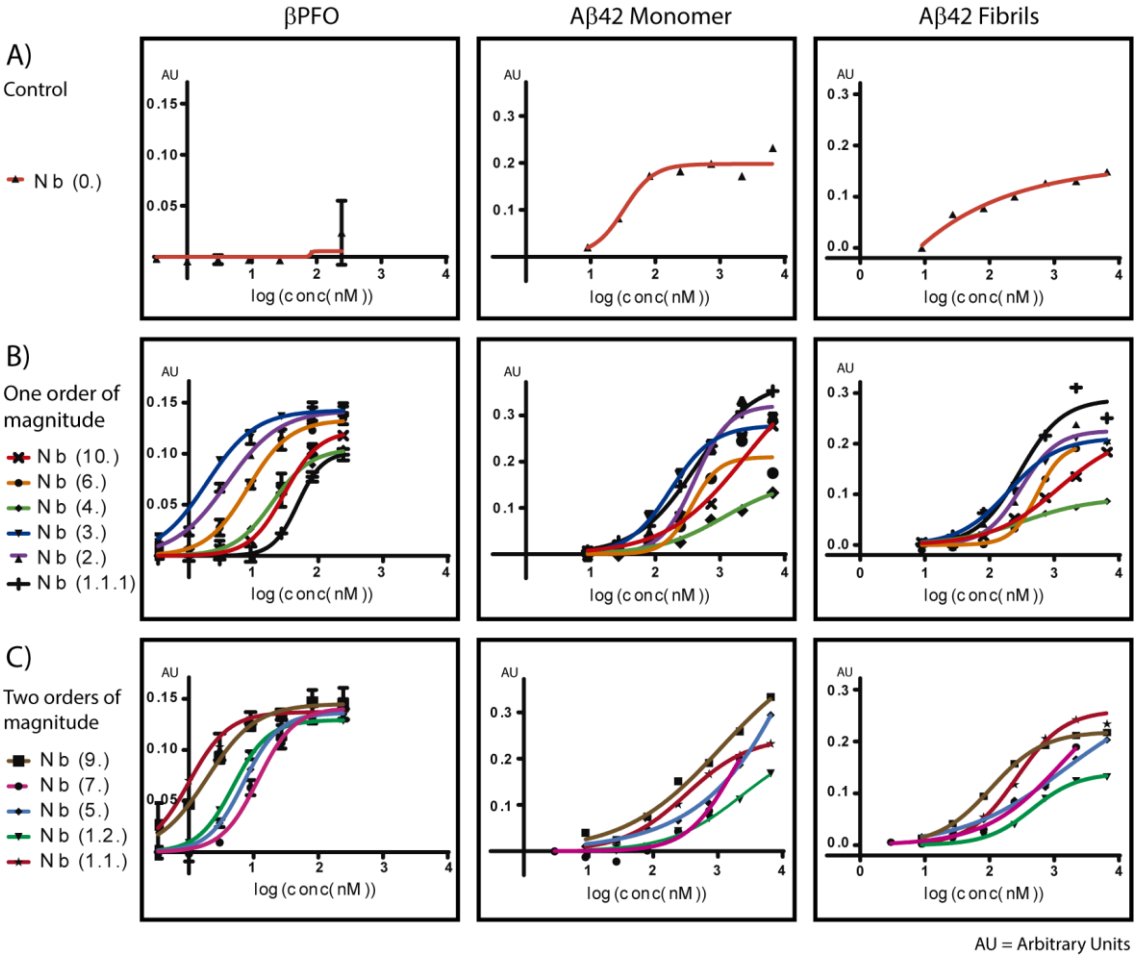

Figure 2-8: Sigmoidal curves from ELISA experiment. Graphs plot absorbance as a function of the logarithm of Nanobody concentration. Each column shows results from coating different Aβ42 species: βPFO, Aβ42 monomers and Aβ42 fibrils. In all the cases the amount of Aβ42 peptide coated was 2 µg/ml. Each row shows results obtained for: (A) Nb (0.) as a negative control; (B) Nanobodies having one order of magnitude of difference in between βPFO and monomer affinity; and (C) Nanobodies having two orders of magnitude difference between βPFO and monomer affinity.

Nanobodies and a secondary Horseadish Peroxidase (HRP)-linked antibody. After developing the signal with Enhanced chemiluminescence (ECL), the concentrations were transformed into logarithmic scale and sigmoidal curves were obtained. The half maximal effective concentration (EC50) values from these sigmoidal curves **[Figure 2-8]**, were taken as a qualitative measure of the affinity of each Nanobody.

Nb (0.) did not recognize βPFO in the range of concentrations we worked with (up to 243 nM). Instead it recognized Aβ42 monomers and the Aβ42 fibrils with an EC50 value of 32 nM and 69 nM, respectively. Because of this behaviour we considered Nb (0.) a good negative control. Next, we determined the EC50 value for each of the Nanobodies that we obtained against βPFO, Aβ42 monomers and Aβ42 fibrils to determined their specificity **[Table 1]**.

We found out that all the obtained Nanobodies had EC50 values in the range of 1-50 nM for the βPFO. While they had EC50 values of at least one order of manitude higher for monomers, and with the exception of Nb (1.1.1.) also for fibrills. Among them, Nb (1.1.1.), Nb (2.), Nb (3.), Nb (4.), Nb (6.) and Nb (10.) had approximatedly one order of magnitud more affinity for βPFO than for the monomer, while Nb (1.1.), Nb (1.2.), Nb

	Oligomer		Monomer		Fibrils	
	EC50 (nM)	95% CI	EC50 (nM)	95% CI	EC50 (nM)	95% CI
Nb (0.)	ND	ND	32	21,13 to 50,9	69	36,54 to 192,5
Nb (1.1.)	1	0,918 to 1,113	327	125,5 to 12573	263	219,2 to 323,7
Nb (1.1.1.)	48	41,42 to 55,99	420	268 to 877,5	293	210,9 to 412,9
Nb (1.2.)	5	4,551 to 5,2	2331	1077 to 16647	454	301,3 to 874,6
Nb (2.)	4	3,322 to 4,597	408	329,4 to 508,6	309	250,3 to 383
Nb (3.)	2	1,604 to 2,232	173	108,9 to 328,5	198	154,8 to 260,1
Nb (4.)	20	17,28 to 22,78	1128	463,2 to 49640	327	140,2 to 6073
Nb (5.)	7	6,248 to 7,963	135725	5311 to ???	1389	442 to 76256
Nb (6.)	8	6,988 to 9,715	367	262,3 to 509	541	356,1 to 1290
Nb (7.)	12	9,431 to 14,87	1629	632 to ???	1281	527,8 to 15914
Nb (9.)	2	1,64 to 2,252	1106	361,6 to 73199	105	83,7 to 135,4
Nb (10.)	30	25,59 to 36,26	1220	680,2 to 6367	1145	522,4 to 12730

Table 1: EC50 values from the sigmoidal curves of the ELISA experiments with its confidence interval. Color gradation is added for an easier comprehension of the results being green the lowest and red the highest. It must be noted that in some cases the 95% confidence interval (CI) is so wide that the EC50 values are just orientative. ND stands for “non-detecatable”.

(5.), Nb (7.) and Nb (9.) had at least two orders of magnitude higher affinity for βPFO than for the monomer **[Figure 2-8]**. To conclude, we have reached to generate 11 high-affinity, βPFO-specific Nanobodies.

Nanobodies interact with βPFO through different mechanisms

One of the characteristics of membrane proteins adopting a β-barrel structure is that when analyzed by SDS-PAGE without boiling them, they can resist SDS denaturation and therefore migrate as a folded protein. Moreover, when β-barrel membrane proteins, are treated with proteases, the exposed flexible regions or loops are proteolyzed while the β-barrel core, protected by the detergent micelle, remains intact. Previous results from our group revealed that βPFO adopts a β-barrel structure[60]. Consistent with this behavior, when βPFO samples are analyzed by SDS-PAGE without boiling them, they migrate mainly as a band with a molecular weight of 18 kDa. When βPFO is proteolyzed by Proteinase K, a lower band at around 12 kDa appears as we saw in the introduction **[Figure 0-7** E**]**. This result indicates that the oligomer has lost the flexible regions and loops thus decreasing its overall size but that the β-barrel core remains intact. We refer to this strategy as limited proteolysis followed by western blot analysis (LP-WB). We next carried out the same experiment but in the presence of each of the Nanobodies under study. We expected that upon Nanobody binding to βPFO, the former could offer some degree of protection from Proteinase K proteolysis. The experiments were performed at two different pHs, physiological pH 7.4 and at pH 9.0 were βPFO is more stable. In order to detect the oligomer we developed the western blot using D9A3A antibody (C-terminal Aβ42-specific) as a primary antibody.

After LP-WB analysis, we compared the migration of the control bands, when LP was carried out in the absence of Nb, to those obtained in the presence of the distinct Nbs **[Figure 2-9]**. For the oligomer sample incubated with Nb (0.) we observed no shift, which is consistent with ELISA experiments showing that this Nanobody did not recognize βPFO. For Nb (9.), we neither observed a band shift towards higher molecular weights. For Nb (5.) and Nb (3.), we either observed very faint band shits or no bands. Somehow these Nanobodies have a behaviour that they expose the oligomer to proteolysis upon binding. For the rest of Nanobodies we observed bands shifted to higher molecular weights to different extents. Notably, while, at pH 7.4 the bands were defined and could

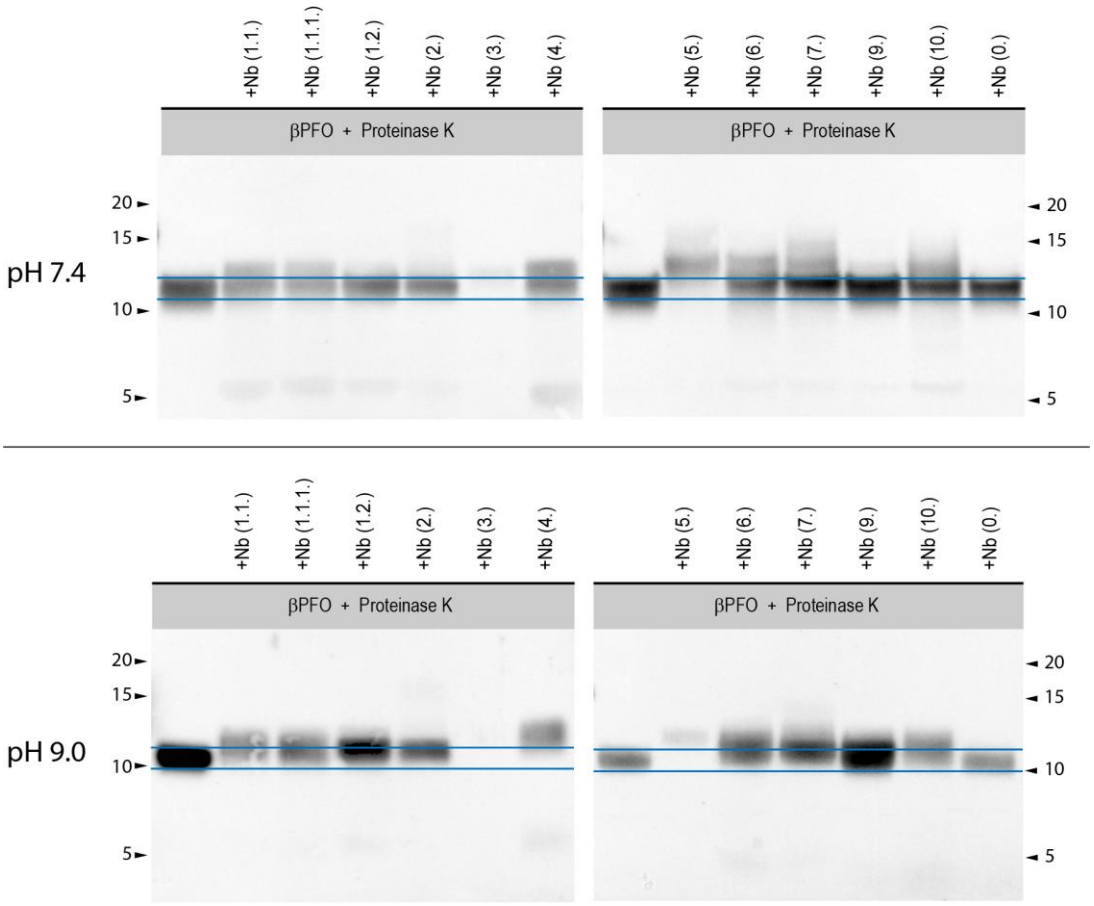

Figure 2-9: Nanobodies' protection to βPFO proteolysis. Nanobodies were added to βPFO and then proteolyzed by Proteinase K for 45 min at 37°C. Proteolysis was stopped with protease inhibitor. Blue lines are guides to the eye. The experiment was done at two pHs, (top) pH 7.4 and (bottom) 9.0.

be distinguished in between double and triple bands. At pH 9.0 we observed sfhifted broad bands. Band broadening widening or double bands, can be explained as distinct proteolysate states that could result from Nanobody bound-unbound equilibria. In the case of Nb (4.), we observed a bigger shift at pH 9 than for the rest of Nanobodies and in the case of Nb (7.) we observed a triple band at pH 7.4. To conclude, we have shown that while Nb (0.) and Nb (9,) are not binding strongly enough to protect it from the proteolysis. In the rest of the cases, Nanobodies are affecting the proteolysis patern, and thus, it is demonstrated that they are strongly interacting with βPFO in different manners as can be seen in **[Table 2]**.

	Western Blot-Limited Proteolysis			
	pH 7.4		pH 9.0	
	Band detection	Shift	Band detection	Shift
Nb (1.1.)	Yes	DB +=	Yes	BB+=
Nb (1.1.1.)	Yes	DB +=	Yes	BB+=
Nb (1.2.)	Yes	=	Yes	+
Nb (2.)	Yes	=	Yes	+
Nb (3.)	(very faint)	+	No	
Nb (4.)	Yes	DB +=	(faint)	BB ++
Nb (5.)	(very faint)	+	(very faint)	+
Nb (6.)	Yes	DB +=	Yes	BB+=
Nb (7.)	Yes	TB ++=	Yes	BB+=
Nb (9.)	Yes	=	Yes	=
Nb (10.)	Yes	DB +=	Yes	BB =+
Nb (0.)	Yes	=	Yes	=

Table 2: Results of the analysis of the WB-LP experiment assessing Nanobodies' protection to βPFO proteolysis. "DB" stands for "Double Band". "TB" stands for "Triple Band". "BB" stands for "Broad Band". "+" stands for an upwards shift. "=" stands for a non-shifted signal. "+=" stands for a shifted upwards band and for an unshifted one.

Nanobodies can block βPFO pores

In a previous study of βPFO[60], we demonstrated in collaboration with Mariam Bayoumi and Dr. Giovanni Maglia from the University of Gröningen, the ability of βPFO to form pores into planar lipid bilayers.[60] Following on this study, our collaborators studied the effect of adding Nanobodies to preformed pores. They added βPFO in the cis chamber and waited until a single pore or several pores were formed. Afterwards, they perfused the chamber to reduce βPFO concentration in solution and thus reduce binding of the Nanobody to the oligomer still present in solution as well as reduce new pore formation. Then, they added each of the different Nanobodies to study their effect in the conductivity across the bilayer. We found out three main different types of behaviors:

- No effect: In four cases the addition of Nanobodies had no effect in the conductivity. Specifically, Nb (0.), Nb (3.), Nb (5.) and Nb (9.) did not show any effect in the pore conductivity. For Nb (0.) this result was expected as ELISA experiments showed that it did not recognize βPFO. For Nb (3.), Nb (5.) and Nb (9.), even though ELISA showed interaction with βPFO, the electrical recordings indicated that their way of interacting with the pore does not affect the

conductivity. We can't rule out the possibility that certain structural elements of βPFO are not the same when reconstituted in detergent micelles, (ELISA) and lipid bilayers, (electrical recordings).

- Pore interaction with partial blockage: For Nb (1.1.), Nb (1.1.1.), Nb (1.2.), Nb (6.) and Nb (10.), an interaction with the pore led to a partial blockage without reaching complete pore blockage. Nb (6.) showed up to a 40 % of conductivity reduction in two steps. Nb (1.2.) and Nb (10.) showed up to a 60-65 % reduction in conductivity in a single step. Nb (1.1.) showed up to a 75 % of conductivity reduction in a single step.
- Complete pore blockage: The addition of Nb (7.) interrupted the current across the bilayer at once. While Nb (2.) interrupted the current in two steps. The first step led to a reduction in the intensity going across the bilayer while in the second step, it reached a complete recovery of 0 pA intensity affording a complete pore blockage **[Figure 2-10]**.

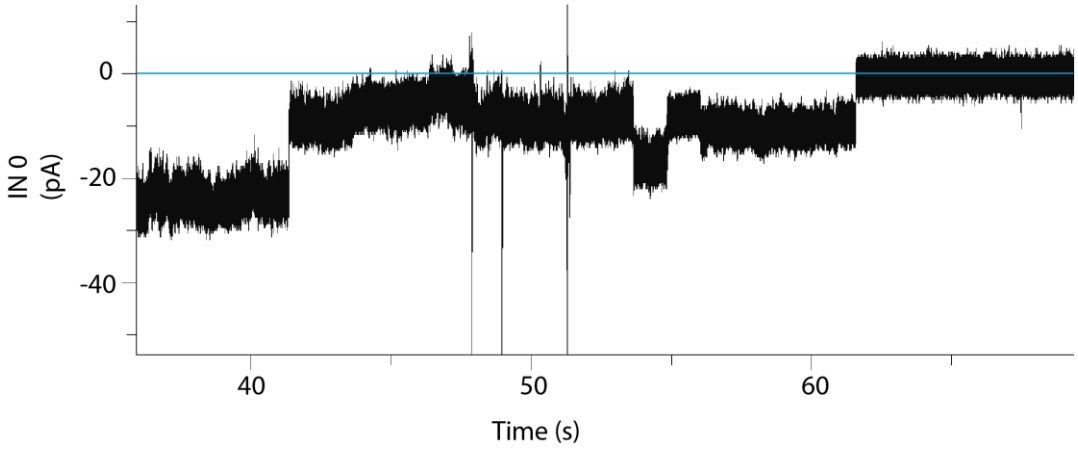

Figure 2-10: Blockage of a pore by Nb (2.). Electrical recordings through planar lipid bilayers. Recordings after addition of Nb (2.) on pre-formed βPFO single-pore conductance. Intensity is recovered to 0 pA in two steps.

The pore blockage effect was produced either in a one-step or in a two-step manner. However, this two-step pore blockage was due to two-step binding or to the binding of two Nanobodies to the same βPFO is still unclear. To conclude, we characterized the way Nanobodies interacts with the pore conductance. Only Nb (0.), Nb (3.), Nb (5.) and Nb (9.) had no effect on the conductance. In contrast, Nb (2.) and Nb (7.), reached a complete blockage of the pore conductance.

Discussion

The aim of this work was to develop a selective probe for βPFO that could allow us to determine its relevance in the context of AD. To this aim, we generated Nanobodies against βPFO, we selected the best and most selective hits to finally get 11 different Nanobodies. By ELISA we demonstrated that all the 11 Nanobodies had higher affinities for βPFO than for Aβ42 monomers and Aβ42 fibrils. Indicating that these Nanobodies targeted βPFO selectively and with high affinity. LP-WB and planar lipid bilayer's electrical recordings certified the interaction of the Nanobodies with βPFO. All together, these results constitute a solid basis for using these Nanobodies in different animal models and AD brain tissue samples to determine βPFO relevance in the disease.

Nb (0.) (Nb_3 in the papers from our collaborators[38,108-109]) was used as a negative control. Nb (0.) was found to have an EC50 of around 30 nM and a K_D of around 100-200 nM[107] against Aβ42 monomer. Based on these and since we were able to reproduce the EC50 value of Nb (0.) in our ELISA experiments, we expect that the anti-βPFO Nanobodies have a K_D in the μM range against monomer and low nM against βPFO. LP-WB and planar lipid bilayer's electrical recordings allowed us to characterize the Nanobody-βPFO interaction. Both techniques showed that the different Nanobodies had different binding mechanism to βPFO. On one hand, there were Nanobodies that did not either affect the pore conductivity such as Nb (3.), Nb (5.) and Nb (9.). These Nanobodies did not show any shift in the WB-LP experiment or were faint bands. For Nb (9.) the binding site may be far enough from the β-barrel and this may not affect the current flow and accessibility to the protease. For Nb (3.) and Nb (5.) WB-LP suggested that they were causing oligomer exposure to proteases, however, electrical recordings suggested that this oligomer exposure happening on the micelle sample was not produced when the pore was inserted in the lipid bilayer as no effect in conductance was detected. On the other hand, Nb (1.1.), Nb (1.1.1.), Nb (1.2.), Nb (2.), Nb (4.), Nb (6.) and Nb (10.) showed some degree of protection in WB-LP. In these cases, their binding affected the current across the bilayer at different levels. In the case of Nb (2.) and Nb (7.) even reaching the complete blockage of the pore. To conclude, we developed 11 new Nanobodies that bind in different ways to βPFO, being two of them able to completely block the pore conductance.

The proposed idea of producing antibodies to validate *in vivo* the presence of Aβ oligomers produced *in vitro* has also been previously proposed by other laboratories. Specifically, it has been used to validate the presence of ADDLS,[36] globulomers[48] and micellar oligomers[110] in brain tissues. However, all these oligomers are not so well structurally characterized as βPFO, and they are also more heterogenous. Moreover, these oligomers are soluble, which implies that if to exert neurotoxicity they need to interact with the membrane, they are most probably changing their structure upon membrane binding. If this would be the case, the oligomers would not be detected at the time of exerting their neurotoxic effect but when in solution. Alternatively, βPFO are membrane oligomers, which implies that they most probably have the same structure to be detected by the Nanobody when produced *in vitro* and when exerting its neurotoxic effect *in vivo*.

The longer CDR3 of Nanobodies, make them more avid for cavities and therefore, conformation-specific rather than sequence-specific. In the same direction as our work, other authors also looked for this structure-specificity of the Nanobodies and produced Nanobodies against other Aβ forms. Habicht and coworkers, and Morgado and coworkers, both used aggregated Aβ40 to select Nanobodies from synthetic libraries, notably, with 10-fold exces Aβ40 monomer in the selection solution to avoid monomer-selective Nanobodies and obtained respectively, B10[111], specific to Aβ40 PF and fibrils, and KW1[112-113], specific to soluble Aβ40 oligomers. Our collaborators from the VUB used Aβ40 monomer inmunization and selection to produce Nb_3[107]. Using this Nanobody, Drews and Flagmeier demonstrated that it avoided calcium influx caused Aβ42 soluble oligomers in both neurons and vesicles.[38,108] David and coworkers inmunized alpacas with AD brain homogenate and panned against untreated Aβ peptide and obtained PrioAD12 specific for Aβ40 and PrioAD13 specific for Aβ42.[113-114] Vandesquille and coworkers used fibrillar synthetic Aβ42 for inmunization to obtain the R3VQ Nanobody.[115] Lafaye and coworkers inmunized an alpaca with overnight incubated at 37 °C Aβ42 peptide and panned the Nanobodies against Aβ42 without any further treatement to finally produce the V31-1 Nanobody.[113,116] Finally, Rutgers and coworkers obtained two different Nanobodies from inmune and non-inmune libraries. From a non-inmune llama-derived phagemid library selected against untreated Aβ42,

they obtained ni3A Nanobody, a Nanobody selective for Aβ42 with a high affinity. Then, using down's sindrome brain parenchyma they generated an inmune library and also selected it against synthetic Aβ42 peptide without any further treatement[113,117-118]. Thus, to our knowledge, our Nanobodies are the first ones specifically selected against a type of Aβ42 oligomer. However, our newly obtained Nanobodies are the only ones described up to now targeting membrane oligomers.

We have obtained Nanobodies that can specifically detect βPFO. This work will open the door to determine whether βPFO is relevant in AD and to establish wether βPFO is the neurotoxic specie in AD. If this is demonstrated, βPFO has the potential to become a new AD drug target and the Nanobodies here developed useful in biomedical research for the development of new drugs to finally treat AD.

Materials & Methods

Reagents

Detergents were purchased from Cube Biotech. Culture media, antibiotics and vitamins were purchased to Duchefa Biochemie. All other reagents were supplied by Sigma-Aldrich unless otherwise stated.

βPFO trapping into NAPol

βPFO was prepared as previously published.[60] NAPol were kindly provided by Dr. Manuela Zoonens and Dr. Jean-Luc Popot. βPFO and NAPol were added at a ratio 1:8 (Aβ42:NAPol) and incubated at 37°C for 20 min. Detergent was depleted by incubating the sample with Bio Beads SM-2 at a ratio 1:50 w/w (DPC:BioBeads) from BioRad at 4°C for 30 min in an orbital wheel. Sample was filtered through a 0.45 µm Ultrafree MC-HV centrifuge filter.

ELISA

Coating. βPFO were prepared, at 150 µM (Aβ42 concentration). For coating, βPFO were diluted to 443 nM (2 µg/ml) in coating buffer (100 mM Sodium Carbonate pH 9.6) supplemented with DPC (1.5 mM final concentration). For coating Aβ42 monomer. Aβ42 was disgreggated with 6,8 M GdnSCN, sonicated and purified by SEC at 4°C using 50 mM $(NH_4)_2CO_3$ as the elution buffer. The collected monomer was quantified and frozen ready

to be diluted before using it. For coating Aβ42 fibrils, Aβ42 monomer was resuspended at 30 µM in 10 mM Tris pH 7.4 buffer and left at 37ºC for 3 days. Both, Aβ42 monomer and Aβ42 fibrils were diluted in coating buffer to a concentration of 443 nM. Next, 100 µL of each preparation were added in each well, including the blanks and left incubating O/N or at least 4-5 h at 4ºC. In the following steps, it is to be noted that when working with βPFO all the buffers used contained 1.5 mM DPC to preserve βPFO stability. Instead, for the Aβ42 monomer and Aβ42 fibrils coated plates, no DPC-containing buffers were used. After coating the wells, they were washed three times. For every wash we emptied the wells by turning the plates down rapidly. We added 150 µL of washing buffer (150 mM NaCl, 10 mM Tris pH 7.4), let it incubate with agitation for 5 min and finally emptied the wells.

Blocking. The surface was blocked to avoid non-specific binding of Nanobodies onto it. To this end, 100 µL of 5 mg/ml BSA in washing buffer was incubated for 1-2 h at room temperature under agitation. Afterwards, wells were washed three times.

Nanobody incubation. When working with PE 100 µL of each PE were incubated for 1 h at room temperature under agitation. When working with pure Nanobodies, they were diluted in washing buffer to 6,561 µM for monomers and fibrils and to 243 µM for βPFO. From the maximal concentration 3-fold dilutions were done 6 times. Then, 100 µL were added into every well except for the blanks where just washing buffer was added. Nanobodies were incubated for 1 hour at room temperature under agitation. Finally, in both cases, plates were washed three times.

Primary antibody. Next, the primary antibody was diluted (1:1500 for AntiHis 6x-His Tag Monoclonal Antibody (HIS.H8), eBioscience™ and 1:2000 for antiHAtag monoclonal antibody). 100 µL were added in every well, and left incubate for 1 h at room temperature under agitation. Wells were washed four times.

Secondary antibody. Secondary antibody was diluted (1:200 for both, ECL Mouse IgG HRP-linked whole Ab from sheep, or anti-mouse IgG alkaline phosphatase (AP) conjugated). Subsequently, 100 µL were added in every well, and left incubate for 1 h at room temperature under agitation. Wells were washed six times.

Plate development. When AP conjugated secondary antibody was used, 100 µL of 4-Nitrophenyl phosphate disodium salt hexahydrate at 2 mg/ml from Sigma were added into the wells. The plate was left to evolve in the dark and analyzed every 10 min in a plate reader at 405 nm until signal saturation for 1h. When HRP conjugated secondary antibody was used, 100 µL of "1-Step™ Ultra TMB-ELISA Substrate Solution" from Thermo Fisher were added into the wells and left incubate until signal visually appeared. When most intense signals were near to saturation we added 100 µL of 2 M H_2SO_4 in every well to stop the reaction. The plate was read in a plate reader at 450 nm.

Phage display panning and screening

Protocol when working with phages

Bacteriophages (or phages) are viruses that attack bacteria. Viruses are so small that can be volatile. A phage infection in a lab can cause the systematic death of the bacterial cultures. Therefore, to avoid phage contamination, phages were confined in a certain room equipped with a laminar flow hood. Work with phages was always done under the laminar flow and only using filter tips. The hood was cleaned before and after working in it with bleach. None of the disposable material (globes, tips, plates, etc.) that got into the phage room were brought outside it while the non-disposable material was only brought outside after previous cleaning with bleach. All the used tips, media or solutions were discarded into bleach. Finally, when working with phages, it was very important to avoid foam formation as they are sensible to it.

Enrichment

The library was generated by our collaborators from VUB. The library consisted on the Nanobodies' sequences inserted in pMECS vector. TG1 cells were transformed with the vector library. Subsequently, transformed TG1 cells were incubated with 300ml of 2xTY culture media (16 g/L of Tryptone, 10 g/L of Yeast Extract and 5 g/L of NaCl pH 7) with 100 µg/ml of ampicillin and 1 % glucose with 100 µL of cell library. Incubation was carried out at 37 ºC and 225 rpm for 2-3 h. Afterwards, 10^7 helper phages M13K07 were added and left incubating for 30 min without agitation. Then, the culture was centrifugated. The resulting phage-containing supernatant was mixed with cold PEG/NaCl solution (20 % / 2.5 M respectively) at 1:5 (v:v) and left incubating for 30 min on ice. Next, the resulting solution was centrifugated to collect the white pellet corresponding to the

phages and the supernatant was discarded. The phages were resuspended with PBS and the resulting solution was centrifugated to get rid of any bacteria. Phage solution was then ready for phage selection. A well in one extreme of the ELISA plate was labeled as "+" and was coated with βPFO as previously detailed. A well in the other extreme of ELISA plate was labeled as "-" and left uncoated. Next, both wells were blocked with BSA. Then, 100 µL of phages were added to each well and left incubating for 1 h at room temperature. Both wells were washed 10-times using 150 µL of washing Buffer containing 1.5 mM DPC. Finally, to elute the bound phages coding for specific Nanobodies, 100 µL of 100 mM Triethylamine (TEA) solution were added. The eluted Nanobodies were kept into Eppendorf tubes and pH was immediately equilibrated by adding 100 µL of 1M Tris pH 7.4.

Evaluation of the success of panning

In order to evaluate the panning success, 10 µL of collected phages were sequentially diluted 10-fold. These dilutions were used to infect TG1 cells by incubating them for 30 min at 37°C without shacking. The cells were then plated as lines in an LB-agar plate with 100 µg/ml of Ampicillin and 1 % of glucose. As only the infected bacteria survived, we could compare the infected bacteria concentrations collected from both, "+" and "-" well. After panning evaluation, the phages were used to infect TG1 cells to reamplify and thus a new panning round was started. In every round of panning, the blocking agent used was changed (skim milk, BSA and casein).

Colony selection

A 96-well U-bottom plate from Nunc was filled with 150 µL of Terrific broth (TB) with 100 µg/ml Ampicillin. Up to 95 single colonies from the last round of panning were picked up with a tip, spread into a new agar plate, and finally sunk into the corresponding well of the 96-well plate. The TB plate was incubated at 37°C for 5 h. Then 10 µL of 100 mM IPTG were added to the cells and left incubating overnight. Next day, the plate was frozen at -80°C to break the outer membrane. The plate was centrifugated and the periplasmic extract (PE) was obtained in the supernatant.

Screening

Screening was performed as the previously detailed ELISA experiment with some differences here described. Alternative rows were coated with/without βPFO. All the

wells were blocked with BSA, and after 3 washing steps, PE was added to pairs of βPFO/blank wells. Nanobody-binding was analyzed through the AP reactivity. The screening was done at two different pHs, 7.4 and 9.0. After the first screening, the selected plasmids were transferred into WK6 cell line. A 2nd ELISA was performed with selected clones by doing triplicates of every clone. In this second ELISA, Nanobody binding to βPFO was compared to that to Aβ42 monomer. Plasmids were purified either by PCR or miniprep kit. Plasmids were finally sequenced.

Production of βPFO specific Nanobodies

Chemically competent cells

To be able to transform the E. coli cells with plasmids through a heat shock we need to first, make them chemically competent. For the Chemically Competent Cell (CCC) production, as no antibiotics were used, to work under very sterile conditions is a must. WK6 cells, were kindly provided by Prof. Serge Muyldermans, were plated in a LB-agar + 1 % glucose plate. From a single colony, pre-cultures were grown on LB 1 % glucose. Then, 300 mL of LB media was inoculated with 3 mL of pre-cultures and incubated at 37ºC and 200 rpm until OD_{600} = 0.7 - 0.8. The cultures were cooled down on ice and from then on, the rest of the procedures were carried out in a cold room. The volume was split in 50 mL falcon tubes and centrifugated at 3.200 rpm for 6 min at 4 °C. Supernatant was discarded and cell pellet resuspended in 50 mL of ice-cooled 0.1 M $CaCl_2$. Resuspended cells were kept on ice for 1 h and then centrifugated again. Supernatant was again discarded and cells were resuspended in 50 mL of ice-cooled 0.1 M $CaCl_2$. After 1 h, cells were centrifugated a third time and were resuspended in 2-3 mL of ice-cooled 0.1 M $CaCl_2$ 25% Glycerol. CCC were aliquoted in pre-cooled sterile Eppendorf tubes and rapidly frozen.

Expression

CCC were thawed on ice, 0.4 ng of plasmid coding for the Nanobody were added and left for 30 min on ice. heat-shock was performed by putting the cells in the thermal block at 42ºC for 40s and afterwards left it for 5 min on ice. Next, 450 µL of LB media were added to the cells and incubated at 37ºC for 1 h at 225 rpm. Then the cells are centrifugated for 1 min at 10.000 g and resuspended in 150 µL of LB. The resuspended

cells were spread on a LB-agar plate containing 1 % glucose and 100 µg/ml of Ampicillin. Plates were incubated overnight at 37°C.

The volumes here described for the expression and purification of Nanobodies are for one liter of cell culture even if we usually produced 300 or 500 mL. From a single colony from the agar plate, 10 mL of LB preculture (with 100 µg/mL Ampicillin, 1 mM $MgCl_2$ and 2 % of glucose) were prepared. The preculture was incubated for 4h (up to OD_{600} = 1.5 - 2) or O/N at 37°C and at 225 rpm. Afterwards, it was centrifugated for 1 min at 10.000 g and the supernatant was discarded. The pellet was resuspended and added to the final 1 L of TB media (with 100 µg/mL Ampicillin, 1 mM $MgCl_2$ and 0.1 % of glucose). The culture was incubated in baffled Erlenmeyers (with a capacity at least 3-fold the culture volume) at 37°C and 200 rpm for 2-3 h until OD_{600} = 1. Then, the incubator temperature was lowered to 28°C and IPTG was added at a final 1 mM concentration. Cultures were left overnight at 28°C and next morning (OD_{600} should be around 20) cells were collected by centrifugation for 10 min at 11.250 g at 4°C. Pellet were stored in 50 mL falcon tubes for the ease of the next steps. They were either frozen and kept at -80 °C or directly purified.

Periplasmic extract purification

Nanobodies were expressed in the periplasmic space of *E. coli*. Thus, cells were not lysed, instead periplasmic space was extracted by an osmotic shock. This method provided a purer sample with good yields. To get better yields, a second periplasmic extraction can be done obtaining almost the same amount of Nanobody but with lower purity. The pellet was completely resuspended with 15 mL of cold TES buffer (200 mM Tris, 0.5 mM Ethylenediaminetetraacetic acid (EDTA), 500mM sucrose, pH 8). The resuspended cells were shacked vigorously for one hour at 4 °C. Next, 30 mL of cold TES/4 solution (4-fold diluted TES) were added to the cells. The cells were shacked vigorously for at least 45 min at 4 °C and afterwards centrifugated for 30 min at11.250 g. The supernatant was transferred to another tube and $MgCl_2$ was added to a final concentration of 1 mM to chelate the EDTA present in the solution (otherwise the EDTA would form a chelate with Nickel stripping it from the IMAC column) and finally filtered. The pellet was conserved at -80 °C for a second extraction. The Nanobody obtained from the PE was purified by IMAC with a 1 ml HisTrap HP column (GE Healthcare). Column

was equilibrated and sample injected using Washing Buffer (10mM Imidazole, 50mM Sodium Phosphate, 300mM NaCl, pH 7.4). Finally, sample was eluted using Elution Buffer (300mM Imidazole, 50mM Sodium Phosphate, 300mM NaCl, pH 7.4). The collected Nanobody was purified and buffer exchanged to PBS with a SEC using HiLoad Superdex75 16:600. Finally, Nanobody was concentrated using Vivaspin centrifugal concentrators and quantified by Abs_{280} taking into account the extinction coefficient of each Nanobody.

Analysis of βPFO/Nanobody affinity by ELISA

The experiment was performed as the previously described in materials and methods ELISA experiment. βPFO, Aβ42 monomers and Aβ42 fibrils were coated in the wells. All the Nanobodies were added in 3-fold sequential dilutions from 6.561 µM to 9 nM in the case of Aβ42 monomers and Aβ42 fibrils coated wells, and from 243 nM to 0.33 nM in the case of the βPFO coated ones. Every Nanobody against each Aβ42 specie was analyzed by triplicate. Once revealed, the signal intensity was corrected substracting the blank and the concentrations transformed into a logarithmic scale. The signal intensity was analyzed using GraphPad Prism 7. Signal was fitted with “log(agonist) vs. response with variable slope” equation with bottom constrained to 0 and automatic outlier elimination active.

Analysis of βPFO – Nb interaction by limited Proteolysis coupled to Western Blot

βPFO was formed at 150 µM (Aβ42 nominal concentration). Afterwards, it was diluted 15-fold with 1.5 mM DPC 10 mM Tris buffer at pH 7.4 or 9. Nanobodies were diluted to 10 µM with the same buffer. Samples were mixed 1:1 and incubated for 15 min at 37 °C. The control was directly diluted to 5 µM. Protease was added at a proteinase K:Aβ42 molar ratio of 1:20 and incubated for 45 min at 37 °C. Afterwards, proteolysis was stopped by adding 1 % (v/v) 4-(2-aminoethyl)benzenesulfonyl fluoride hydrochloride (AEBSF) solution. Samples were run in SDS-PAGE without being boiled. The proteins were transferred onto a nitrocellulose membrane (Amersham Protran 0.2 NC) and boiled. Then, membranes were blocked with 5 % BSA, then incubated with primary antibody D9A3A (diluted 1:5000), thirdly with secondary antibody Antirabbit-HRP

(diuted 1:5000) and finally developed with substrate HRP Immobilon Western from Millipore and read on a ChemiDoc XRS+ from Bio-Rad.

Analysis of βPFO – Nb interaction by electrical recordings with planar lipid bilayers

Electrical recordings with planar lipid bilayers were performed as previously described in this and previous works.[60] Pore was formed by adding βPFO to a final 0.6 μM concentration for single pore or to a final 1.5 μM concentration for multiple pore. In both cases, βPFO concentration corresponds to the nominal Aβ42 concentration. After pore formation, the chamber was perfused three times with buffer to reduce βPFO concentration in the chamber and thus avoid Nanobody binding to non-inserted βPFO. All the Nanobody samples were analyzed with single pores and with multiple pores. Results were reproduced at least three times. Nanobodies were added to a final concentration of 0.4-0.5 μM for single pore and 2 μM for multiple pore.

Appendix: Formation of amyloid oligomers in liposomes

Context

As described in the introduction, Aβ is produced from the sequential cleavage of APP by β- and γ-secretases. It is generally considered that after being generated, the Aβ peptide is completely released to the extracellular space where it starts to oligomerize to finally evolve to amyloid fibrils. Previous literature reports have described how soluble oligomers interact with lipid membranes causing calcium dysregulation.[38,47,97-98,119-120] Thus, it is well-accepted within the Aβ hypothesis on AD, that extracellular Aβ oligomers act on the membrane. However, given that the Aβ42 sequence comprises part of the transmembrane domain of APP, the possibility that after Aβ is produced, a partition remains embedded into the membrane cannot be ruled out. If a partition of the Aβ produced is not released upon cleavage, the peptide could remain monomeric in the lipid bilayer and when accumulated at high concentrations start to oligomerize directly in the bilayer **[Figure A-1]**.

To test the hypothesis of Aβ42 oligomerization directly in the membrane, we designed the following experiments. We envisioned that mixing liposomes with soluble Aβ42 would not mimic the scenario of Aβ42 peptide embedded into the bilayer, as the lipid-

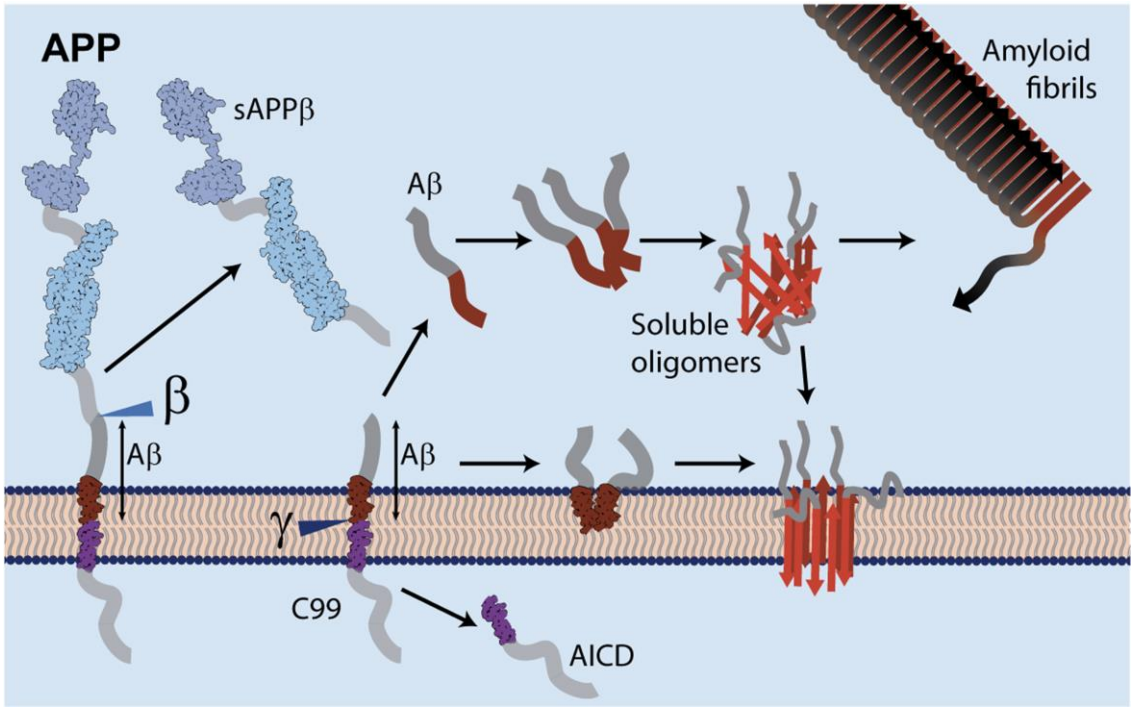

Figure A-1: Scheme describing two hypothetical mechanisms of oligomer formation in membrane. Either monomeric Aβ is released and it forms soluble oligomers that interact with the membrane or else the Aβ peptide is not completely released and remains in the membrane where it oligomerizes.

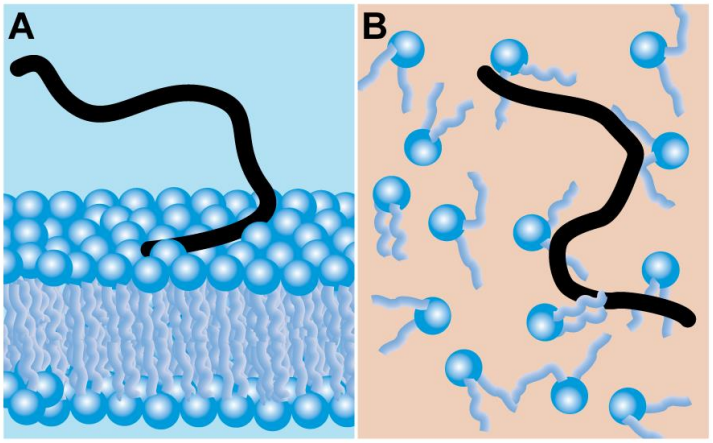

Figure A-2: Scheme of peptide lipid interactions. (A) Peptide interacting with the surface of a lipid bilayer. (B) Peptide co-dissolved with lipids in organic solvent.

peptide contact would be through the polar heads of lipids **[Figure A-2** A**]**. Instead, we proposed to co-solubilize Aβ42 with the lipids in organic solvent, dry the mixture and afterwards resuspend it in aqueous solution. In this manner, we would have direct peptide-hydrophobic chain interaction between the peptide and the lipids in the same way as when Aβ is generated in the membrane **[Figure A-2** B**]**. However, complete Aβ solubilization in organic solvents is not trivial[89]. Different solvents have been proposed in the literature: Chloroform, where lipids are soluble[53] but apparently Aβ is not [89]. TFA, where both lipids[121] and Aβ42[122] are soluble. However, the effect of such a strong acid on the lipid's ester should be determined. Benzene was also used to dissolve Aβ[123]. Alternatively, DMSO is also known to dissolve Aβ. However, because of its high boiling point it is hard to eliminate.

In this appendix, we show a way to insert Aβ42 into bicelles through co-solubilization. This strategy had already been proposed. It's the case, for instance, of the membrane-oligomers that Hai Lin *et al.* showed by AFM. However, they did not show any solubility of Aβ42 in chloroform.[53] Bokvist *et al*. performed similar experiments using Aβ40. They used TFA to solubilize the peptide, and showed a different effect between the membrane anchored peptide and the superficially bound.[121] Others like Nakazaga used benzene to co-solubilize lipids in chloroform/methanol and Aβ without showing peptide solubility neither.[123]

The study of the formation of Aβ oligomers in liposomes doesn't allow the use of solution NMR as in chapter 2 in a technical aspect, due to the high molecular weight of the samples under study. In this sense, I did a research stage in the solid-state NMR (ssNMR) laboratory of Antoine Loquet at the "Institut Européen de Chimie et Biologie" (IECB), with the invaluable help of Denis Martinez.

Results

HFIP is able to dissolve both Aβ42 and POPC

As I have just explained there are several contradictory reports in the literature regarding the solubility of Aβ42 in organic solvents.[53,89,121] Moreover, the solubility of the peptide may also depend on the aggregation state in which it is found at the time of resuspending it. Because of these reasons, we carried out a screening to establish solubility of the previously purified Aβ42 peptide in different organic solvents. We first used organic solvents commonly used to solubilize lipids such as chloroform, methanol, chloroform:methanol 2:1 and 1:1 and dichloromethane:methanol 1:1. Then, we also used benzene, isopropanol, acetonitrile, acetone, ethanol and HFIP. From all these solvents, only benzene and HFIP reached to make optically disappear peptide powder. Thus, we analyzed theses samples by ^{1}H-NMR spectrum **[Figure A-3]**. We compared these spectra with the one obtained from Aβ42 solubilized in DMSO. As it is known, Aβ42 is soluble in DMSO. However, the boiling point of DMSO is 189 °C and has a very low vapor pressure what makes it hard to eliminate by lyophilization or speed-vac. Remaining traces of DMSO would disrupt lipid membrane and is therefore not an appropriate solvent to work with liposomes.[124] Nevertheless, it is a good solvent to be used as a control for complete Aβ42 solubilization.

As a control, the analysis of Aβ42 dissolved in DMSO showed all the regions expected for a peptide. The amide peaks, the aromatic peaks, the H_α and the aliphatic peaks **[Figure A-3** top**]**. On the contrary, when using benzene to solubilize Aβ42, despite that physical aspect showed the disappearance of the solid peptide, we could not find those characteristic peaks from the peptide, only aliphatic peaks most probably from impurities coming from the synthesis of the peptide. **[Figure A-3** mid-top**]**. Indeed, after the NMR analysis, a deposit was visible at the bottom of the tube. Therefore, even if it

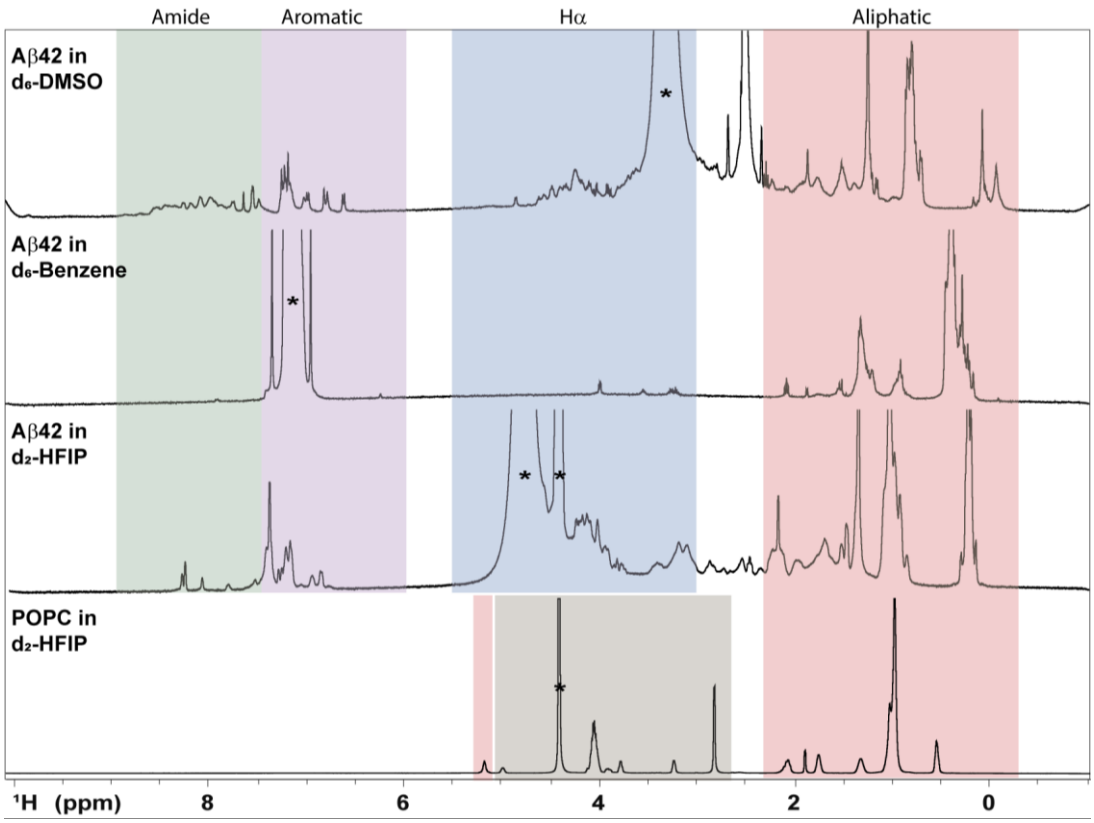

Figure A-3: Aβ42 solubility in different organic solvents. The (green) amide, (purple) aromatic, (blue) Hα and (red) aliphatic regions of the peptide are highlighted. At top, Aβ42 dissolved in DMSO. At mid-top Aβ42 dissolved in benzene. At mid-bottom Aβ42 dissolved in HFIP. At bottom POPC dissolved in HFIP. The polar head of the phosphocholine is highlighted in brown. The peak at 5.2 ppm in the POPC spectra corresponds to the unsaturation of the oleyl chain. (*) solvent peaks.

had been used in the literature to solubilize Aβ40,[123] we conclude that Aβ42 was insoluble in benzene. When the peptide was resuspended in HFIP, we could not detect the amide peaks because of the proton amide exchange with the acidic deuterium of d_2-HFIP, thus silencing the amide signals. However, we could find the aromatic peaks, the Hα peaks and the aliphatic peaks **[Figure A-3** mid-bottom**]**. On the basis of this result, we concluded that Aβ42 was soluble in HFIP. Next, we were interested in knowing whether the lipids could be dissolved in the same solvent or not. For these experiments, we selected 1-palmitoyl-2-oleoyl-sn-glycero-3-phosphocholine (POPC), that is, zwitterionic as DPC. Then, we used HFIP to solubilize the POPC and analyzed the resulting sample by 1D ^{1}H NMR. We found POPC peaks with very narrow linewidths indicating that POPC were completely solubilized as monomers **[Figure A-3** bottom**]**.

Liposomes containing Aβ42 are stable

Next, we developed a protocol to produce Aβ42-containing liposomes. Briefly, Aβ42 was co-solubilized with lipids in HFIP, then the solution was dried and the film resuspended and lyophilized. The latter step was performed to remove HFIP traces as it has been shown that traces of HFIP can disrupt lipid bilayers.[119] To establish liposome formation in the presence of Aβ42 as well as its stability, we prepared two samples following the above described protocol. One sample consisting of POPC liposomes and another one of POPC:Aβ42 50:2 proteoliposomes. We measured the 1D ^{31}P NMR spectra of the samples after immediate preparation and after 6 and 40 days to analyze its isotropy and bandwidth **[Box 1]**.

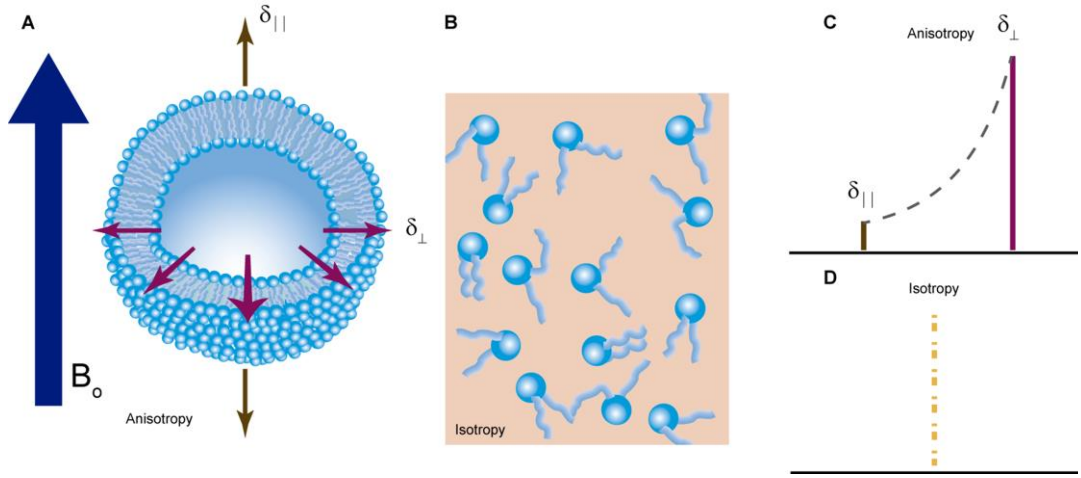

Box 1: ^{31}P NMR signals' interpretation. Liposome with the purple arrows showing the section perpendicular to the magnetic field (Bo) and the brown arrows showing the regions parallel to it (A). Isotropic lipids (B). Scheme of a typical spectra of liposomes (C). Scheme of a spectra of isotropic lipids (D).

When working with anisotropic samples, NMR signals depend on the direction of the atoms relative to the magnetic field. In the case of liposomes, a lamellar phase structure, there are two extreme states, the one parallel to the magnetic field ($\delta_{||}$) and the one perpendicular to it ($\delta_{\perp}$). Between these two extreme locations, the atoms perpendicular to the field are the most populated as this location comprises the whole circular section of the liposome. In contrast, the parallel location, only comprises the few atoms from the upper and lower part of the liposome.

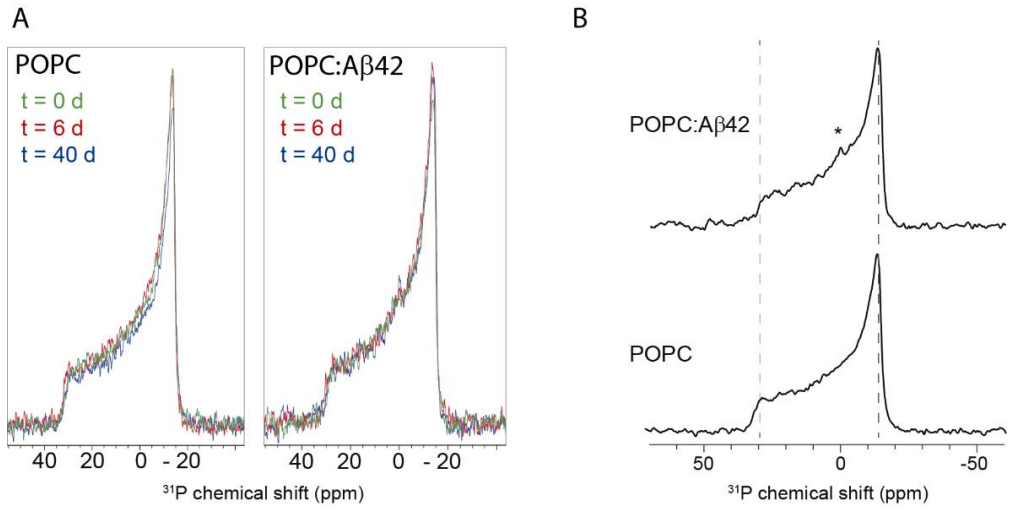

Figure A-4: Liposome stability with the time. Both POPC liposomes (A, left) and Aβ-inserted POPC proteoliposomes (A, right) stay stable after 40 days at 4 °C. Comparison of the bandwidth of the POPC:Aβ42 and the POPC spectrums at t = 0 d (B). (*) Isotropic signal.

These spectra indicate that a lamellar phase in form of liposomes is formed both in the absence and in the presence of Aβ42. Moreover, the analysis also showed no significant loss in stability after 40 days at 4 °C in none of the samples **[Figure A-4** A**]**. At time 0 d, a small but non-significant isotropic signal could be observed **[Figure A-4** B**]** but it did not appear in the rest of experiments.

Aβ affects every part of the POPC molecule

Another information that we can obtain from ^{31}P NMR spectrum is the bandwidth of the peak. Since the chemical shift depends on the relative orientation of the atom to the magnetic field, a more mobile system in the polar heads will have a narrower bandwidth. When comparing the spectrum of POPC and POPC:Aβ42, we observed a decrease in bandwidth **[Figure A-4** B**]**. This indicates that even if there is not a significant part of isotropic lipids, the overall anisotropy is reduced. Implying that the mobility of the polar heads containing the ^{31}P is increased after the Aβ42 insertion.

To determine whether the peptide was inserted in the bilayer or, on the contrary, its effect was just superficial, the same samples were prepared but using partially deuterated liposomes. In the POPC used, the palmitic chain was fully deuterated whereas the oleic chain and the glycerol-phosphocholine was fully protonated. The samples were analyzed using 1D ^{2}H NMR analysis **[Box 2]**. The quadrupolar splitting of

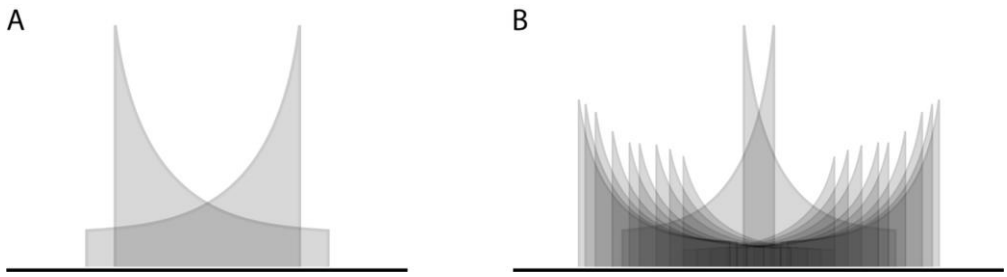

Box 2: Representations of (A) Pake doublet and the (B) ^{2}H signal of an acyl chain from an anisotropic liposome.

In ssNMR, when analyzing deuterated samples, the peak shape changes. As deuterium is a quadrupolar nuclei having a spin of 1, it behaves differently than ½ spin nuclei like ^{31}P. In this case, every spatial direction regarding the magnetic field, shows two opposed peaks instead of one, to finally produce the overlay of two opposed shapes like the one in **[Box 1 C]**. The peak-to-peak separation is called quadrupolar splitting. This effect, with a single deuterium would make a "Pake doublet"[1] **[Box 2** A**]**. When working with fully deuterated acyl chain, successive overlays of "Pake doublets" are found forming a more complex shape where every doublet of maxima represent a set of equivalent deuterium **[Box 2** B**]**.

every doublet of peaks is related to the order parameter of each atom in the acyl chain, which is related to the mobility change at every point across the lipid bilayer. The order parameter of C-^{2}H (S_{CD}) is calculated through the **[Equation 3]**.

Equation 3

(1) $\Delta\vartheta_Q = \frac{3}{4} S_{CD} \cdot A_Q \qquad A_Q = 167\ kHz\ \ (for\ a\ methylene\ CD\ bond)$ [125]

Three samples were analyzed. POPC liposomes, POPC:Aβ42 at 50:2 and at 50:1 giving the spectra from **[Figure A5** A**]**. As just commented, the order parameters were obtained and compared among the three samples **[Figure A5** B**].** It could be seen in all the samples a decrease in order parameter at the end of the palmitoyl chain where the last methyl moves freely. These decrease in order parameter could be also seen at the same level that the instauration of the oleyl chain is found. For the samples prepared in

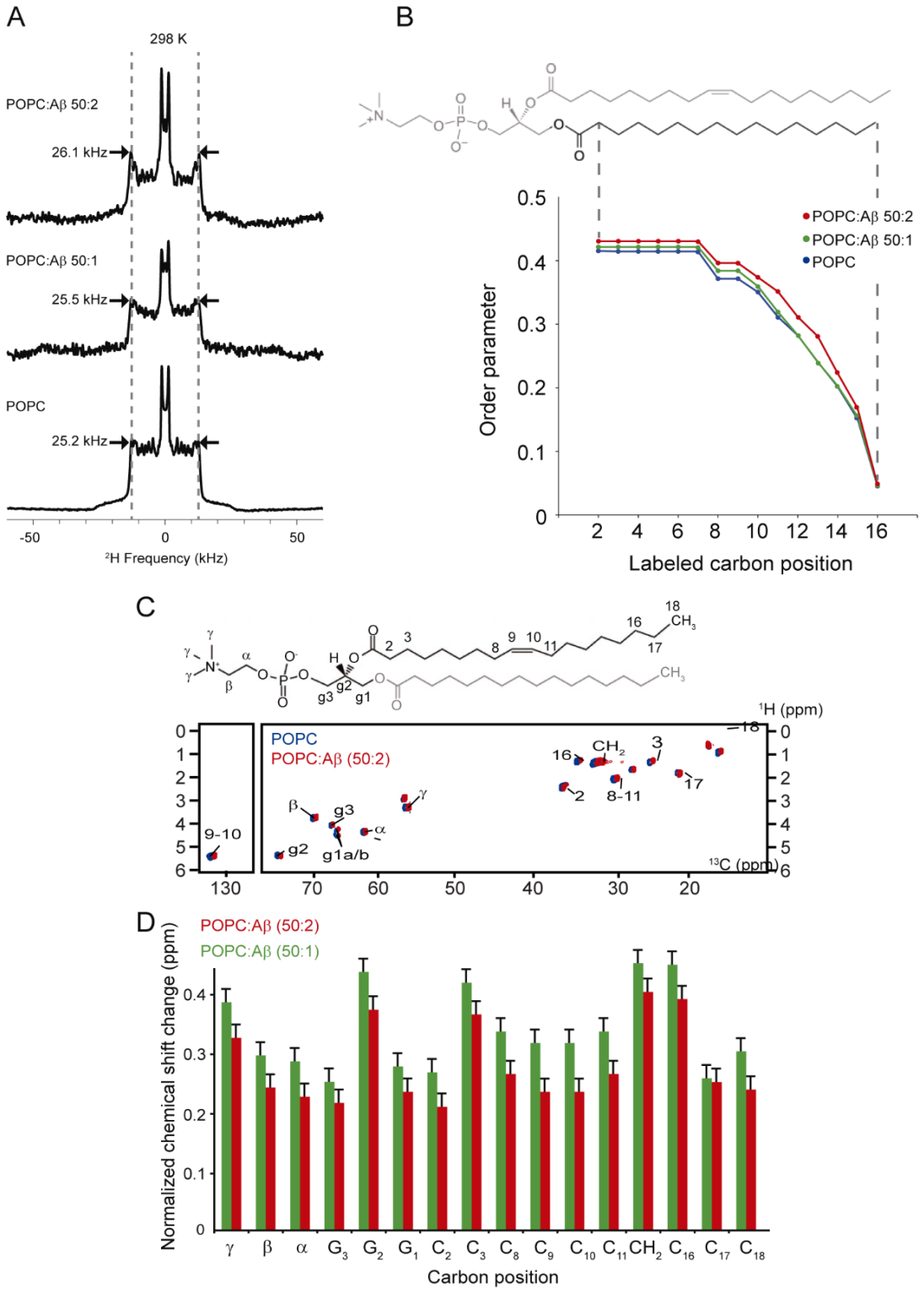

Figure A-5: Effect of Aβ on POPC order parameters and chemical shifts. (A) Spectra of ^{2}H-NMR of (from top to bottom) POPC:Aβ42 50:2, 50:1 and POPC, analyzed at 25°C. (B) Plot of the order parameter of the palmitoyl acyl chain for the three samples studied. (C) 2D ^{1}H-^{13}C INEPT-HSQC using magic angle spinning (MAS). (blue) POPC and (red) POPC:Aβ42 50:2 samples. Peaks corresponding to the protonated oleyl chain and the glycerol-phosphocholine group of POPC shown in black on the atomic structure. (D) Plot of the change in chemical shift as a function of the different concentrations of Aβ42 compared to the POPC control sample.

the presence of Aβ42, the higher the Aβ42 concentration, the more ordered that all the carbons were along the palmitoyl chain.

Moreover, using the same partly deuterated sample, we studied the change in chemical shifts of lipids in the absence and in the presence of Aβ42. To do so, we measured a ^{1}H-^{13}C HSQC, taking advantage of the natural abundance of ^{13}C in the protonated oleic chain while the deuterated palmitic chain stayed invisible **[Figure A** C**]**. The insertion of Aβ42 peptide changed the ^{1}H-^{13}C chemical shift of all the carbons all along the acyl chain. The more significant changes were found at most of the acyl chain between carbons C3 and C16 (except for the unsaturated and unsaturation-bound carbons 8,9,10 and 11), in the carbon G2 from the glycerol group and in the methyl carbons γ of the choline **[Figure A** D**]**. These results showed that Aβ42 peptide was inserted and affecting the carbons of all along the POPC lipid.

Discussion

Following the hypothesis that a partition of Aβ42 is not secreted to the extracellular space and stays attached to the membrane after cleavage, we mimicked this scenario by using a lipid-peptide co-solubilization protocol. This allowed us to have Aβ42 and lipids already mixed before bilayer formation. Other authors co-solubilized Aβ with lipids but without previously showing peptide solubility in their system.

In this work, first, ^{31}P NMR analysis showed that using the co-solubilization protocol, a lamellar phase was formed and the overall structure of the liposome bilayer was preserved in the presence of Aβ42 and thus membrane integrity was preserved **[Figure A-4]**. Moreover, either by ^{31}P or ^{2}H NMR, we showed that peptide insertion in the bilayer was affecting the dynamics of both, polar head and hydrophobic chains by increasing and decreasing their mobility respectively **[Figure A-4** B **and Figure A5** A and B**]**. Therefore, the incorporation of Aβ42 constrained the hydrophobic space while freed space for the polar head mobility. Finally, the ^{1}H-^{13}C INEPT HSQC experiment showed that also the all the atoms were perturbed either from the oleic chain, from the glycerol group or from the choline. Therefore, we can conclude that Aβ42 is in contact with all the structure of the lipids and thus is not only superficially embedded. These results

open the door to the option that it interacts in a transmembrane manner, but further experiments must be done.

The work carried out so far resolves around the study of the effect of Aβ42 on the liposome. Future work will involve the study of the effects of the liposome on Aβ42. To this end appropriately labelled Aβ42 samples will be required. We expect that this work opens new avenues to study Aβ42 oligomer formation in a lipid environment.

Material & Methods

Reagents

Lipids were purchased from Avanti Polar Lipids (Birmingham, AL). Aβ42 was synthesized and purified by Dr. James I. Elliott (New Haven, CT, USA). The rest of reagents were supplied by Sigma-Aldrich.

Aβ42 proteoliposomes preparation

Liposome samples always contained 5 mg of POPC. The amounts of Aβ42 peptide were calculated to prepare samples at a molar POPC:Aβ42 ratio of 50:1 (0,6 mg Aβ42) and 50:2 (1,2 mg Aβ42). The Aβ42 peptide was previously purified as detailed in chapter 1, the required amount aliquoted and then lyophilized. To prepare Aβ42 proteoliposomes, the required amount of Aβ42 was first resuspended resuspended in 500 µL of HFIP. Afterwards, the Aβ42 solution was used to resuspend the 5mg of POPC. In the POPC liposome control sample, the first step was not required and POPC was directly resuspended with HFIP. Finally, solvent was evaporated under a N_2 flow in a fume hood rolling the tube in order to produce a lipid film on the glass walls. When the solvent was completely evaporated, 1 mL of 50 mM $(NH_4)_2CO_3$ (non-adjusted pH) was added and the lipid film resuspended using the vortex. The sample was transferred into an Eppendorf and lyophilized overnight to eliminate HFIP traces. The lyophilized sample could be stored at -20ºC for long-term. To prepare the sample for ssNMR studies, it was resuspended with the required volume of 10 mM Tris pH 9.0 to have a final 70-80% w/w hydration by vortexing it. In the case of ^{2}H-NMR analysis, the buffer was prepared using deuterium-depleted H_2O while in the case of phosphorous analysis the buffer contained

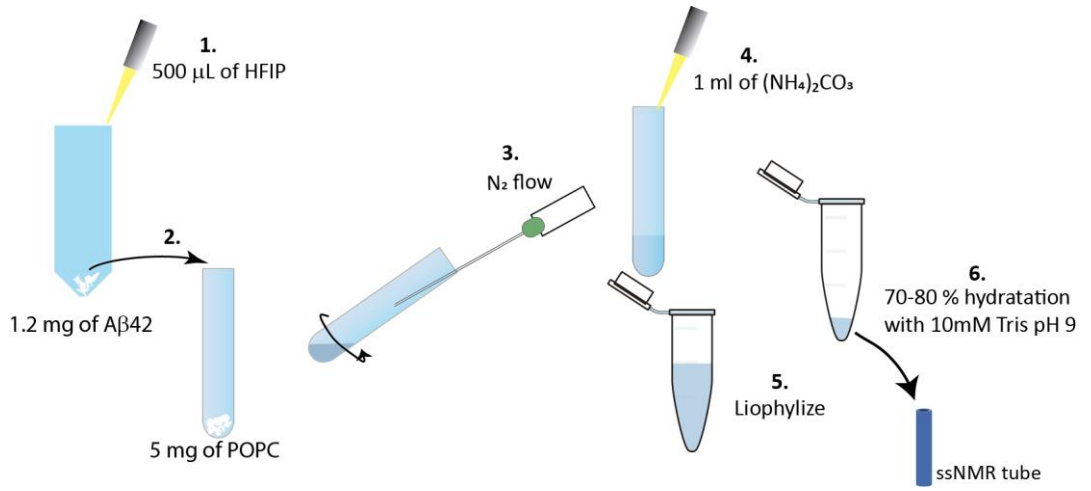

Figure A-6: Scheme of sample preparation.

10% D_2O for the lock. Three freeze-thaw cycles were performed by freezing the sample in liquid N_2 and next incubating it at 37 °C for 10 min. Sample was analyzed using ZrO_2 rotors. The whole process is depicted in **[Figure A-6]**. DSS was added directly to the rotor to be used as a reference.

NMR spectroscopy

^{1}H NMR and ^{31}P NMR experiments were carried out on a Bruker 400 MHz spectrometer at 25 °C. Deuterium NMR experiments on labeled d_{31}-POPC and 2D ^{1}H-^{13}C INEPT-HSQC experiments were carried out in a Bruker 500 MHz spectrometer at 25 °C. Samples were allowed to equilibrate at least 10 min before the NMR spectrum was acquired.

Conclusions

The aim of this thesis was to advance in the validation of βPFO as a new druggable target for AD.

First, we focused on the study of βPFO in bicelles, a biomimetic membrane environment comprising lipids. We showed that the classical DHPC-DMPC bicelle system was not an appropriate system to study βPFO as it caused its aggregation. Next, we developed a new system with DPC-DMPC that could be used at low bicelle concentrations. Afterwards, we showed that βPFO could be reconstituted and could directly be formed into DPC-DMPC bicelles. Moreover, we proved that the overall βPFO structure was preserved as well as its pore-forming activity. On this basis, we concluded that βPFO is stable in a lipid environment.

Second, we focused on obtaining conformational-specific Nanobodies against βPFO to validate βPFO relevance in AD. We obtained eleven Nanobodies, which showed to have higher affinity for βPFO than for Aβ42 monomer and fibrils. Indeed, the difference of affinity between βPFO and Aβ42 monomers and fibrils, was from one to two orders of magnitude. Next, we established that Nanobody binding to βPFO offered different protections to proteases such as Proteinase K. Then, we demonstrated that βPFO-specific Nanobodies were active against the βPFO pores inserted in lipid bilayers. These experiments revealed that the Nanobodies bind to βPFO through different mechanisms: not affecting the electrical recording across a lipid bilayer, and partially or completely blocking the pore formed by βPFO.

Finally, we developed a co-solubilization protocol to produce Aβ42 proteoliposomes. Using solid-state NMR, we showed that, Aβ42 was inserted in the membrane affecting the dynamics of all the atoms of the lipid employed, what could indicate a transmembrane disposition.

References

[1] G. E. Pake, Nuclear resonance absorption in hydrated crystals: Fine structure of the proton line. *J Chem Phys* 1948, *16*, 327-336.

[2] E. Bagyinszky, Y. C. Youn, S. S. A. An, S. Kim, The genetics of Alzheimer's disease. *Clin Interv Aging* 2014, *9*, 535-551.

[3] T. G. Watkinson, A. N. Calabrese, F. Giusti, M. Zoonens, S. E. Radford, A. E. Ashcroft, Systematic analysis of the use of amphipathic polymers for studies of outer membrane proteins using mass spectrometry. *Int J Mass Spectrom* 2015, *391*, 54-61.

[4] A. Van den Abbeele, S. De Clercq, A. De Ganck, V. De Corte, B. Van Loo, S. H. Soror, V. Srinivasan, J. Steyaert, J. Vandekerckhove, J. Gettemans, A llama-derived gelsolin single-domain antibody blocks gelsolin–G-actin interaction. *Cellular and molecular life sciences : CMLS* 2010, *67*, 1519-1535.

[5] R. Katzman, Education and the prevalence of dementia and Alzheimer's disease. *Neurology* 1993, *43*, 13-13.

[6] R. E. Tanzi, The genetics of Alzheimer disease. *Cold Spring Harb Perspect Med* 2012, *2*.

[7] A. C.-H. Martin Prince, Martin Knapp, Maëlenn Guerchet, Maria Karagiannidou, World Alzheimer Report 2016. in *World Alzheimer Report* Alzheimer's Disease International, London, 2016.

[8] H. N. S. Rainulf A. Stelwmann, and F. Reed Muriiagh, An English translation of Alzheimer's 1907 Paper, "Über eine eigenartige Erlranliung der Hirnrinde". *Clin Anat* 1995, *8*, 429-431.

[9] R. Dahm, Alzheimer's discovery. *Curr Biol* 2006, *16*, R906-910.

[10] I. Grundke-Iqbal, K. Iqbal, Y. C. Tung, M. Quinlan, H. M. Wisniewski, L. I. Binder, Abnormal phosphorylation of the microtubule-associated protein tau (tau) in Alzheimer cytoskeletal pathology. *Proc Natl Acad Sci U S A* 1986, *83*, 4913-4917.

[11] C. L. Masters, G. Simms, N. A. Weinman, G. Multhaup, B. L. McDonald, K. Beyreuther, Amyloid plaque core protein in Alzheimer disease and Down syndrome. *Proc Natl Acad Sci U S A* 1985, *82*, 4245-4249.

[12] G. G. Glenner, C. W. Wong, Alzheimer's disease and Down's syndrome: Sharing of a unique cerebrovascular amyloid fibril protein. *Biochem. Biophys. Res. Commun.* 1984, *122*, 1131-1135.

[13] R. Jakob-Roetne, H. Jacobsen, Alzheimer's disease: From pathology to therapeutic approaches. *Angew Chem Int Edit* 2009, *48*, 3030-3059.

[14] W. J. Strittmatter, A. M. Saunders, D. Schmechel, M. Pericak-Vance, J. Enghild, G. S. Salvesen, A. D. Roses, Apolipoprotein E: high-avidity binding to beta-amyloid

and increased frequency of type 4 allele in late-onset familial Alzheimer disease. *Proc Natl Acad Sci U S A* 1993, *90*, 1977-1981.

[15] A. C. Slooter, M. Cruts, S. Kalmijn, et al., Risk estimates of dementia by apolipoprotein e genotypes from a population-based incidence study: The rotterdam study. *Arch Neurol* 1998, *55*, 964-968.

[16] D. M. Walsh, D. J. Selkoe, Ab Oligomers - a decade of discovery. *J Neurochem* 2007, *101*, 1172-1184.

[17] L. M. Ittner, J. Gotz, Amyloid-beta and tau-a toxic pas de deux in Alzheimer's disease. *Nat Rev Neurosci* 2011, *12*, 65-72.

[18] D. W. Dickson, Neuropathology of non-Alzheimer degenerative disorders. *Int J Clin Exp Pathol* 2010, *3*, 1-23.

[19] V. W. Chow, M. P. Mattson, P. C. Wong, M. Gleichmann, An overview of APP processing enzymes and products. *Neuromolecular Med* 2010, *12*, 1-12.

[20] X. C. Bai, C. Yan, G. Yang, P. Lu, D. Ma, L. Sun, R. Zhou, S. H. W. Scheres, Y. Shi, An atomic structure of human gamma-secretase. *Nature* 2015, *525*, 212-217.

[21] W. T. Kimberly, M. J. LaVoie, B. L. Ostaszewski, W. Ye, M. S. Wolfe, D. J. Selkoe, γ-Secretase is a membrane protein complex comprised of presenilin, nicastrin, aph-1, and pen-2. *Proc Natl Acad Sci U S A* 2003, *100*, 6382-6387.

[22] C. Haass, Take five—BACE and the γ-secretase quartet conduct Alzheimer's amyloid β-peptide generation. *EMBO J* 2004, *23*, 483-488.

[23] C. Haass, C. Kaether, G. Thinakaran, S. Sisodia, Trafficking and proteolytic processing of APP. *Cold Spring Harb Perspect Med* 2012, *2*, a006270.

[24] M. Vestergaard, T. Hamada, M. Takagi, Using model membranes for the study of amyloid beta:lipid interactions and neurotoxicity. *Biotechnol Bioeng* 2008, *99*, 753-763.

[25] M. G. Zagorski, J. Yang, H. Shao, K. Ma, H. Zeng, A. Hong, in *Methods Enzymol, Vol. 309*, Academic Press, 1999, pp. 189-204.

[26] D. J. Selkoe, J. Hardy, The amyloid hypothesis of Alzheimer's disease at 25 years. *EMBO Mol Med* 2016, *8*, 595-608.

[27] K. Herrup, The case for rejecting the amyloid cascade hypothesis. *Nat Neurosci* 2015, *18*, 794-799.

[28] E. Karran, M. Mercken, B. De Strooper, The amyloid cascade hypothesis for Alzheimer's disease: an appraisal for the development of therapeutics. *Nat Rev Drug Discov* 2011, *10*, 698-712.

[29] J. Hardy, B. De Strooper, Alzheimer's disease: where next for anti-amyloid therapies? *Brain* 2017, *140*, 853-855.

[30] J. Sevigny, P. Chiao, T. Bussière, P. H. Weinreb, L. Williams, M. Maier, R. Dunstan, S. Salloway, T. Chen, Y. Ling, J. O'Gorman, F. Qian, M. Arastu, M. Li, S. Chollate, M. S. Brennan, O. Quintero-Monzon, R. H. Scannevin, H. M. Arnold, T. Engber, K. Rhodes, J. Ferrero, Y. Hang, A. Mikulskis, J. Grimm, C. Hock, R. M. Nitsch, A. Sandrock, The antibody aducanumab reduces Aβ plaques in Alzheimer's disease. *Nature* 2016, *537*, 50-56.

[31] J. L. Price, D. W. McKeel, Jr., V. D. Buckles, C. M. Roe, C. Xiong, M. Grundman, L. A. Hansen, R. C. Petersen, J. E. Parisi, D. W. Dickson, C. D. Smith, D. G. Davis, F. A. Schmitt, W. R. Markesbery, J. Kaye, R. Kurlan, C. Hulette, B. F. Kurland, R. Higdon, W. Kukull, J. C. Morris, Neuropathology of nondemented aging: presumptive evidence for preclinical Alzheimer disease. *Neurobiol Aging* 2009, *30*, 1026-1036.

[32] C. J. Pike, A. J. Walencewicz, C. G. Glabe, C. W. Cotman, In vitro aging of β-amyloid protein causes peptide aggregation and neurotoxicity. *Brain Res* 1991, *563*, 311-314.

[33] C. A. McLean, R. A. Cherny, F. W. Fraser, S. J. Fuller, M. J. Smith, V. Konrad, A. I. Bush, C. L. Masters, Soluble pool of Aβ amyloid as a determinant of severity of neurodegeneration in Alzheimer's disease. *Ann Neurol* 1999, *46*, 860-866.

[34] L.-F. Lue, Y.-M. Kuo, A. E. Roher, L. Brachova, Y. Shen, L. Sue, T. Beach, J. H. Kurth, R. E. Rydel, J. Rogers, Soluble Amyloid β Peptide Concentration as a Predictor of Synaptic Change in Alzheimer's Disease. *Am J Pathol* 1999, *155*, 853-862.

[35] D. Huang, M. I. Zimmerman, P. K. Martin, A. J. Nix, T. L. Rosenberry, A. K. Paravastu, Antiparallel β-sheet structure within the C-terminal region of 42-residue Alzheimer's amyloid-β peptides when they form 150-kDa oligomers. *J Mol Biol* 2015, *427*, 2319-2328.

[36] E. H. Rakez Kayed, Jennifer L. Thompson, Theresa M. McIntire, Saskia C. Milton, Carl W. Cotman, Charles G. Glabe, Common structure of soluble amyloid oligomers implies common mechanism of pathogenesis. *Science* 2003, *300*.

[37] M. P. Lambert, A. K. Barlow, B. A. Chromy, C. Edwards, R. Freed, M. Liosatos, T. E. Morgan, I. Rozovsky, B. Trommer, K. L. Viola, P. Wals, C. Zhang, C. E. Finch, G. A. Krafft, W. L. Klein, Diffusible, nonfibrillar ligands derived from Aβ1–42 are potent central nervous system neurotoxins. *Proc Natl Acad Sci U S A* 1998, *95*, 6448-6453.

[38] A. Drews, J. Flint, N. Shivji, P. Jonsson, D. Wirthensohn, E. De Genst, C. Vincke, S. Muyldermans, C. Dobson, D. Klenerman, Individual aggregates of amyloid beta induce temporary calcium influx through the cell membrane of neuronal cells. *Sci Rep* 2016, *6*, 31910.

[39] D. C. Bode, M. D. Baker, J. H. Viles, Ion channel formation by amyloid-β42 oligomers but not amyloid-β40 in cellular membranes. *J Biol Chem* 2017, *292*, 1404-1413.

[40] D. M. Walsh, I. Klyubin, J. V. Fadeeva, W. K. Cullen, R. Anwyl, M. S. Wolfe, M. J. Rowan, D. J. Selkoe, Naturally secreted oligomers of amyloid β protein potently inhibit hippocampal long-term potentiation in vivo. *Nature* 2002, *416*, 535.

[41] R. Kayed, Y. Sokolov, B. Edmonds, T. M. McIntire, S. C. Milton, J. E. Hall, C. G. Glabe, Permeabilization of lipid bilayers is a common conformation-dependent activity of soluble amyloid oligomers in protein misfolding diseases. *J Biol Chem* 2004, *279*, 46363-46366.

[42] B. Serra-Vidal, L. Pujadas, D. Rossi, E. Soriano, S. Madurga, N. Carulla, Hydrogen/deuterium exchange-protected oligomers populated during Abeta fibril formation correlate with neuronal cell death. *ACS Chem Biol* 2014, *9*, 2678-2685.

[43] G. M. Shankar, S. Li, T. H. Mehta, A. Garcia-Munoz, N. E. Shepardson, I. Smith, F. M. Brett, M. A. Farrell, M. J. Rowan, C. A. Lemere, C. M. Regan, D. M. Walsh, B. L. Sabatini, D. J. Selkoe, Amyloid-β protein dimers isolated directly from Alzheimer's brains impair synaptic plasticity and memory. *Nat Med* 2008, *14*, 837.

[44] S. Lesné, M. T. Koh, L. Kotilinek, R. Kayed, C. G. Glabe, A. Yang, M. Gallagher, K. H. Ashe, A specific amyloid-β protein assembly in the brain impairs memory. *Nature* 2006, *440*, 352.

[45] R. Pujol-Pina, S. Vilaprinyo-Pascual, R. Mazzucato, A. Arcella, M. Vilaseca, M. Orozco, N. Carulla, SDS-PAGE analysis of Abeta oligomers is disserving research into Alzheimer s disease: appealing for ESI-IM-MS. *Sci Rep* 2015, *5*, 14809.

[46] D. M. Walsh, A. Lomakin, G. B. Benedek, M. M. Condron, D. B. Teplow, Amyloid β-protein fibrillogenesis: Detection of a protofibrillar intermediate. *J Biol Chem* 1997, *272*, 22364-22372.

[47] D. M. Hartley, D. M. Walsh, C. P. Ye, T. Diehl, S. Vasquez, P. M. Vassilev, D. B. Teplow, D. J. Selkoe, Protofibrillar intermediates of amyloid β-protein induce acute electrophysiological changes and progressive neurotoxicity in cortical neurons. *J Neurosci* 1999, *19*, 8876-8884.

[48] S. Barghorn, V. Nimmrich, A. Striebinger, C. Krantz, P. Keller, B. Janson, M. Bahr, M. Schmidt, R. S. Bitner, J. Harlan, E. Barlow, U. Ebert, H. Hillen, Globular amyloid beta-peptide1-42 oligomer - a homogenous and stable neuropathological protein in Alzheimer's disease. *J Neurochem* 2005, *95*, 834-847.

[49] E. Cerf, R. Sarroukh, S. Tamamizu-Kato, L. Breydo, S. Derclaye, Y. F. Dufrene, V. Narayanaswami, E. Goormaghtigh, J. M. Ruysschaert, V. Raussens, Antiparallel beta-sheet: a signature structure of the oligomeric amyloid beta-peptide. *Biochem J* 2009, *421*, 415-423.

[50] J. Laurén, D. A. Gimbel, H. B. Nygaard, J. W. Gilbert, S. M. Strittmatter, Cellular prion protein mediates impairment of synaptic plasticity by amyloid-β oligomers. *Nature* 2009, *457*, 1128-1132.

[51] N. Arispe, E. Rojas, H. B. Pollard, Alzheimer disease amyloid beta protein forms calcium channels in bilayer membranes: blockade by tromethamine and aluminum. *Proc Natl Acad Sci U S A* 1993, *90*, 567-571.

[52] H. B. P. Nelson Arispe, and Eduardo Rojas, Zn2+ interaction with Alzheimer amyloid beta protein calcium channels. *Proc Natl Acad Sci U S A* 1996, *93*, 1710-1171.

[53] R. B. Hai Lin, and Ratneshwar Lal, Amyloid beta protein forms ion channels: implications for Alzheimer's disease pathophysiology. *FASEB J* 2001, *15*, 2433-2444.

[54] J. I. Kourie, C. L. Henry, P. Farrelly, Diversity of amyloid β protein fragment [1–40]-formed channels. *Cell Mol Neurobiol* 2001, *21*, 255-284.

[55] Y. Hirakura, M.-C. Lin, B. L. Kagan, Alzheimer amyloid Aβ1–42 channels: Effects of solvent, pH, and congo red. *J Neurosci Res* 1999, *57*, 458-466.

[56] P. K. Mandal, J. W. Pettegrew, Alzheimer's Disease: Soluble Oligomeric Aβ(1–40) Peptide in Membrane Mimic Environment from Solution NMR and Circular Dichroism Studies. *Neurochem Res* 2004, *29*, 2267–2272.

[57] R. E. Liping Yu, John E. Harlan, Thomas F. Holzman, Ana Pereda Lopez, Boris Labkovsky, Heinz Hillen, Stefan Barghorn, Ulrich Ebert, Paul L. Richardson, Laura Miesbauer, Larry Solomon, Diane Bartley, Karl Walter, Robert W. Johnson, Philip J. Hajduk and Edward T. Olejniczak, Structural characterization of a soluble amyloid β-peptide oligomer. *Biochemistry* 2009, *48*, 1870–1877.

[58] H. Shao, S.-c. Jao, K. Ma, M. G. Zagorski, Solution structures of micelle-bound amyloid β-(1-40) and β-(1-42) peptides of Alzheimer's disease11Edited by P. E. Wright. *J Mol Biol* 1999, *285*, 755-773.

[59] J. L. Popot, Amphipols, nanodiscs, and fluorinated surfactants: three nonconventional approaches to studying membrane proteins in aqueous solutions. *Annu Rev Biochem* 2010, *79*, 737-775.

[60] M. Serra-Batiste, M. Ninot-Pedrosa, M. Bayoumi, M. Gairí, G. Maglia, N. Carulla, Aβ42 assembles into specific β-barrel pore-forming oligomers in membrane-mimicking environments. *Proc Natl Acad Sci U S A* 2016, *113*, 10866-10871.

[61] D. E. Otzen, K. K. Andersen, Folding of outer membrane proteins. *Arch Biochem Biophys* 2013, *531*, 34-43.

[62] N. K. Burgess, T. P. Dao, A. M. Stanley, K. G. Fleming, β-barrel proteins that reside in the Escherichia coli outer membrane in vivo demonstrate varied folding behaviorin vitro. *J Biol Chem* 2008, *283*, 26748-26758.

[63] E. Wallin, G. V. Heijne, Genome-wide analysis of integral membrane proteins from eubacterial, archaean, and eukaryotic organisms. *Protein Sci* 1998, *7*, 1029-1038.

[64] S. Hiller, R. G. Garces, T. J. Malia, V. Y. Orekhov, M. Colombini, G. Wagner, Solution structure of the integral human membrane protein VDAC-1 in setergent micelles. *Science* 2008, *321*, 1206-1210.

[65] Y. Song, K. F. Mittendorf, Z. Lu, C. R. Sanders, Impact of bilayer lipid composition on the structure and topology of the transmembrane amyloid precursor C99 protein. *J Am Chem Soc* 2014, *136*, 4093-4096.

[66] A. M. Seddon, P. Curnow, P. J. Booth, Membrane proteins, lipids and detergents: not just a soap opera. *Biochem. Biophys. Res. Commun.* 2004, *1666*, 105-117.

[67] R. A. a. J.-L. P. Christophe Tribet, Amphipols: Polymers that keep membrane proteins soluble in aqueous solutions. *Proc Natl Acad Sci U S A* 1996, *93*, 15047–15050,.

[68] A. Jonas, K. E. Kézdy, J. H. Wald, Defined apolipoprotein A-I conformations in reconstituted high density lipoprotein discs. *J Biol Chem* 1989, *264*, 4818-4824.

[69] M. A. Schuler, I. G. Denisov, S. G. Sligar, in *Lipid-Protein Interactions: Methods and Protocols* (Ed.: J. H. Kleinschmidt), Humana Press, Totowa, NJ, 2013, pp. 415-433.

[70] C. R. Sanders, *Development and application of bicelles for use in biological NMR and other biophysical studies*, 2005.

[71] D. E. Warschawski, A. A. Arnold, M. Beaugrand, A. Gravel, É. Chartrand, I. Marcotte, Choosing membrane mimetics for NMR structural studies of transmembrane proteins. *BBA-Biomembranes* 2011, *1808*, 1957-1974.

[72] E. A. Morrison, K. A. Henzler-Wildman, Reconstitution of integral membrane proteins into isotropic bicelles with improved sample stability and expanded lipid composition profile. *BBA-Biomembranes* 2012, *1818*, 814-820.

[73] K. F. A. W. Donghan Lee, Ann-Kathrin Brückner, Christian Hilty, Stefan Becker, and Christian Griesinger, Bilayer in small bicelles revealed by lipid-protein interactions using NMR spectroscopy. *J Am Chem Soc* 2008, *130*, 13822–13823.

[74] J. A. W. Kerney J. Glover, Guohua Wu, Nan-jun Yu, Raymond Deems, Jochem O. Struppe, Ruth E. Stark, Elizabeth A. Komives, and Regitze R. Vold, Structural evaluation of phospholipid bicelles for solution-state studies of membrane-associated biomolecules. *Biophys J* 2001, *81*, 2163–2171.

[75] L. Frey, N.-A. Lakomek, R. Riek, S. Bibow, Micelles, bicelles, and nanodiscs: Comparing the impact of membrane mimetics on membrane protein backbone dynamics. *Angew Chem Int Edit* 2017, *56*, 380-383.

[76] J. T. S. Hopper, Y. T.-C. Yu, D. Li, A. Raymond, M. Bostock, I. Liko, V. Mikhailov, A. Laganowsky, J. L. P. Benesch, M. Caffrey, D. Nietlispach, C. V. Robinson, Detergent-free mass spectrometry of membrane protein complexes. *Nat Methods* 2013, *10*, 1206-1208.

[77] T. A. H. John Katsaras, Jeremy Pencer, Mu-Ping Nieh, "Bicellar" lipid mixtures as used in biochemical and biophysical studies. *Naturwissenschaften* 2005, *92*, 355–366.

[78] I. Kucharska, T. C. Edrington, B. Liang, L. K. Tamm, Optimizing nanodiscs and bicelles for solution NMR studies of two β-barrel membrane proteins. *J Biomol NMR* 2015, *61*, 261-274.

[79] J. Liebau, W. Ye, L. Mäler, Characterization of fast-tumbling isotropic bicelles by PFG diffusion NMR. *Magn Reson Chem* 2017, *55*, 395-404.

[80] Z. Lu, W. D. Van Horn, J. Chen, S. Mathew, R. Zent, C. R. Sanders, Bicelles at low concentrations. *Mol Pharm* 2012, *9*, 752-761.

[81] B.-B. Lucyanna, R. Gelen, C. Merce, R. Laia, L.-I. Carmen, D. l. M. Alfons, L. Olga, Structural versatility of bicellar systems and their possibilities as colloidal carriers. *Pharmaceutics* 2011, *3*, 636-664.

[82] A. Piai, Q. Fu, J. Dev, J. J. Chou, Optimal bicelle q for solution NMR studies of the protein transmembrane partition. *Chem Eur J* 2017, *23*, 1361-1367.

[83] M. Vestergaard, J. F. Kraft, T. Vosegaard, L. Thøgersen, B. Schiøtt, Bicelles and Other Membrane Mimics: Comparison of Structure, Properties, and Dynamics from MD Simulations. *J Phys Chem B* 2015, *119*, 15831-15843.

[84] O. V. Nolandt, T. H. Walther, S. L. Grage, A. S. Ulrich, Magnetically oriented dodecylphosphocholine bicelles for solid-state NMR structure analysis. *BBA-Biomembranes* 2012, *1818*, 1142-1147.

[85] D. Lee, C. Hilty, G. Wider, K. Wüthrich, Effective rotational correlation times of proteins from NMR relaxation interference. *J Mag Res* 2006, *178*, 72-76.

[86] S. S. S. Wang, Y.-T. Chen, S.-W. Chou, Inhibition of amyloid fibril formation of β-amyloid peptides via the amphiphilic surfactants. *Biochim Biophys Acta* 2005, *1741*, 307-313.

[87] K. Dahse, M. Garvey, M. Kovermann, A. Vogel, J. Balbach, M. Fändrich, A. Fahr, DHPC Strongly Affects the Structure and Oligomerization Propensity of Alzheimer's Aβ(1–40) Peptide. *J Mol Biol* 2010, *403*, 643-659.

[88] M. Beaugrand, A. A. Arnold, S. Bourgault, P. T. F. Williamson, I. Marcotte, Comparative study of the structure and interaction of the pore helices of the hERG and Kv1.5 potassium channels in model membranes. *Eur Biophys J* 2017, *46*, 549-559.

[89] L. Malavolta, M. R. S. Pinto, J. H. Cuvero, C. R. Nakaie, Interpretation of the dissolution of insoluble peptide sequences based on the acid-base properties of the solvent. *Protein Sci* 2006, *15*, 1476-1488.

[90] K. J. Korshavn, A. Bhunia, M. H. Lim, A. Ramamoorthy, Amyloid-β adopts a conserved, partially folded structure upon binding to zwitterionic lipid bilayers prior to amyloid formation. *Chem commun* 2016, *52*, 882-885.

[91] D. Bhowmik, K. R. Mote, C. M. MacLaughlin, N. Biswas, B. Chandra, J. K. Basu, G. C. Walker, P. K. Madhu, S. Maiti, Cell-membrane-mimicking lipid-coated nanoparticles confer raman enhancement to membrane proteins and reveal membrane-attached amyloid-β conformation. *ACS Nano* 2015, *9*, 9070-9077.

[92] M. Serra-Batiste, R. Garcia-Castellanos, M. Ninot-Pedrosa, B. Serra-Vidal, N. Simon Berrow, N. Carulla, Alzheimer's disease-associated Aβ42 peptide: Expression and purification for NMR structural studies. *Curr Chem Biol* 2017, *11*, 50-62.

[93] R. C. Tyler, H. K. Sreenath, S. Singh, D. J. Aceti, C. A. Bingman, J. L. Markley, B. G. Fox, Auto-induction medium for the production of [U-15N]- and [U-13C, U-15N]-labeled proteins for NMR screening and structure determination. *Protein Expression and Purif* 2005, *40*, 268-278.

[94] F. W. Studier, Protein production by auto-induction in high-density shaking cultures. *Protein Expression and Purif* 2005, *41*, 207-234.

[95] R. Assenberg, O. Delmas, S. C. Graham, A. Verma, N. Berrow, D. I. Stuart, R. J. Owens, H. Bourhy, J. M. Grimes, Expression, purification and crystallization of a lyssavirus matrix (M) protein. *Acta Crystallogr F* 2008, *64*, 258-262.

[96] C. R. Sanders, F. Sönnichsen, Solution NMR of membrane proteins: practice and challenges. *Magn Reson Chem* 2006, *44*, S24-S40.

[97] C. Di Scala, N. Yahi, A. Flores, S. Boutemeur, N. Kourdougli, H. Chahinian, J. Fantini, Broad neutralization of calcium-permeable amyloid pore channels with a chimeric Alzheimer/Parkinson peptide targeting brain gangliosides. *BBA-Mol Basis Dis* 2016, *1862*, 213-222.

[98] C. Di Scala, N. Yahi, S. Boutemeur, A. Flores, L. Rodriguez, H. Chahinian, J. Fantini, Common molecular mechanism of amyloid pore formation by Alzheimer's β-amyloid peptide and α-synuclein. *SCI REP* 2016, *6*.

[99] S. Muyldermans, Single domain camel antibodies: current status. *Rev Mol Bio/Technol* 2001.

[100] C. Hamers-Casterman, T. Atarhouch, S. Muyldermans, G. Robinson, C. Hamers, E. B. Songa, N. Bendahman, R. Hamers, Naturally occurring antibodies devoid of light chains. *Nature* 1993, *363*, 446-448.

[101] S. Muyldermans, Nanobodies: Natural single-domain antibodies. *Annu Rev Biochem* 2013, *82*, 775-797.

[102] M. Zoonens, J. L. Popot, Amphipols for each season. *J Membr Biol* 2014, *247*, 759-796.

[103] J. L. Popot, T. Althoff, D. Bagnard, J. L. Banères, P. Bazzacco, E. Billon-Denis, L. J. Catoire, P. Champeil, D. Charvolin, M. J. Cocco, G. Crémel, T. Dahmane, L. M. de la Maza, C. Ebel, F. Gabel, F. Giusti, Y. Gohon, E. Goormaghtigh, E. Guittet, J. H. Kleinschmidt, W. Kühlbrandt, C. Le Bon, K. L. Martinez, M. Picard, B. Pucci, J. N. Sachs, C. Tribet, C. van Heijenoort, F. Wien, F. Zito, M. Zoonens, Amphipols From A to Z*. *Ann Rev Biophys* 2011, *40*, 379-408.

[104] K. S. S. Paola Bazzacco, Grégory Durand, Fabrice Giusti, Christine Ebel, Jean-Luc Popot and Bernard Pucci, Trapping and stabilization of integral membrane proteins by hydrophobically grafted glucose-based telomers. *Biomacromolecules* 2009, *10*, 3317–3326.

[105] M. Serra-Batiste, F. Giusti, M. Zoonens, N. Carulla, Antigen preparation for the validation of a membrane-associated amyloid-β oligomer in Alzheimer's disease. in *"Structural and Molecular Biology of Alzheimer's Disease"*, Front. Mol. Biosci. , (under revision).

[106] E. Pardon, T. Laeremans, S. Triest, S. G. F. Rasmussen, A. Wohlkönig, A. Ruf, S. Muyldermans, W. G. J. Hol, B. K. Kobilka, J. Steyaert, A general protocol for the generation of Nanobodies for structural biology. *Nat Protoc* 2014, *9*, 674-693.

[107] G. Paraschiv, C. Vincke, P. Czaplewska, M. Manea, S. Muyldermans, M. Przybylski, Epitope structure and binding affinity of single chain llama anti-beta-amyloid antibodies revealed by proteolytic excision affinity-mass spectrometry. *J Mol Recognit* 2013, *26*, 1-9.

[108] P. Flagmeier, S. De, D. C. Wirthensohn, S. F. Lee, C. Vincke, S. Muyldermans, T. P. J. Knowles, S. Gandhi, C. M. Dobson, D. Klenerman, Ultrasensitive measurement of Ca2+ influx into lipid vesicles induced by protein aggregates. *Angew Chem Int Edit* 2017, *56*, 7750-7754.

[109] G. Paraschiv, C. Vincke, P. Czaplewska, M. Manea, S. Muyldermans, M. Przybylski, Epitope structure and binding affinity of single chain llama anti-β-amyloid antibodies revealed by proteolytic excision affinity-mass spectrometry. *Journal of Molecular Recognition* 2013, *26*, 1-9.

[110] A. Sebollela, G.-M. Mustata, K. Luo, P. T. Velasco, K. L. Viola, E. N. Cline, G. S. Shekhawat, K. C. Wilcox, V. P. Dravid, W. L. Klein, Elucidating molecular mass and shape of a neurotoxic Aβ oligomer. *ACS Chem Neurosci* 2014, *5*, 1238-1245.

[111] C. H. Gernot Habicht, Ralf P. Friedrich, Peter Hortschansky, Carsten Sachse, Jessica Meinhardt, Karin Wieligmann, Gerald P. Gellermann, Michael Brodhun, Jürgen Götz, Karl-Juürgen Halbhuber, Christoph Röcken, Uwe Horn, and Marcus Fändrich, Directed selection of a conformational antibody domain that prevents mature amyloid fibril formation by stabilizing Aβ protofibrils. *Proc Natl Acad Sci U S A* 2007, *104*, 19232–19237.

[112] I. Morgado, K. Wieligmann, M. Bereza, R. Rönicke, K. Meinhardt, K. Annamalai, M. Baumann, J. Wacker, P. Hortschansky, M. Malešević, C. Parthier, C. Mawrin, C. Schiene-Fischer, K. G. Reymann, M. T. Stubbs, J. Balbach, M. Görlach, U. Horn, M. Fändrich, Molecular basis of β-amyloid oligomer recognition with a conformational antibody fragment. *Proceedings of the National Academy of Sciences* 2012, *109*, 12503-12508.

[113] C. Pain, J. Dumont, M. Dumoulin, Camelid single-domain antibody fragments: Uses and prospects to investigate protein misfolding and aggregation, and to treat diseases associated with these phenomena. *Biochimie* 2015, *111*, 82-106.

[114] M. A. David, D. R. Jones, M. Tayebi, Potential candidate camelid antibodies for the treatment of protein-misfolding diseases. *J Neuroimmunol* 2014, *272*, 76-85.

[115] M. Vandesquille, T. Li, C. Po, C. Ganneau, P. Lenormand, C. Dudeffant, C. Czech, F. Grueninger, C. Duyckaerts, B. Delatour, M. Dhenain, P. Lafaye, S. Bay, Chemically-defined camelid antibody bioconjugate for the magnetic resonance imaging of Alzheimer's disease. *mAbs* 2017, *9*, 1016-1027.

[116] P. Lafaye, I. Achour, P. England, C. Duyckaerts, F. Rougeon, Single-domain antibodies recognize selectively small oligomeric forms of amyloid beta, prevent Abeta-induced neurotoxicity and inhibit fibril formation. *Mol Immunol* 2009, *46*, 695-704.

[117] K. S. Rutgers, A. van Remoortere, M. A. van Buchem, C. T. Verrips, S. M. Greenberg, B. J. Bacskai, M. P. Frosch, S. G. van Duinen, M. L. Maat-Schieman, S. M. van der Maarel, Differential recognition of vascular and parenchymal beta amyloid deposition. *Neurobiol Aging* 2011, *32*, 1774-1783.

[118] K. S. Rutgers, R. J. Nabuurs, S. A. van den Berg, G. J. Schenk, M. Rotman, C. T. Verrips, S. G. van Duinen, M. L. Maat-Schieman, M. A. van Buchem, A. G. de Boer, S. M. van der Maarel, Transmigration of beta amyloid specific heavy chain antibody fragments across the in vitro blood-brain barrier. *Neuroscience* 2011, *190*, 37-42.

[119] R. Capone, F. G. Quiroz, P. Prangkio, I. Saluja, A. M. Sauer, M. R. Bautista, R. S. Turner, J. Yang, M. Mayer, Amyloid-beta-induced ion flux in artificial lipid bilayers and neuronal cells: resolving a controversy. *Neurotox Res* 2009, *16*, 1-13.

[120] A. Quist, I. Doudevski, H. Lin, R. Azimova, D. Ng, B. Frangione, B. Kagan, J. Ghiso, R. Lal, Amyloid ion channels: A common structural link for protein-misfolding disease. *Proc Natl Acad Sci U S A* 2005, *102*, 10427-10432.

[121] M. Bokvist, F. Lindström, A. Watts, G. Gröbner, Two types of Alzheimer's β-amyloid (1–40) peptide membrane interactions: Aggregation preventing transmembrane anchoring versus accelerated surface fibril formation. *J Mol Biol* 2004, *335*, 1039-1049.

[122] P. L. Yeagle, R. M. Epand, C. D. Richardson, T. D. Flanagan, Effects of the 'fusion peptide' from measles virus on the structure of N-methyl dioleoylphosphatidylethanolamine membranes and their fusion with Sendai virus. *BBA-Biomembranes* 1991, *1065*, 49-53.

[123] Y. Nakazawa, Y. Suzuki, H. Saitô, T. Asakura, The interaction of Aβ(1-40) peptide with lipid bilayers and ganglioside as studied by multinuclear solid-state NMR. *ACS Sym Ser* 2011, *1077*, 299-316.

[124] R. Notman, M. Noro, B. O'Malley, J. Anwar, Molecular basis for dimethylsulfoxide (DMSO) action on lipid membranes. *J Am Chem Soc* 2006, *128*, 13982-13983.

[125] J. P. Douliez, A. Léonard, E. J. Dufourc, Restatement of order parameters in biomembranes: calculation of C-C bond order parameters from C-D quadrupolar splittings. *Biophys J* 1995, *68*, 1727-1739.